MOVAGHAR, MOHAMMAD ESMAEEL

SECOND-ORDER ANALYSIS OF GABLED FRAMES WITH TAPERED MEMBERS

The University of Oklahoma PH.D. 1979

THE UNIVERSITY OF OKLAHOMA

GRADUATE COLLEGE

SECOND-ORDER ANALYSIS OF GABLED FRAMES WITH TAPERED MEMBERS

A DISSERTATION

SUBMITTED TO THE GRADUATE FACULTY

in partial fulfillment of the requirements for the

degree of

DOCTOR OF PHILOSOPHY

BY

MOHAMMAD ESMAEEL MOVAGHAR

Norman, Oklahoma

1979

SECOND-ORDER ANALYSIS OF GABLED FRAMES

WITH TAPERED MEMBERS

APPROVED BY

Thomas M. Murray

A. Ghali

Fulton K. Fears

Lloyd A. Herrmann

DISSERTATION COMMITTEE

ACKNOWLEDGMENTS

I wish to express my sincere gratitude to my advisor, Dr. Thomas M. Murray, for his valuable guidance, supervision and support during the course of this research. I also wish to thank Dr. A.R. Kukreti, Dr. F.K. Fears and Professor L.E. Iverson who served as members of the Doctoral Advisory Committee.

Special appreciation is extended to my wife Mana for her patience and understanding, and my family for their support throughout the years of my study.

TABLE OF CONTENTS

TABLE OF CONTENTS, Cont.

TABLE OF CONTENTS, Cont.

LIST OF FIGURES

LIST OF FIGURES, Cont.

LIST OF FIGURES, Cont.

LIST OF TABLES

LIST OF SYMBOLS

A = Area

b_T = Member length

C_{ij} = Carry-over factor for memer ij from i to j

C_f = Width of residual stress tension block due to flame cutting

C_m = A coefficient applied to bending term in interaction equation

C_v = A coefficient for determination of shrinkage force due to welding

C_w = Width of residual stress tension block due to welding

D = Inclination of column

d = Depth of member

E = Modulus of elasticity of steel

e = Rise of frame rafter

F = Shinkage force of weld

$F_{a\gamma}$ = Allowable stress for a tapered axially loaded compression member

F_y = Yield stress of steel

G = Stiffness ratio

H = Distance from the center of support to midspan of frame

H_w = A coefficient for the heat input of a weld

h = Height of column

I_e = Equivalent moment of inertia

I_n = Moment of inertia

K_{ij} = Stiffness of member ij at the i end

k_{ij} = Stiffness factor of member ij at the i end

$K_{x\gamma}$ = Effective length factor

L = Length

M = Moment

M_p = Plastic moment capacity of a cross-section

P = Vertical concenterated load

P_{cr} = $1.7\ A\ F_{a\gamma}$

$$P_{e'\gamma} = \frac{12\pi^2 EA}{23(K_{x\gamma} x \frac{L}{r_x})^2}$$

Q = Lateral concenterated load

Qw/η = Heat input per unit length of weld

R = Equivalent joint loads

r_x = Radius of gyration

t = Thickness of plate

V = Vertical deflection

v = Transverse imaginary load

w = Uniform load

X_{ij} = Horizontal projection of member ij

Y_{ij} = Vertical projection of member ij

Y = Distance from the centeroidal x axis of a cross-section to the center of gravity of a segment of the cross-section

$\alpha, \beta, \delta, \rho$	=	Coefficients for computation of deflections in trial and error method
γ	=	Tapering ratio
θ	=	Slope of rafter
θ_{ij}	=	Rotation of one end of member ij with respect to the other end
Δ	=	Horizontal or transverse deflection
σ	=	Normal stress

Subscripts

A,B,C,D,E	=	Locations on frame
b	=	Beam
c	=	Column
L	=	Left side
R	=	Right side
rc	=	Compressive residual stress
T	=	Total
1	=	First stage loading
2	=	Second stage loading

ABSTRACT

This study deals with the second-order analysis of unbraced, single story, gabled frames with singly or doubly symmetrical tapered members and hinged supports. Only in-plane behavior is considered with adequate bracing to prevent out-of-plane deflections. Two methods of analysis were developed: a modified stiffness method procedure in the form of a computer program and a manual trial and error method. The trial and error procedure is based on the slope deflection method and moment area principles. Numerical integration was used for computation of the stiffness matrix elements and slope deflection stiffness and carry-over factors. In both procedures, P-Δ effects are taken into account by formulating the equilibrium equations on the deformed structure. Effects of residual stresses are studied by assuming a residual stress pattern at all cross-sections. The yielded portions of members due to combined effects of residual stresses and applied normal stresses are eliminated during the incremental loading process. Reinforcement effect of rigid connections is considered by assuming that a hinge cannot form on members adjacent to reinforced connections within a distance equal to depth of the member from the connection. Loading is incremental and continues until the failure of the frame.

Using the modified stiffness and trial and error methods, the maximum load capacity of several example frames was calculated. Comparison of load-deflection relationships from the two procedures showed good agreement. Comparison with analytical and experimental results found in the literature also showed good agreement. Results for a frame constructed of double symmetric H-shaped cross-sections and constant tapering angle in all members were compared to the maximum load computed by the AISC design provisions for similar frames. The maximum load computed by this procedure was slightly less than the maximum load carrying capacity estimated by the proposed procedures.

CHAPTER I

1.1 Introduction

1.1.1 Nature of Tapered Members

In 1952 Amirikian (1) first proposed the use of tapered members or wedge-beams. The suggestion was made for better and more efficient use of materials. Today, tapered members are used in gabled frames with one or more bays, single-story framed structures, cantilevered elements of structures, and sometimes end portions of beams in low-rise structures to increase their resistance to bending moment and shear at connections.

The frames containing this type of members are called tapered frames. Tapered frames are widely used in pre-engineered metal building industry. Typically, the analysis of tapered frames is first order using design criterion of American Institute of Steel Construction, which is based on empirical formulas of Column Research Counsel, and no inelastic buckling study was considered. Here the effect of some factors on behavior and load capability of tapered frames are attempted to study. These factors are: P-Δ

effect, residual stresses, and the reinforcement effect of rigid connections.

The flexural behavior of a prismatic element with rigid or simple end connections does not follow a consistent form due to variation of moment along the element. The location of maximum bending moment and the variation of the moment along the beam depends on type, location and composition of loads, and for rigid frames it is related to relative stiffness of the member.

It is possible to shape an element to produce uniform maximum stress over its entire length, but economically it is not feasible because of labor cost in fabrication and manufacturing. However, efficient use of material can be attained through the use of tapering. For example, if the prismatic rafter of a rigid frame is increased in cross-section near the supports, the bending moment under vertical or lateral loads will increase also near the supports and decrease toward the middle. If the increase of the cross-section at the ends is accompanied by a decrease of the cross-section at the mid-span , the change of shape of the bending moment diagram becomes more apparent. With an appreciable change of a prismatic to a tapered shape, the bending moment diagram of the rafter may change from reverse flexure to single flexure (like two hinged cantilever beams). This change of shape can be translated into a practical and suitable pattern of cross-sections, which provides a near

consistant stress pattern and consequently better use of material along the member.

Tapered members are also used for columns in frames for the same advantages. Because of low bending moment capability at the narrow end of a tapered element, the joint at this end can be considered hinged or sometimes partially hinged. The other end, which has higher bending moment capacity, is used in rigid connections.

1.1.2 Types of Tapered Members

In general, a tapered member can be defined as a member composed of wedge-shaped elements arranged for better stress distribution and better control of stress along the member. A tapered member may be made of steel, wood, or concrete. In the case of steel the member is constructed by welding all elements to each other. The cross-section can be constructed in any desirable shape. Some of the shapes that are widely used are H-shaped sections, channel sections, box sections, and rectangular sections, Figure 1.1. A tapered member may be single tapered, which means only the web or only the flanges of the member is tapered or double-tapered where both web and flanges are tapered.

1.1.3 Analysis

In the design of steel structures, a major concern is assessment of the overall stability of the structure. When the analysis used by the designer to determine the

distribution of forces and moments throughout the structure is first order, stability effects are not included and the results must be adjusted to reflect the reduction in strength of the structure due to stability effects. In the North American steel design specification, this adjustment is accomplished through the use of interaction equations for the design of beam-columns.

In braced frames, the resistance to lateral loads imposed on a structure is provided by flexural action, diagonal bracing shear walls, claddings, etc. When shear walls and diagonal bracing are not used and the effects of cladding are negligible, the frame of such a structure is called "unbraced." The lateral stiffness of an unbraced frame must be supplied by flexural action of beams and columns and the rigidity of their connections.

The behavior of unbraced frames has been the subject of many studies in the last few decades. Some of the recent studies deal with second order analysis of this type of frame. In second order analysis, the equilibrium equations are formulated considering the deformed structure. In other words, the secondary moments of the structure, resulting from eccentricity of axial loads due to transverse displacements of members, are accounted for in the analysis. The consideration of these secondary bending moments is commonly referred to as including "P-Δ effects."

The behavior of an unbraced plane frame with rigid joints can be studied under gravity, lateral and combined gravity and lateral loadings. Under gravity loadings, at a certain critical load a bifurcation of equilibrium is possible, and failure occurs as the column buckle, Figure 1.2. Under lateral loads, as the bending moments increase, hinges form at or between the rigid joints, Figure 1.3. After the formation of sufficient number of hinges to define mechanism, the frame becomes instable and failure occurs. Under combined lateral and gravity loads, which is the most general type of loading, horizontal deflection is present from the beginning, Figure 1.4. The failure of a frame under combined loading may occur due to sidesway buckling or plastic mechanism.

The purpose of this study is to investigate nonlinear behavior of tapered frames. This nonlinearity can be caused by several factors: P-Δ effects, residual stresses, rigidity of joints, etc. In this study the effects of the first three factors on the behavior of tapered frames are considered.

1.2 Review of Literature

1.2.1 Classical Methods

A basic approach to analyze tapered frames was first introducted by Amirikian (1). This procedure starts with the assumption that a hinge is placed at the narrow end of all tapered elements. The structure is then a series of

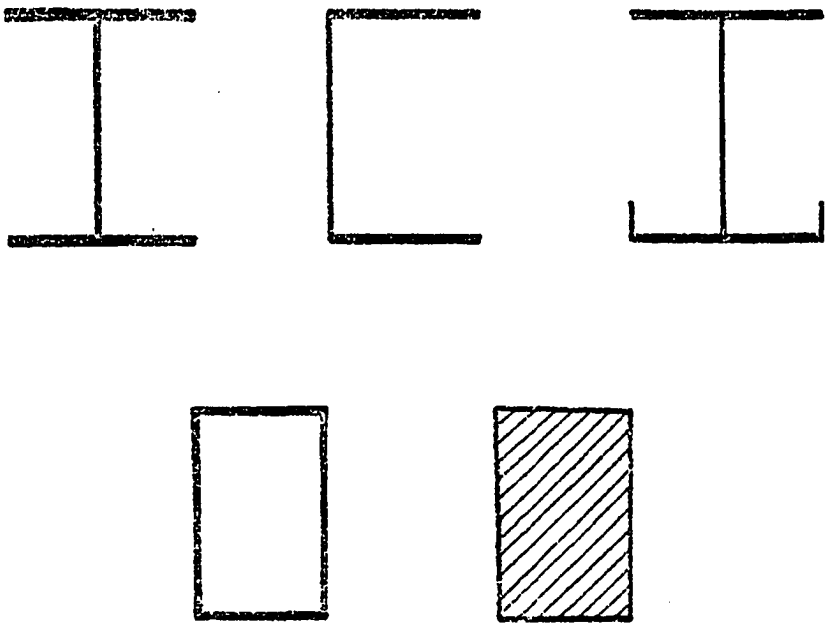

Figure 1.1 Types of Cross-Sections Used in Tapered Members

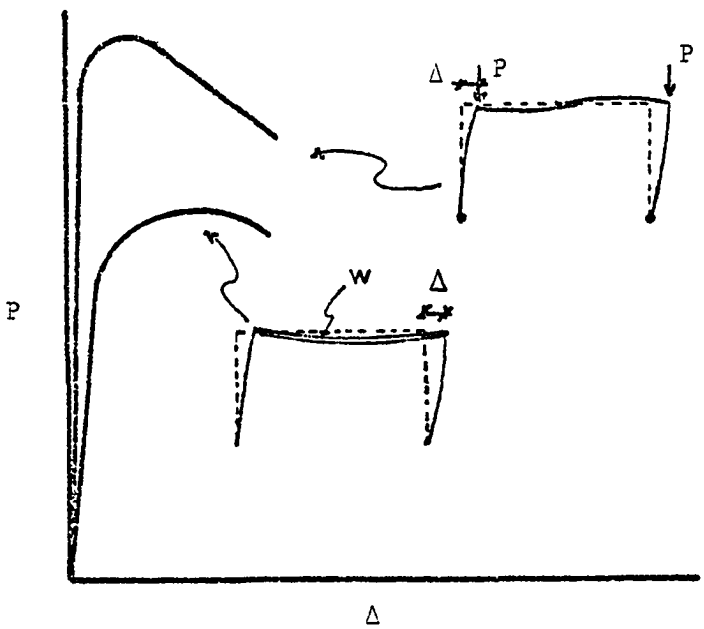

Figure 1.2 Load-Deflection Curve of Frame Loaded with Gravity Load

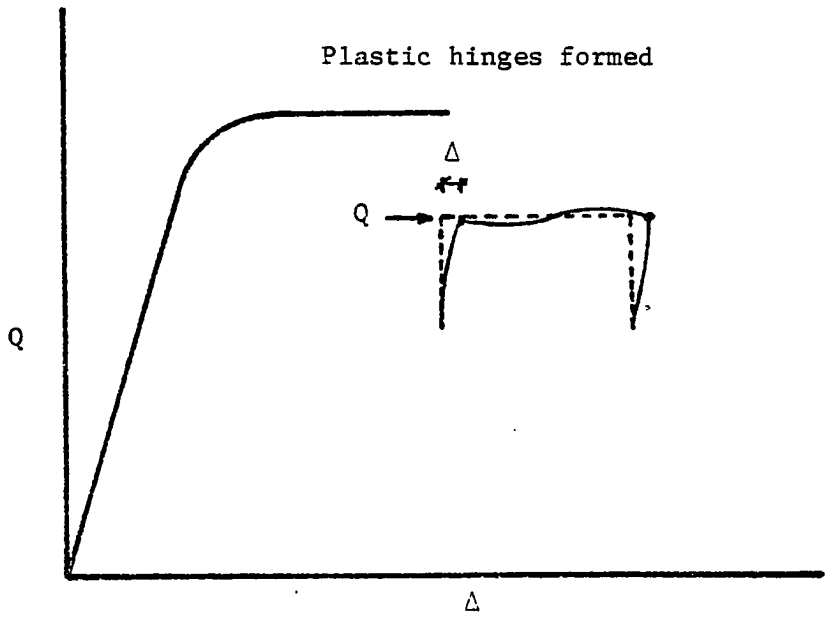

Figure 1.3 Load-Deflection Curve of a Frame Loaded with Lateral Load

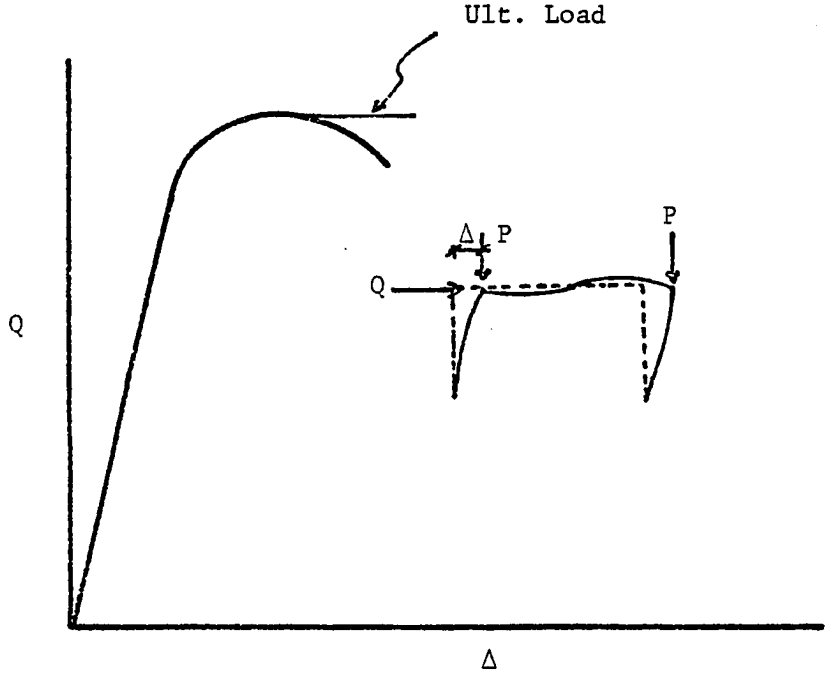

Figure 1.4 Load-Deflection Curve of a Frame Loaded with Gravity and Lateral Loads

statistically determinate frames called simple frames. A simple frame is composed of one, two, or more subassemblages, each of which is formed by two or three tapered members rigidly jointed at their deep end, Figure 1.5. It is assumed that, because of adequate bracing out-of-plane lateral deflection and twist are not a factor in this study and buckling is not considered. Because of these assumptions, analysis of two legged, three hinged frames is very simple. In practice, the joints at the narrow ends are not hinged, therefore, the proposed method by Amirikian underestimates the load capacity of tapered frames, and some of the frames currently in use are multiple tapered to which Amirikian's method is not applicable, Figure 1.6.

Theoretical analysis of tapered members used as columns or beams in frames has been studied by several authors. Fogel and Ketter (7) studied the effect of a combination of axial compression load, bending moment, and slenderness of elastic nonprismatic members pinned at both ends. In their study, the in-plane behavior of two types of member was considered: (a) members with I cross-sections and taper web; and (b) members with rectangular cross-sections and variable depth. They concluded that the interaction among axial load, bending moment, and slenderness is dependent on variation of cross-section along the member and the loadings and provided formulas to locate cross-sections where yielding occurs and their interaction equation, for

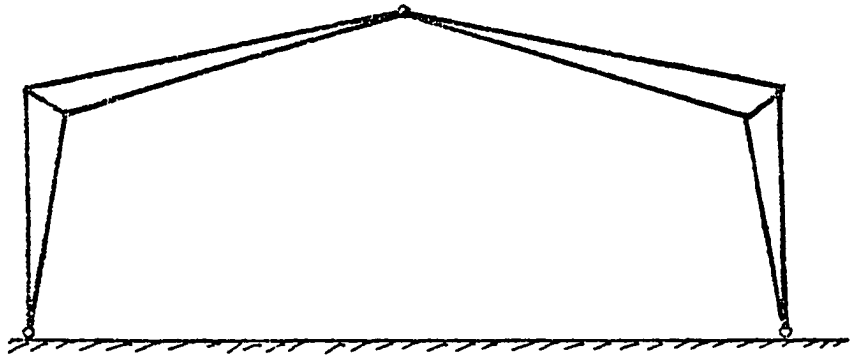

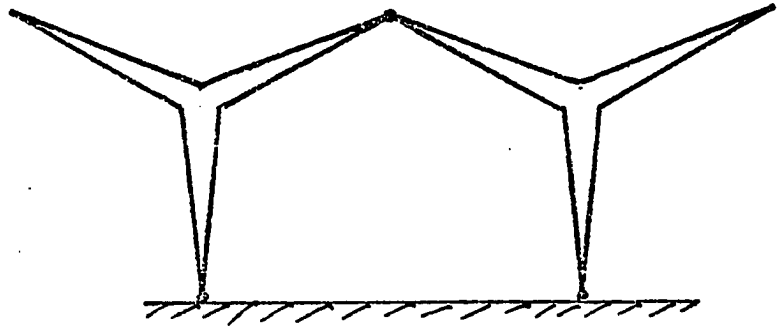

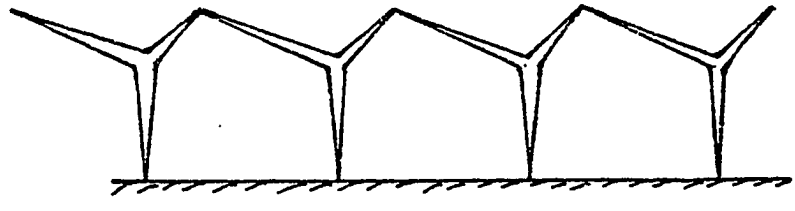

Figure 1.5 Multi-Bay Single Story Simple Tapered Frames

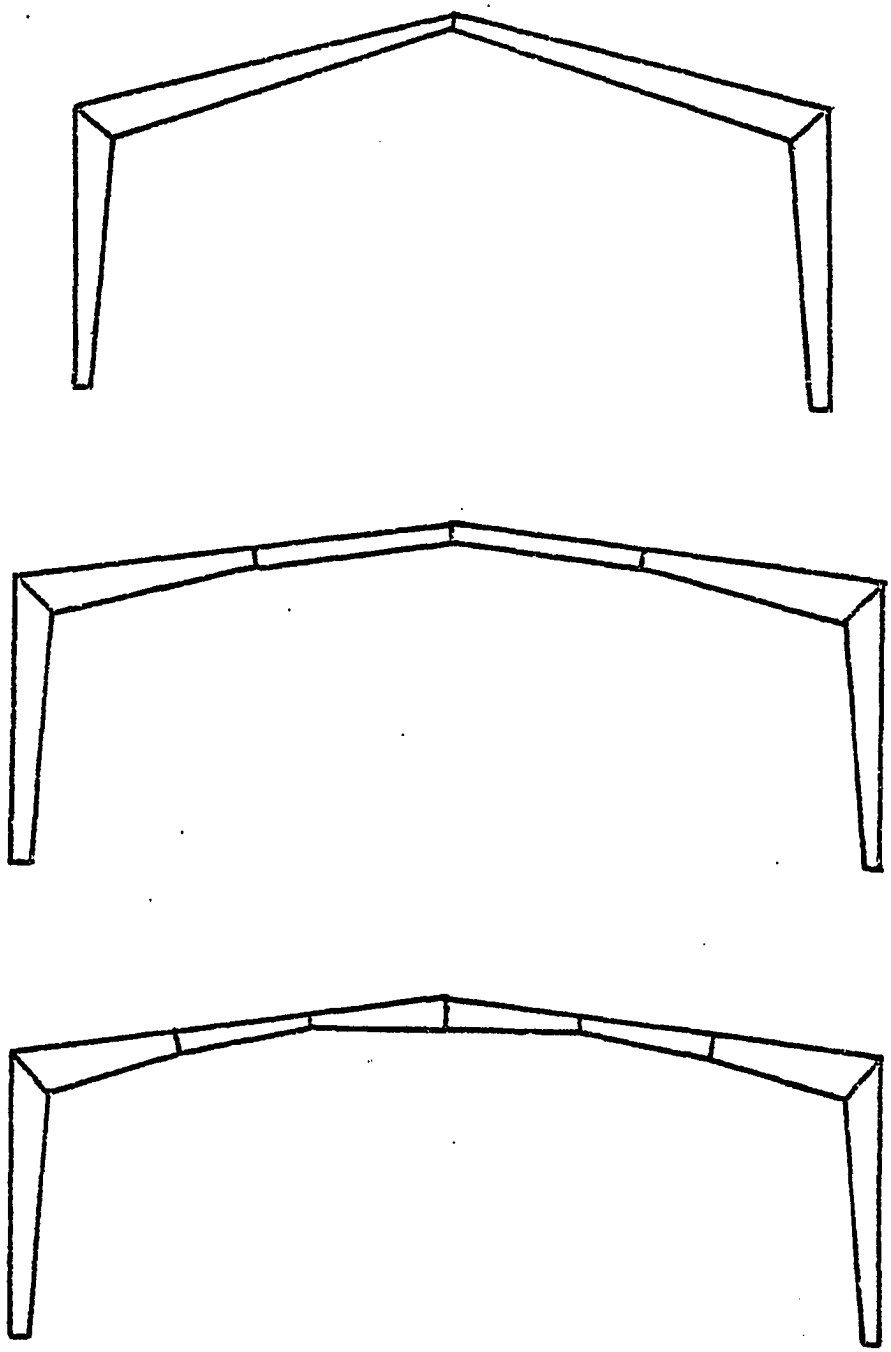

Figure 1.6 Multiple Tapered Beam Gabled Frames

both types of elements.

Moses, F. (3) presented a numerical iterative method suitable for digital computers to solve the stability problem associated with sidesway buckling of inelastic frames. In his procedure, which is called the "fixed deflection method," a deflected shape or a buckled mode is assumed and the load associated with the assumed deflected shape computed by first analyzing each member of the frame subjected to end moments, axial forces, and transverse loads and then applying equilibrium equations, compatibility, and boundary conditions to solve for the applied loads. Since the computations are based on the deflected shape of the frame, this is a second order method. In computing the load for an assumed deflected shape, the method cannot be used for as a neutral equilibrium criteria for buckling, but it can be conveniently used for numerical computation by computer.

For the stability analysis of rigid frames, Wang (10) used a trial and error method to make the determinant of the stability stiffness matrix equal to zero. For each value of the standard stability angle ($\phi = L\sqrt{\frac{P}{EI}}$), a value of the determinant can be computed. The lowest value of the stability angle for which the determinant is zero is the critical standard stability angle, from which the buckling load is computed. For frames with nonprismatic members, Wang suggests that each member be divided into small elements assuming average properties at the two ends as properties

of the element. With this procedure the size of stiffness matrix increases proportionally with the number of elements in the frame and, therefore, more computer time and storage is required.

Wang used an iterative procedure for second order analysis. In the first cycle of iteration, the computations are based on the geometry of the frame using the joint displacements from the first order analysis. In the second cycle, the computations are based on the geometry of the frame at the end of the first cycle of iteration. This procedure is repeated to any desired degree of accuracy.

Galambos (5), using the slope deflection method, formulated equilibrium equations for the analysis of frames. In his procedure, the equilibrium equations are formulated on the undeformed frame for first order analysis. For second-order elastic analysis, the equilibrium equations are formulated on the deformed structure. The moments in the members are magnified by the product of the axial force and the deflection, which results an increase in deformations. These deformations become quite large when the load approach the buckling load of the frame. For rigid plastic analysis Galambos assumed that no deformation occurs until plastic moment is reached at sufficient locations in the frame to develop a mechanism. At this point the load is called plastic collapse load or plastic failure load.

1.2.2 Design Methods

Lee, Morrell and Ketter (2,9) conducted a comprehensive study of the stability and design of tapered frames. This study was concerned with the analysis of frames with members having linearly tapered webs and doubly symmetric H-shaped cross-sections. To develop a design procedure, they suggested the use of design formulas for prismatic members but with modification factors. The result of this study was the development of a set of curves for several types of frames from which the effective length of tapered column with or without sidesway can be computed. These results are contained in the 1978 American Institute of Steel Construction specification as Appendix D (4). The application of this design procedure is given in Reference 8. The procedure is based on finding an imaginary prismatic beam-column with cross-section of the small end of the tapered member and with a length equal to effective length factor times the length of the tapered member. The provisions for prismatic members are used to determine allowable stresses of the members. The maximum load of the frame is the load where the stress at a location on the frame is at the allowable stress for that member.

1.3 Effects of Residual Stresses

Since tapered members are normally fabricated from flame cut or hot rolled flat plates or rolled sections, significant residual stresses are to be expected. Because

of these residual stresses, a frame constructed of tapered members may exhibit a lower capacity than a frame constructed with initially stress-free section.

Extensive investigations by Frost and Schilling (7) Nagarajarao, Marek, and Tall (16), Dwight and Maxham (21), and Nethercot (18,19) on the magnitude of residual stresses in hybrid H-shaped test beams and stub columns, shows that tension residual stresses near the weld area and flame cut edges may be as high as the yield stress of the material, and that compressive residual stresses in the remainder of the cross-sectional area balancing the tension stresses. In an elasto-plastic analysis, residual stresses do not have a direct effect on the load capacity of tapered frames. In other words, the residual stresses do not reduce the plastic moment capacity of cross-sections, however, the presence of residual stresses does increase frame flexibility, which, in turn, causes a reduction of load capacity due to second order effects.

1.4 Present Analysis

1.4.1 Elasto-Plastic Stiffness Analysis of Tapered Frames

In this study a computer program was developed to analyze the elasto-plastic behavior of tapered frames under vertical and horizontal loads applied in one or two stages. The computer program is a general program and considers non-linear behavior of frames due both to material properties

and P-Δ effects. Residual stresses are considered by assuming the same pattern at every cross-section. The effect of reinforcement of a connection (11,12) is considered by assuming that a hinge does not form within a distance equal to the depth of member from the center of connection.

A frame may be loaded by two sets of loads, in two stages. In the first stage the loads are applied to the frame in one cycle, and in the second stage the loads are applied incrementally. In both stages, an iterative procedure is used to include P-Δ effects in the analysis. When it is desired to load the frame with only one load set, the loads of the second set are taken equal to zero.

The stiffness method is used for analysis. Using the moment area principle and numerical integration on small elements of members, the stiffness matrices for members are computed. The structure stiffness matrix is then assumbled and solution for a given load obtained by multiplying the inverse of frame stiffness matrix by load matrix. At the end of each loading, stresses resulted from axial froce and bending moment are combined with residual stresses in every cross-sections and yielded portions of all cross-sections are eliminated. Elimination of the yielded portions causes change in member stiffness, therefore, new properties for the member elements are computed for the next loading. If all segments at a cross-section are eliminated, e.g., when the bending moment reaches the plastic moment capacity of

the cross-section including the effect of axial load, a hinge has formed at that location. Subsequent analysis is made with a real hinge inserted at that location on the frame. The analysis is continued by further loading the frame until sufficient hinges are found to form a plastic mechanism or sidesway buckling of the frame occurs.

1.4.2 Trial and Error Method of Analysis

The purpose of this part of study is to develop an alternative to the stiffness method to analyze a plane frame.

Here a manual trial and error technique is presented to estimate the load-deflection relationship for tapered gable frame hinged at the supports. This technique takes into account in-plane behavior of the frame, and the slope-deflection method is used for the analysis.

The analysis of the frame by this technique contains two stages of incremental loading as follows:

1. In the first stage, the frame is indeterminate and the equilibrium equations are formulated on deformed structure including P-Δ effects. The computation for an increment of load starts by assuming a value for the horizontal reaction at one of the supports. With this assumed value, the remaining reactions and the horizontal deflection at one end of the rafter with respect

to other end are calculated. The horizontal deflection is calculated in two different ways, if the two computed values are equal or within an acceptable range, the assumed value is accepted and all other deflections computed; otherwise, the procedure is repeated until convergence. The loading in this stage continues until a hinged forms on the frame.

2. In the second stage, the frame is determinate and the reactions and deflections for an increment of load are computed directly from equilibrium equations, iterated for the effect of deformations on reactions. This stage of loading continues until a plastic mechanism occurs or the frame fails due to sideway buckling.

1.5 Summary

Although previous studies have produced a variety of methods to analyze tapered frames, almost all of these methods are in the elastic range. The overall concept of inelastic behavior of frames is dependent on P-Δ effect (or secondary moments due to deflections and axial forces), residual stresses, true stress-strain relations, joint rigidity, and, finally, strain reversal in fibers. It is difficult and sometimes impossible to consider all of these factors in the solution. However, an attempt has been made to develop a method of solution for the analysis of tapered

frames in the plastic as well as elastic range including some of these factors. Two different analysis methods were developed and results compared. The effect of residual stress is considered in the form of a pattern of stress at cross-sections of all members. It is assumed all joints except supports are rigid, and the secondary effect of axial force due to transverse deflection of a member is considered for each loading and iterated until convergence occurs.

CHAPTER II

COMPUTER ANALYSIS OF TAPERED FRAMES

2.1 General

This chapter is a discussion of a computer program for the elastro-plastic analysis of planar frames. The program analyzes nonlinear behavior of a plane frame caused by P-Δ effects and considers effects caused by partial yielding of the cross-sections due to residual stresses.

2.2 Assumptions

The members of the frame are assumed to be web tapered only and with constant tapering angle. The flunges have constant width and thickness, and with minor adjustment the program can be used for variable flunge dimensions. It is also assumed that the location of the centroidal axis of a member varies linearly and that it lies in the plane of the frame. Therefore, whenever the location of the centroidal axis varies significantly from the assumptions, that section is considered as a separate member, Figure 2.1. The connections between the member can be assumed either rigid or

pinned. The positive direction of joint forces, joint displacements, member end forces, and member end displacements are as shown in Figure 2.2. The loads are assumed concenterated at joints or uniformly distributed along a member and are assumed to be applied in the plane of the frame.

All deflections and deformations are assumed to occur in the plane of the frame. The out-of-plane behavior, including biaxial bending, local, and torsional buckling are assumed not to occur in this study.

Sidesway of the frame is not prevented and the resistance to sidesway is assumed to be provided by stiffness of the members and rigidity of the connections.

All members are assumed to be built-up from plates and/or hot-rolled sections and assembled by welding. The cross-sections of the members considered in this study are limited to two types, as shown in Figure 2.3. The cross-section of the type shown in Figure 2.3(b) is commonly used for columns.

The joints of the frame are assumed to be located at the ends of the members where the centroidal axes of the adjacent members intersect. However, a short stiff member is assumed to exist immediately adjacent to all rafter to column connections to account for the reinforcement effect of the knee area. This increased stiffness forces the formation of the plastic hinges some distance away from the

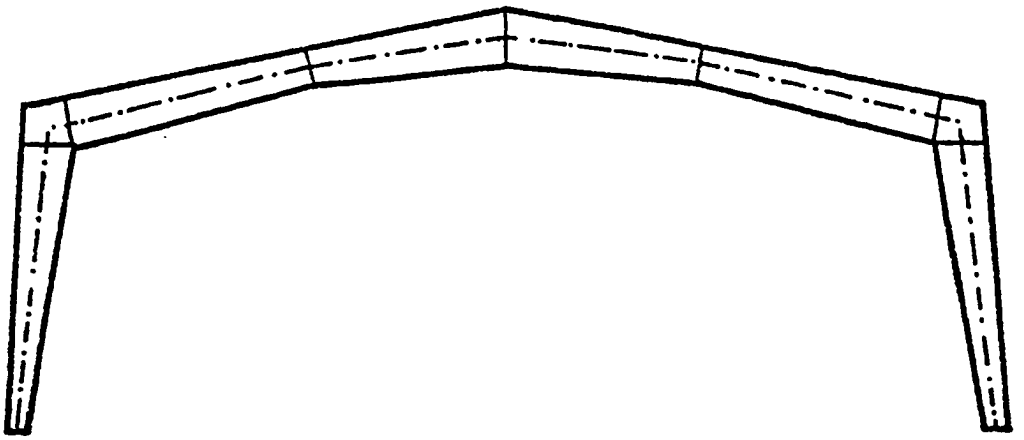

Figure 2.1 A Typical Frame with Six Members

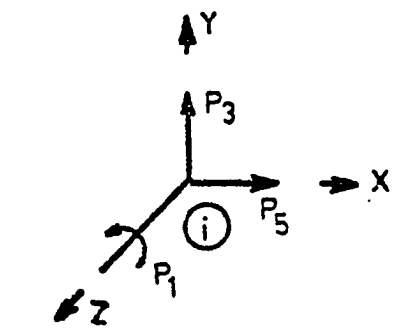

(a) Joint Forces

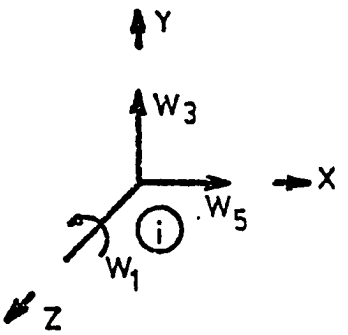

(b) Joint Displacements

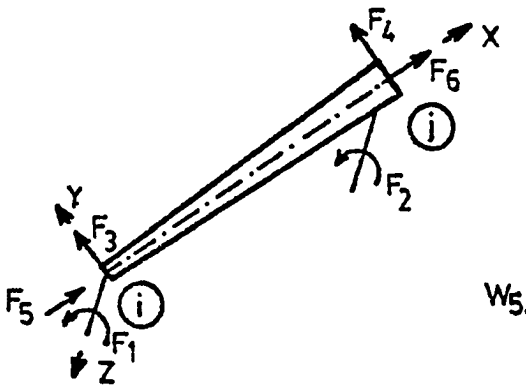

(c) Member End Forces

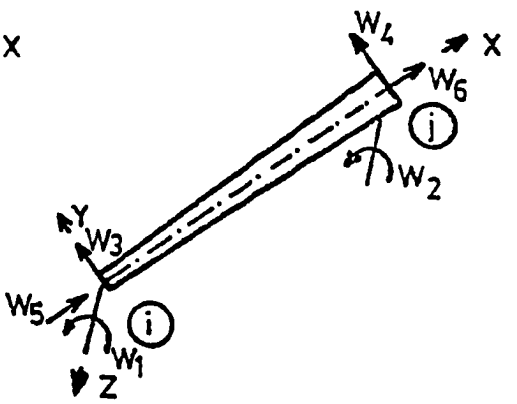

(d) Member End Displacements

Figure 2.2 Sign Conventions of Analysis Procedure

connection. Later in this chapter the reinforcement effect will be discussed in more detail.

2.3 Solution Method

The method of analysis presented here is a stiffness method (13), modified to account for P-Δ and inelastic effects caused by residual stress and local yielding.

Since section properties vary along the length of a member, elements of the member stiffness matrix cannot be computed by the standard methods used for prismatic members. It is convenient to use the moment area principle (22), to calculate the elements of the member stiffness matrix. Figure 2.4 shows a typical tapered member. From the moment area principle, carry-over factors and stiffness coefficients for this member are:

$$C_{AB} = \frac{L\int_A^B \frac{x\,dx}{I_x} - \int_A^B \frac{x^2\,dx}{I_x}}{\int_A^B \frac{x^2\,dx}{I_x}} \tag{2.1}$$

$$K_{AB} = \frac{EL^2}{\int_B^A \frac{x_1^2\,dx_1}{I_x} + C_{AB}\int_B^A \frac{(L-x_1)x_1\,dx_1}{I_x}} \tag{2.2}$$

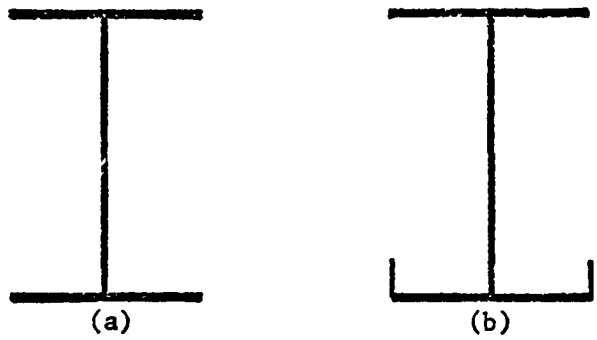

Figure 2.3 Types of Cross-Sections

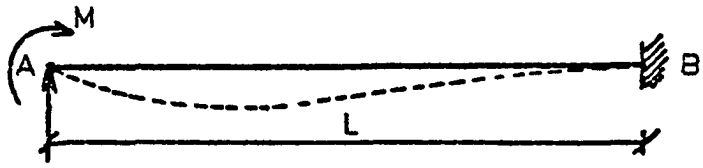

(a) Beam AB with a Moment at A

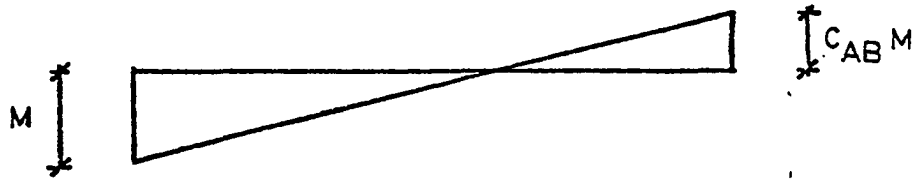

(b) Moment Diagram

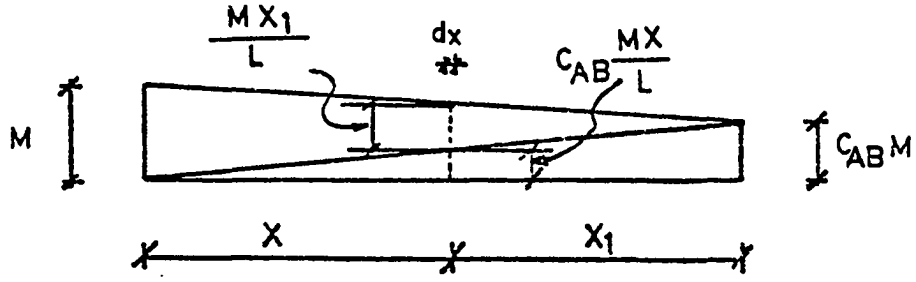

(c) Equivalent Form of Moment Diagram

Figure 2.4 The Deflected Shape and Moment Diagram of a Typical Beam

where C_{AB} = the ratio of moment at B to the moment at A, and K_{AB} = the stiffness at A. By the same procedure C_{BA} and K_{BA} are:

$$C_{BA} = \frac{L\int_B^A \frac{x_1 dx_1}{I_x} - \int_B^A \frac{x_1^2 dx_1}{I_x}}{\int_B^A \frac{x_1^2 dx_1}{I_x}} \tag{2.3}$$

$$K_{BA} = \frac{EL^2}{\int_A^B \frac{x^2 dx}{I_x} + C_{BA}\int_A^B \frac{(L-x)x dx}{I_x}} \tag{2.4}$$

The moment of inertia along a tapered member is variable, and the relationship between the coordinate of the location where the moment of inertia is desired, and the moment of inertia is complicated for some types of tapered members. Furthermore, it is not possible to establish a relationship between the location and moment of inertia for cross-sections which are partially yielded. Numerical integration is used in this study by dividing the member into a number of small segments and using the average properties at the two ends of each element as the properties of the element. Thus, it is assumed that the member is stepped

(i.e., each element is prismatic), and integration is performed along the stepped member. The accuracy of solution depends on two factors: 1. the number of element in the members, the larger the number of elements, the more accurate the results obtained from the calculation; and 2. the tapering angle of the member. As the tapering angle increases the variation of moment of inertia along the member also increases. The increase of tapering angle may increase the depth of the member drastically, so the deep beam effect becomes a factor in stress distribution in deep cross-sections, but this study is not concerned with this effect. For accurate results, the number of elements along a member must be increased with increased tapering angle. However, the size of computer and computer time economics limits the practical number of the elements.

2.4 P-Δ Effects

Transverse displacement of one end of a member with respect to the other end causes an eccentricity of the axial load which creates an additional moment along the member. This moment is termed the P-Δ effect.

The analysis of a structure considering this effect is called a "second order" analysis. In a second order analysis, the shear equilibrium equations are formulated on a deformed structure and, thus, the secondary moments produced by eccentricity of axial loads in all members are considered in the analysis.

2.4.1 Formulation for P-Δ Effects

Consider the column of Figure 2.5(a) under a vertical load P and horizontal load Q. The column is pinned at the support and restrained by the girder, which is replaced by a rotational spring at the top. Figure 2.5(b) shows the deflected shape of the column and the moment at the top of the column is:

$$M = Qh + P\Delta \tag{2.5}$$

The moment M consists of two parts: Qh, a first order moment due to the horizontal load, and PΔ, the second order moment caused by the deformation Δ and the axial load P. This moment can be replaced by a pair of transverse loads at the ends of the column. From

$$P\Delta = hV \tag{2.6}$$

the transverse loads can be written as:

$$V = \frac{P\Delta}{h} \tag{2.7}$$

where V is an imaginary load which is placed at both ends of the column to create a moment equivalent to PΔ, see Figure 2.5(c).

Starting with a load increment acting on the frame, values of V for all members are computed for known P and Δ.

In the first iteration the values of V are used as a new set of loads for the frame, and the displacements, moments and axial forces introduced by these loads are computed and added to the existing displacements, moments and axial forces. In other iterations, in each cycle the deflections and axial forces introduced by the imaginary load of the previous iteration are used to compute the values of V which are used as the new set of loads. The cycles of iterations continues until all of the computed values of V drop to less than a specified value, which in this study is assumed to be equal to 0.001 kips.

2.5 Residual Stresses

Residual stresses in the plates and rolled shapes have been the subject of a number of investigations which have resulted in a better understanding of the behavior and load capacity of structural elements. Residual stresses are introduced in a structural members during the following processes: welding, flame cutting, hot-rolling, cold bending and cambering. Tapered members are usually fabricated from rolled plates cut to the desired size by a flame torch or mechanical plate shear. However, rolled shapes are sometimes used to construct tapered members, for example, a hot rolled channel may be used as a compression flange of a column. In either case, the elements are assembled by welding which introduces residual stresses in the member. Residual stresses caused by welding and flame cutting in built-up members are

the only types of residual stresses considered in this study.

The unresisted thermal expansion of steel for each 100°C is approximately equal to the strain of mild steel at yield (21). The temperature of steel around a welded area or near a flame cut edge rises to about 1200°C. This localized increase in temperature causes a change in the physical properties of the cross-section after cooling. The residual stresses in these areas may reach as high as the yield stress of the base material. The residual stresses immediately adjacent to the weld or flame cut are usually tensile and are balanced by lower compressive residual stresses spread over a larger portion of the cross-section.

The pattern of residual stresses in a rolled section depends on the rate of cooling and rolling process. Bjorhovde, et al., (20) investigated and measured residual stresses in hot rolled thick plates before and after flame cutting. It was found that the maximum compressive residual stress increases with increased plate size and that variation of residual stress through the thickness is negligible in plates thinner than about one inch. Figure 2.6 shows that the isostress diagram of a 12 in. by 3½ in. universal mill plate, which indicates the variation of the residual stress through the thickness of the plate.

The residual stresses of several hybrid H shaped test beams have been measured (17). The results of these

tests confirm the yielding of the area around the weld and the flame cut edges, and show similar patterns in all cross-sections.

Nagarajarao, Marek and Tall (16) measured residual stresses in five hybrid H shaped specimens. The specimens were three feet long and fabricated from cut plates and universal-mill plates and were not subjected to cold bending or straightening. The specimens were not straightened or cold-bent or trimmed after welding. The results of residual stress measurement for two specimens are shown in Figure 2.7. The flanges of the specimen shown in Figure 2.7(a) are universal-mill plates; the flanges of the specimen shown in Figure 2.7(b) are flame cut plates. The shape of the residual stress distributions are very similar to the stress distribution in homogeneous shapes. The tensile residual stress at the flame cut flange tips ranges from 30 ksi to 70 ksi and is about 25 ksi at the welds. The compressive residual stress is about 20 ksi. The web has high tensile residual stress in the area close to the weld and a compressive residual stress of about 10 ksi in the remaining area.

To analyze the effect of residual stresses in frames, a simple geometrical pattern is needed to approximate the residual stress pattern found from experimental investigation.

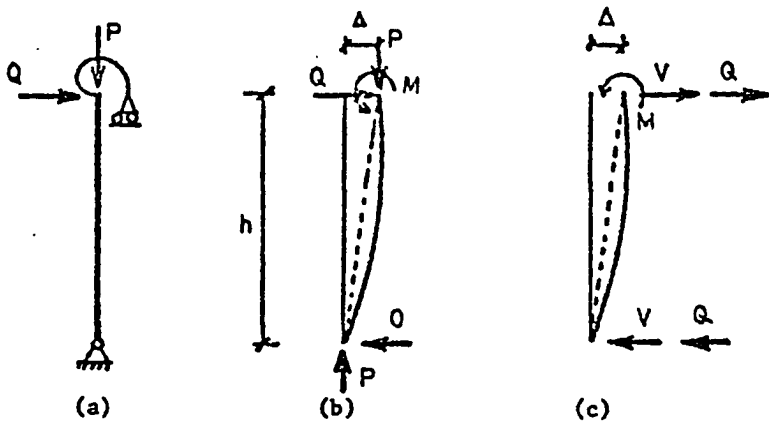

Figure 2.5 A Column Deflected under Vertical and Horizontal Loads

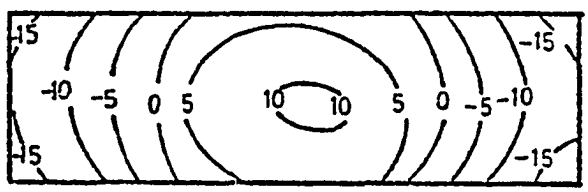

Figure 2.6 Isostress Diagram for Residual Stresses in Thick Plate of A36 Steel

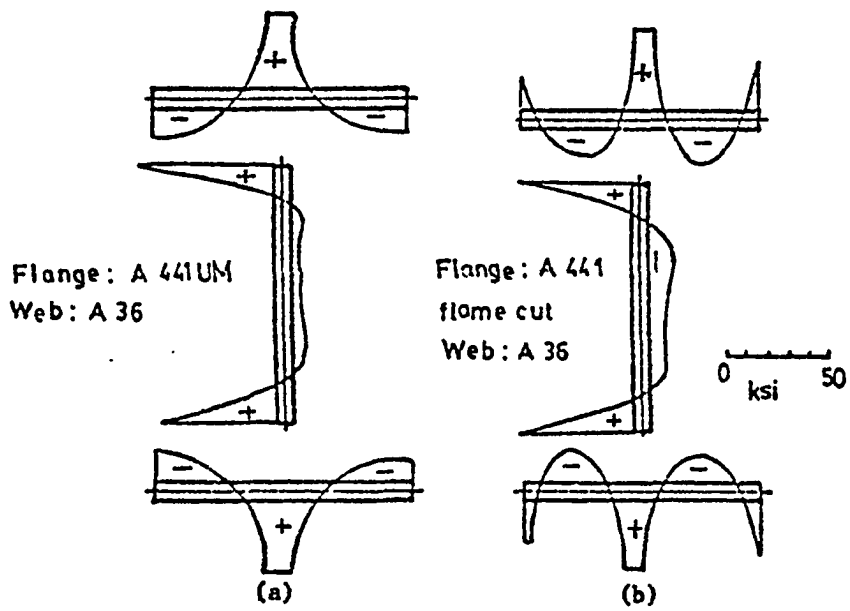

Figure 2.7 Residual Stress Distribution in Two Hybrid H-Shaped Specimens

Dwight and Maxham (21) have used the rectangular residual stress pattern shown in Figure 2.8(a) for box sections, and later Nethercot (18, 19) adapted the same pattern for hybrid I sections, Figure 2.8(b). In this type of pattern, the area around the weld is in tension at the yield stress level, and the rest of the cross-section is in compression, thus balancing the tensile residual stresses.

Theoretical investigations at Cambridge by Dwight and Maxham (21), supported by test results, produced a simple procedure to compute the width of the tension block. The procedure computes the shrinkage force of a weld by:

$$F = Hw \times {}^{Qw}/_{\eta} \tag{2.8}$$

or

$$F = C_v \times A \tag{2.9}$$

where F = the shrinkage force of the weld, Hw = a constant estimatd to be about 0.13 (18), ${}^{Qw}/_{\eta}$ = the heat input for a unit length of the weld, C_v = a constant, approximately equal to 870 kips/in^2 (18), and finally A = the added area of the weld in square inches which can be computed by:

$$A = 0.6 \times W_e^2 \tag{2.10}$$

in which W_e= weld size.

The width of the yielded tension block is calculated by:

$$c_w = \frac{F}{\sigma y \Sigma t} \tag{2.11}$$

where Σt = summation of thickness of the plates welded together. When the weld is not located in the edge of a plate, like in flanges of an I section, twice the plate thickness is included in computing Σt.

When the plates used for the flanges of the I section are flame cut, a portion of the plates at the edges is also assumed to be yielded in tension. Dwight suggested that the width of the tension block induced by flame cutting and due to shrinkage to be

$$C_f = \frac{28.783\sqrt{t}}{\sigma y} \qquad (2.12)$$

where t = thickness of the plate in inches, σy = yield stress in ksi and C_f = the width of the tension block. Figure 2.8(c) shows the residual stress pattern in the flame cut flange of an I section.

Tall and Yu, in a study on stub column test results at Lehigh University (33), used triangular residual stress pattern for H shape cross-section, Figure 2.9. The H shapes were built-up from mild steel plates flame cut and universal mill. The residual stress in the tips of flame cut flanges was approximately 75% of the yield stress.

The buckling curves of beams based on this type of residual stress pattern is very similar in most of their range to the curves obtained by an analysis based on rectangular patterns, for the same values of the compressive residual stress (19).

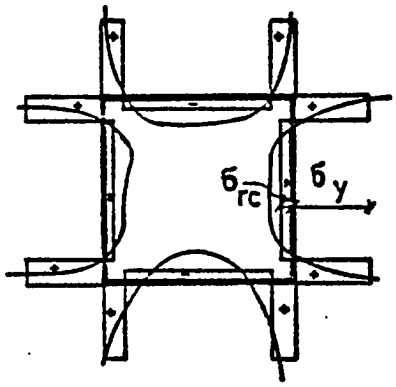

(b) Rectangular R.S. Pattern

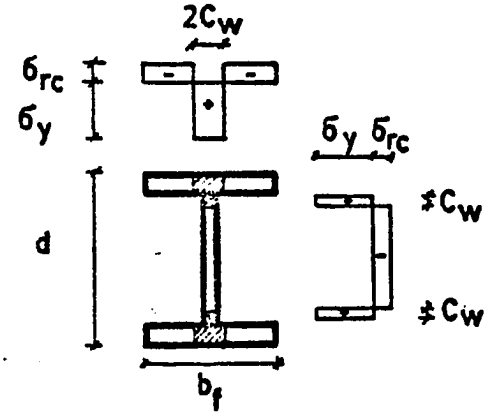

(a) Rectangular and Actual R.S. Pattern

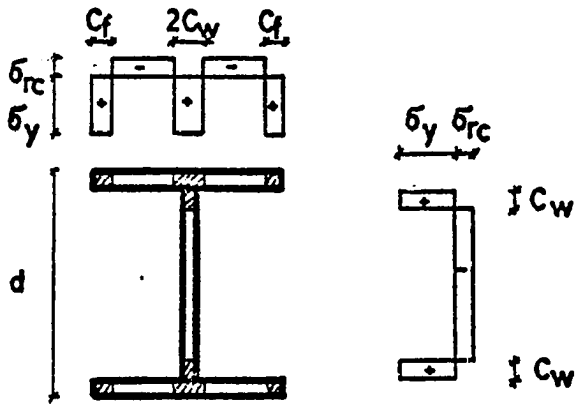

(c) Rectangular R.S. Pattern for Cross-Section with F.C. Plates

Figure 2.8 Rectangular Residual Stress Patterns for Box Sections and I Beam due to Welding and Flame Cutting

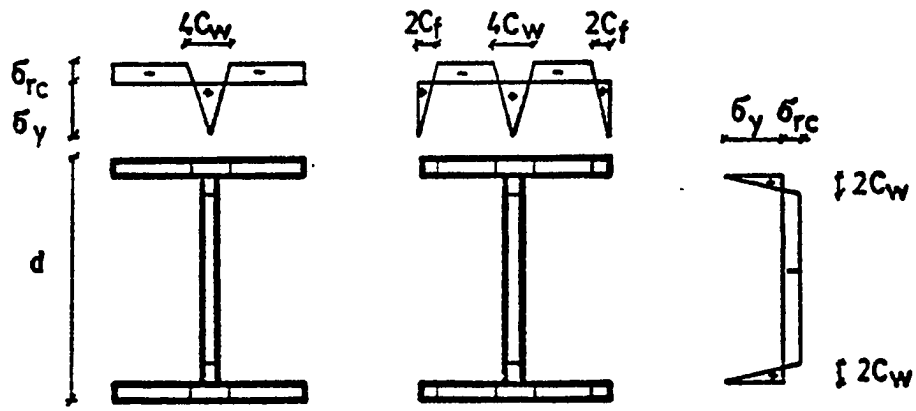

(a) U.M. Plates (b) F.C. Plates

Figure 2.9 Triangular Residual Stress Pattern

Nethercot (19) mentioned that Dwight recently suggested to modify the rectangular tension block of the residual stress into the trapezoidal shape for columns, see Figure 2.10. He used welding data together with the Cambridge approach (Equations 2.8, 2.9, 2.10, 2.11). The theoretical beam buckling curves based on this type of pattern, and curves by experimental results of two sections, were in substatial agreement.

The purpose of this study is not to establish a definitive residual stress pattern for welded sections, but to consider several possible patterns and study their effects on the behavior of tapered gabled frames. For this purpose, three procedures are included in the computer program, so that frames can be analyzed for any of the three patterns shown in Figures 2.8, 2.9, 2.10.

2.6 Elimination of Yielded Portions from Cross-Sections

After loading the frame with both real and imaginary loads, caused by P-Δ effects in a cycle of loading, the total end actions of members are computed by adding the end actions resulting from that cycle to the end actions due to previous load increments. Using the total end actions, member loads and standard static formulas, the moment diagram and the axial force along a member are determined. These are used to establish normal stress distribution of cross-sections along the member. Boley (6), using a series

solution and the Bernoulli-Euler theory for tapered rectangular beams, found that for tapered angles of less than 15^{o}, the error on normal stress computed by the general method was less than a few percent. Since the tapering angle of the members used in this study is considerably less than 15^{o}, the Bernoulli-Euler theory is used to compute stresses due to bending moment and axial loads.

For elimination of yielded portions, the cross-section is divided into small segments. To reduce computer core usage and computing time, the stress at the center of gravity of a segment is considered to be the stress along the length of the segment.

According to Bernoulli-Euler theory the normal stresses due to bending moment and axial load in any location of a cross-section are:

$$\sigma_m = \frac{M_x Y}{I_x} \tag{2.12}$$

$$\sigma_p = \frac{P}{A} \tag{2.13}$$

where M_x = the bending moment, y = the distance from the centroidal x axis of the cross-section to the center of gravity of the segment, and p = the axial load. The total stress at each point is then:

$$\sigma_t = \sigma_r + \sigma_m + \sigma_p \tag{2.14}$$

where σ_r = the residual stress of the segment. After

computation of σ_t, those segments having a σ_t larger than the yield stress are replaced by a fictitious force and moment. The magnitude of this force is equal to area of the yielded segment times the yield stress. The moment arm of this force is defined at the distance from the center of gravity of the yielded portion to the neutral axis as calculated for the non-yielded parts of the cross-section. The next step is to combine all fictitious forces and moments with the axial force and bending moment on the cross-section. Based on this new moment and axial force, the stresses in the rest of segments are computed. The process of eliminating the yielded segments continues until only segments with stress less than the yield stress are left. At this point the cycle of computation for a real or imaginary loading is completed. For the next cycle of computation, new properties of all cross-section must be computed.

A typical cross-section used in this study is divided into 28 areas, see Figure 2.11. The center portion of the flanges which are closest to the weld areas are assumed to be in tension due to residual stresses. The remaining portion of the flange area are compressed to balance the tension forces of the center portion. The compresses portions of the flange are in two separate parts, but the stresses in the identical horizontal layers of these portions are the same. Therefore these two separate portions are treated as one compressed block.

Each flange is divided into four horizontal layers and the flanges of the channel section, located in the lower part of Figure 2.11, are divided into two segments. The web of the cross-section is divided into eight segments. The lower and upper segments of the web are in tension because they are closest to the weld area, and the rest of the web area is in compression, balancing the residual stresses of the other two segments which are in tension. By assigning a zero value to the width of flanges of channel in Figure 2.11, the cross-section is transformed into a H-shaped section. If all or some of the tension blocks of cross-sections of any or all members of a frame are equated to zero, the frame will be analyzed partially or totally free of residual stresses.

2.7 Reinforcement Effect of Rigid Connections

In classical plastic analysis of rigid frames, it is usually assumed that a hinge can form at the center of all connections. Laboratory tests have shown that when two members (usually a column and a rafter) are framed together by a reinforced connection, the plastic hinge will form at a distance from the face of the connection in the weaker member (32). This phenomenon is caused by the increased strength of the portion of member adjacent to the connection, and to the combined stress condition at the face of the connection. This effect tends to increase the stiffness of the frame, which in turn results in an increase of the ultimate load

capacity of the frame. One approach to consider this effect in analysis is to introduce a short, stiff member between the column or the rafter and the reinforced connection. This short member behaves elastically during the loading process and, therefore, a hinge cannot form in the member. A full scale frame with prismatic members was tested at Lehigh University to study this effect (11). A theoretical analysis using the fictitious member concept produced results very close to those found experimentally when the location of hinge formation was moved to a location with a distance equal to depth of column or girder from the face of the connection. The use of this type of fictitious member is considered in this study.

2.8 Computer Program

A computer program for this study was written for an IBM 370/158 computer with the OS/VS2 JCL system. The language of the program is FORTRAN-IV Level N and double precision was used in all computations.

The following assumptions are made in the development of the program:

1. All members of the frame are straight in their original position, i.e., no crookedness due to fabrication is considered.
2. Plane cross-sections remain plane after deformation.

3. Bernoulli-Euler law for stress distribution of all cross-sections is applicable.
4. Deformations are small and shear deformations are negligible.
5. Due to adequate bracing, the possibility of lateral buckling and out-of-plane deformation does not exist.

Linear analysis of the frame by the matrix method is incorporated with elimination of yielded portions of the frame members, the presence of residual stresses, and the P-Δ effects. These refinements are incorporated to analyze nonlinear inelastic behavior of the tapered frames. The sign conventions for joint forces, joint displacements, end actions and forces are shown in Figure 2.2. The input format for cross-section data, material properties, load information, joint coordinates, and boundary conditions are explained in Appendix A.

The computer program operates in the following stages:

Step 1.

Cross-section properties along the members are computed, and the member stiffness matrices in local coordinates are assembled. All member stiffness matrices are then transformed to global coordinates and the stiffness matrix of the frame is assembled. The ISML library routine LINV2F (31) is used to invert the stiffness matrix.

Step 2.

The following equations, which are based on the moment-area principles, are used to compute fixed end actions of a member. Figure 2.12 shows a loaded fixed ended member and its equivalent moment diagram.

$$M_B \int_A^B \frac{x^2 dx}{Ix} + M_A \int_A^B \frac{(L-x)xdx}{Ix} + \frac{wL}{2} \int_A^B \frac{(L-x)x^2 dx}{Ix} = 0 \qquad (2.15)$$

$$M_B \int_B^A \frac{(L-x_1)x_1 dx_1}{Ix} + M_A \int_B^A \frac{x^2_1 dx_1}{Ix} + \frac{wL}{2} \int_B^A \frac{(L-x_1)x^2_1 dx_1}{Ix} = 0 \qquad (2.16)$$

$$R_A = \frac{wL}{2} - \frac{M_A - M_B}{L} \qquad (2.17)$$

$$R_B = \frac{wL}{2} + \frac{M_A - M_B}{L} \qquad (2.18)$$

The load matrix is formed from the applied joint loads, and equivalent joint forces are computed by Equations (2.15) to (2.18). The solution of the equations so generated gives joint rotations and displacements.

Step 3.

The P-Δ effect is accounted for by computing the transverse deflection of one end of a member with respect to the other end, and using this deflection and the axial force in the number, a pair of imaginary loads are computed. These

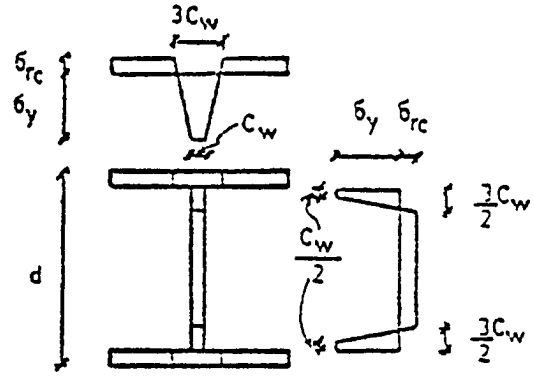

Figure 2.10 Trapezoidal Residual Stress Pattern

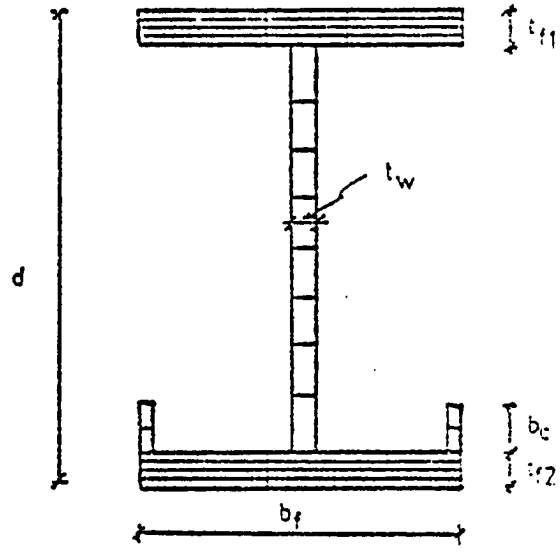

Figure 2.11 A Typical Cross-Section Divided in Small Segments

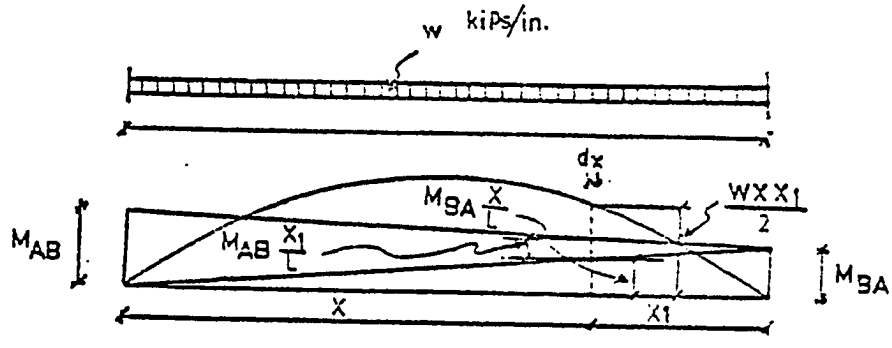

Figure 2.12 Fixed Ended Beam and Moment Diagram

loads are located at the ends of the member and replace the moment created by the eccentricity of axial load due to transverse deflection of the member. After every cycle of loading by a load increment or imaginary loads, the pair of imaginary loads for all members are computed and are included in the set of loads for next cycle. This iterative process was found to converge very fast since the computed imaginary loads are very small compared with the loads of the previous cycle of loading. The iteration stops when the summation of absolute values of imaginary loads of all members is less than 0.001 kips.

Step 4.

Multiplication of the member stiffness matrix and the member displacement matrix converted to the local coordinate systems gives the member end actions for the loading increment. These actions are added to the end actions of the previous increments to obtain the total end action. Using the total end actions and total member loads the bending moment and axial force at each cross-section of all members are computed for each loading or at each iteration. With the bending moment and axial force of a cross-section known, stresses in cross-section segments are calculated and yielded portions eliminated. New properties of all cross-sections are then computed for the next increment of loading or iteration.

Step 5.

If all the segments of a cross-section are eliminated, a hinge has formed at that location, e.g., the bending moment has reached the plastic moment capacity of the cross-section in the presence of axial force. If the formation of the hinge occurs because of a real load increment, computed values related to this increment of loading are deleted, and a smaller increment is used to ensure a more accurate result.

The magnitude of the hinge forming load is considered to be determined with adequate accuracy if the hinge forms during application of a small load increment or during iteration for P-Δ effects. If the number of hinges is not sufficient to define a mechanism, the analysis process continues until a mechanism is found.

The above process for determining the collapse load is a lower bound procedure. The existence of a mechanism is an upper bound solution, hence, the solution is unique, and the maximum load computed is the ultimate load of the frame.

2.9 Computer Program Capability

The program has the capability for analyzing a one story tapered or prismatic gable frame in both the elastic and plastic ranges with consideration of P-Δ effects, residual stresses and localized yielding.

The frame may be loaded by two load sets. Loads in the first set are applied to the frame in one cycle of loading followed by iteration for P-Δ effects. The second set may then be applied incrementally. If either of the two sets is not required, zero loads are used for that set. The flow chart of the computer program is shown in Figure 2.13.

2.10 Computer Analysis Results

Several frames were analyzed to verify the analysis technique and the results are summarized as follows:

Number of elements in members

Three frames with maximum tapering angles of less than 4° were analyzed with different element patterns in the members. For each analysis the loading remained the same but the number of elements in each member was varied. Figure 2.14 shows the results of the analysis of one of the frames. The results for the other two frames are similar. This figure shows that the centerline deflection increases with the increasing number of elements, but that the rate of increase is much smaller when the number of elements per member is between 15 and 25. It also shows that there is little change when the number of elements is increased from 20 to 25. Taking computer storage limitation into consideration, the optimum number of elements seems to be 20 and this number was used for all members of frames analyzed in this study.

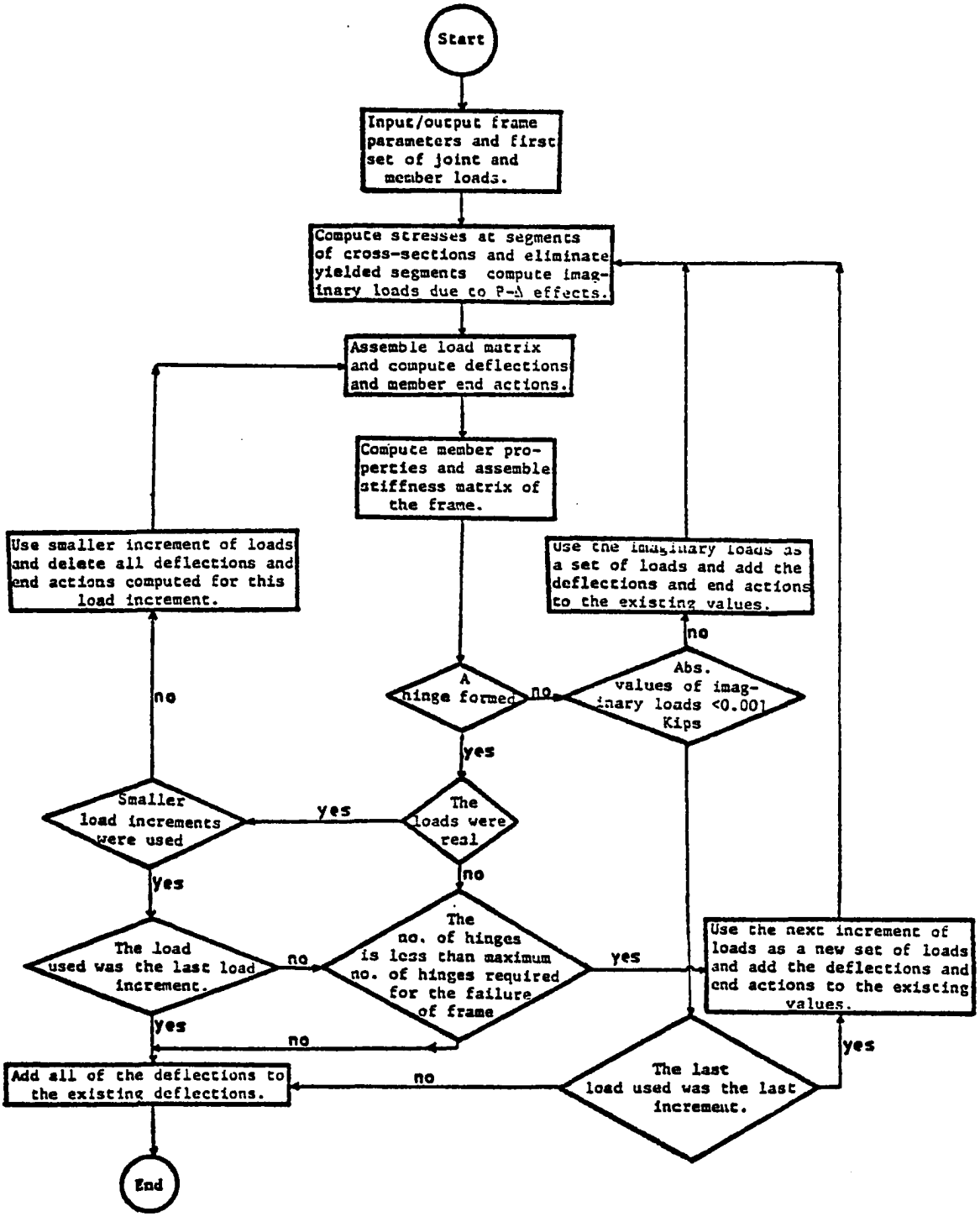

Figure 2.13 Flow Chart of the Computer Program

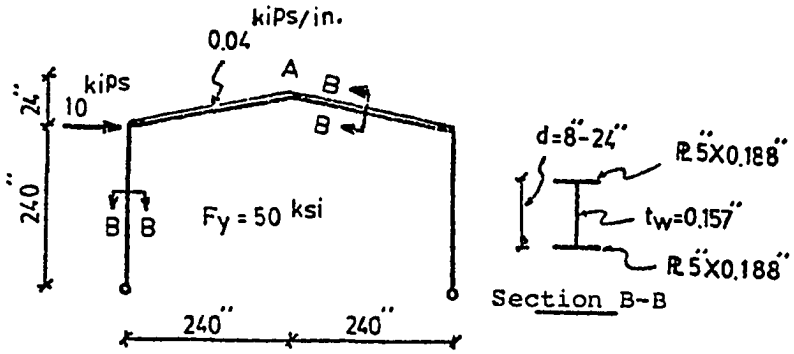

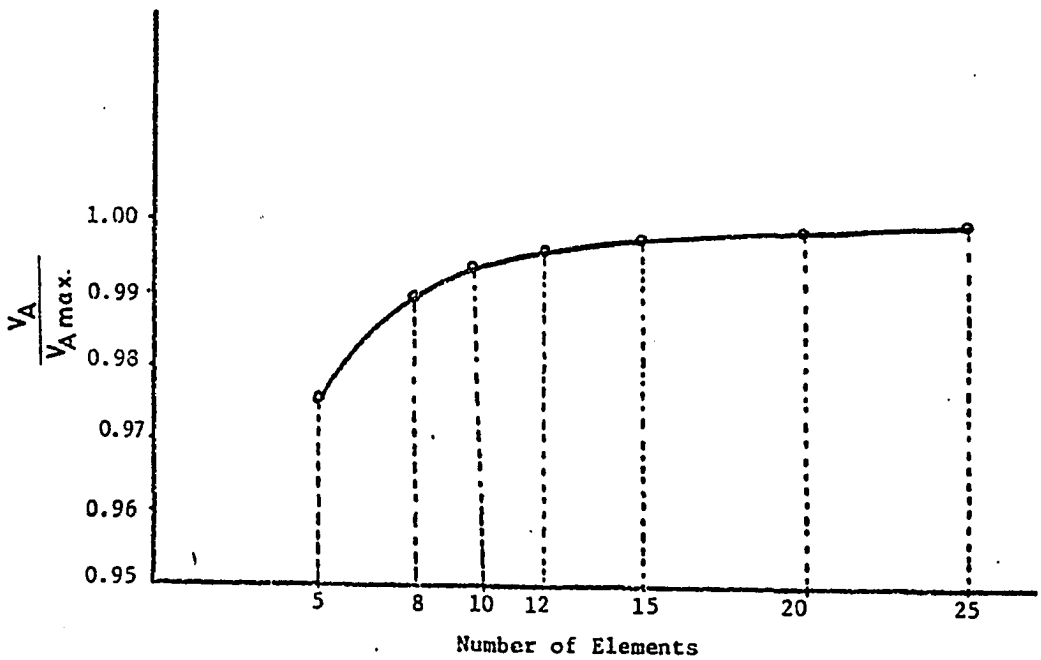

Figure 2.14 Variation of Midspan Deflection Versus Number of Member Elements

P-Δ Effects

Figure 2.15 shows a single story frame subjected to horizontal and vertical loads. Also shown are load-deflection curves for the frame. The upper broken line is from a first order analysis and the solid line is from a second order analysis. The load-deflection curves show that the second order effect decreases the ultimate load capacity of the frame and increases the deflections.

Comparison of first and second order analysis results for several frames showed that the behavior of a frame, under either gravity or combined gravity and lateral loads, cannot be adequately predicted by a first order analysis. This is especially true when the axial load in a member is significant. Figure 2.16 shows a frame loaded by lateral load only. Because of the absence of gravity loads, the axial force in the members is not significant and the load-deflection curves from first and second order analyses do not vary significantly.

Residual Stress Effects

To study the effect of residual stress block width, four frames were analyzed, with five different residual stress patterns. The basic pattern was assumed to be rectangular, Figure 2.8(b), and the ratio of tension block width to flange width varied. The results of the analyses were similar for all frames. Figures 2.17 and 2.18 show the load-deflection relation of two of the frames. As the tension

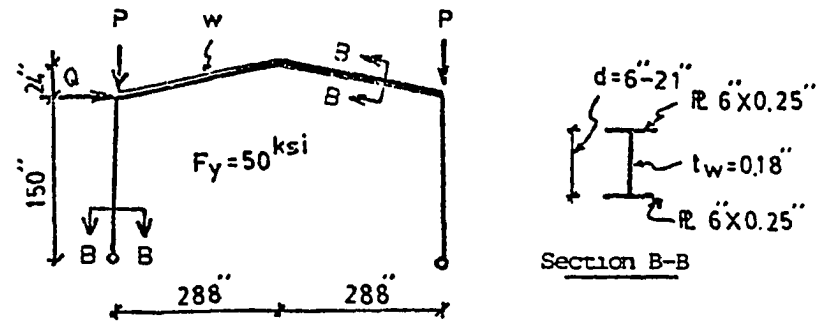

------ First order analysis results

——— Second order analysis results

P = 10Q

w = 0.1Q kips/in.

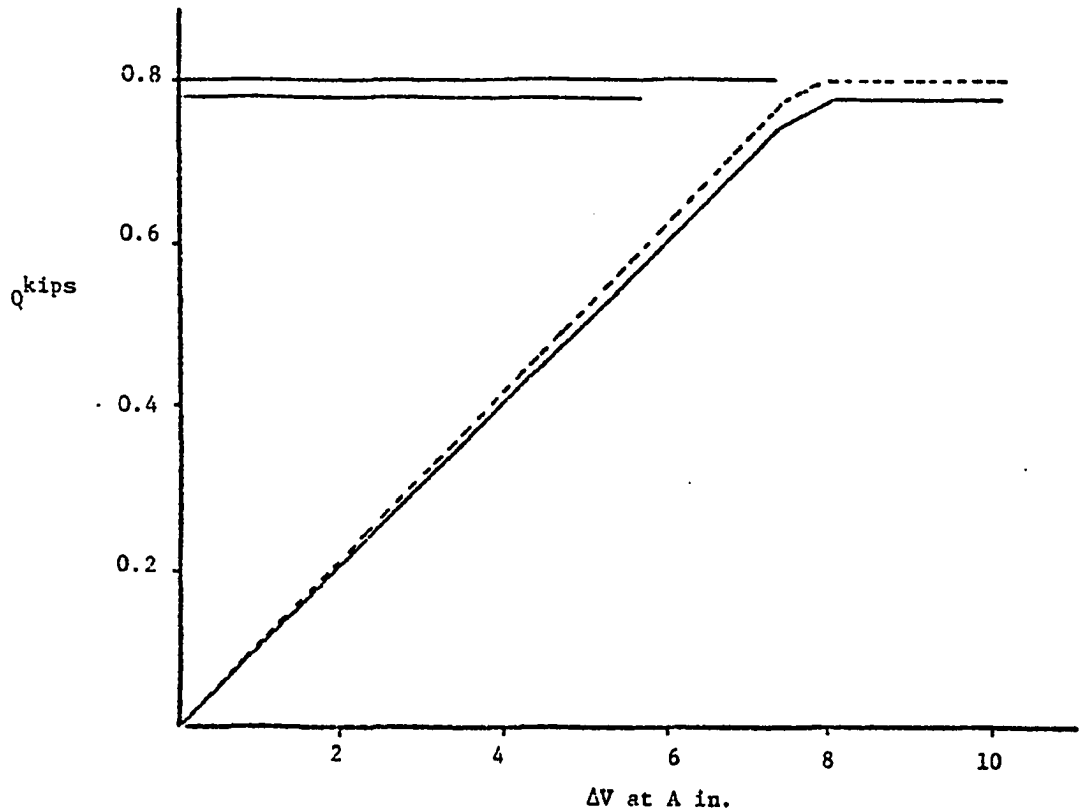

Figure 2.15 Load-Deflection Curves for First and Second Order Analysis of the Frame Shown Above

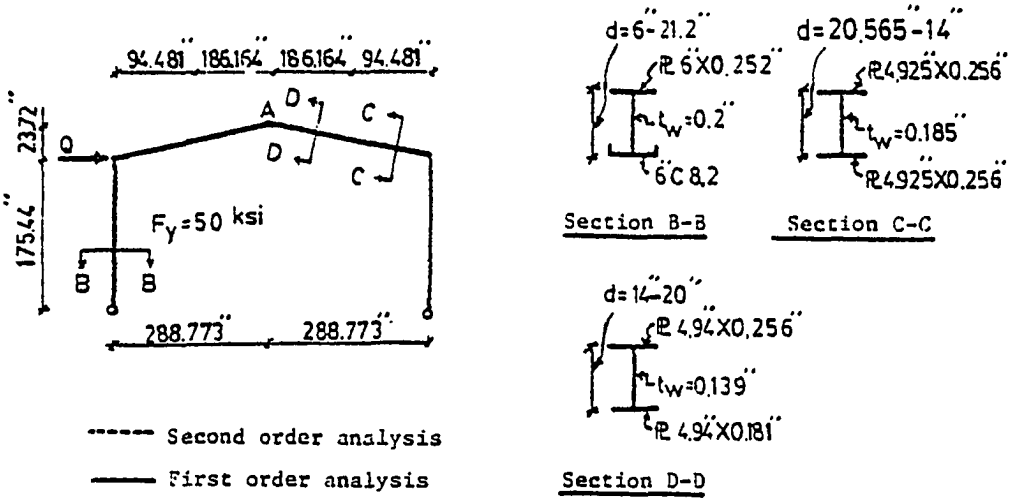

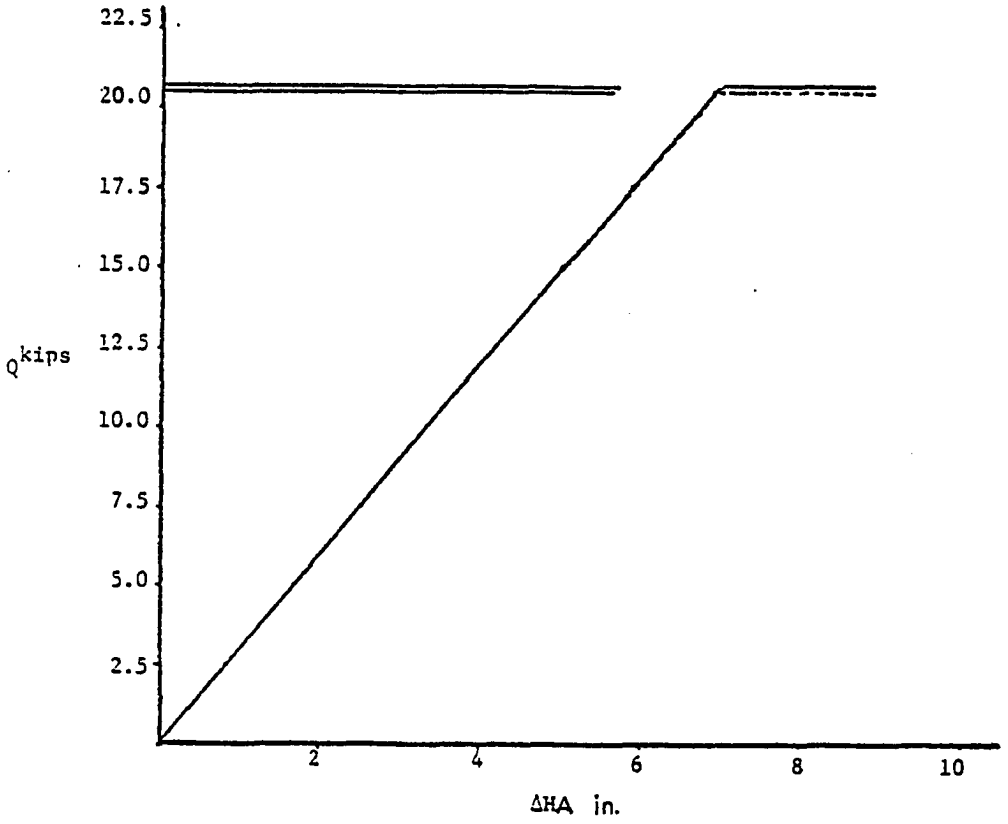

Figure 2.16 Load-Deflection Curves for First and Second Order Analysis of a Frame for Lateral Loading

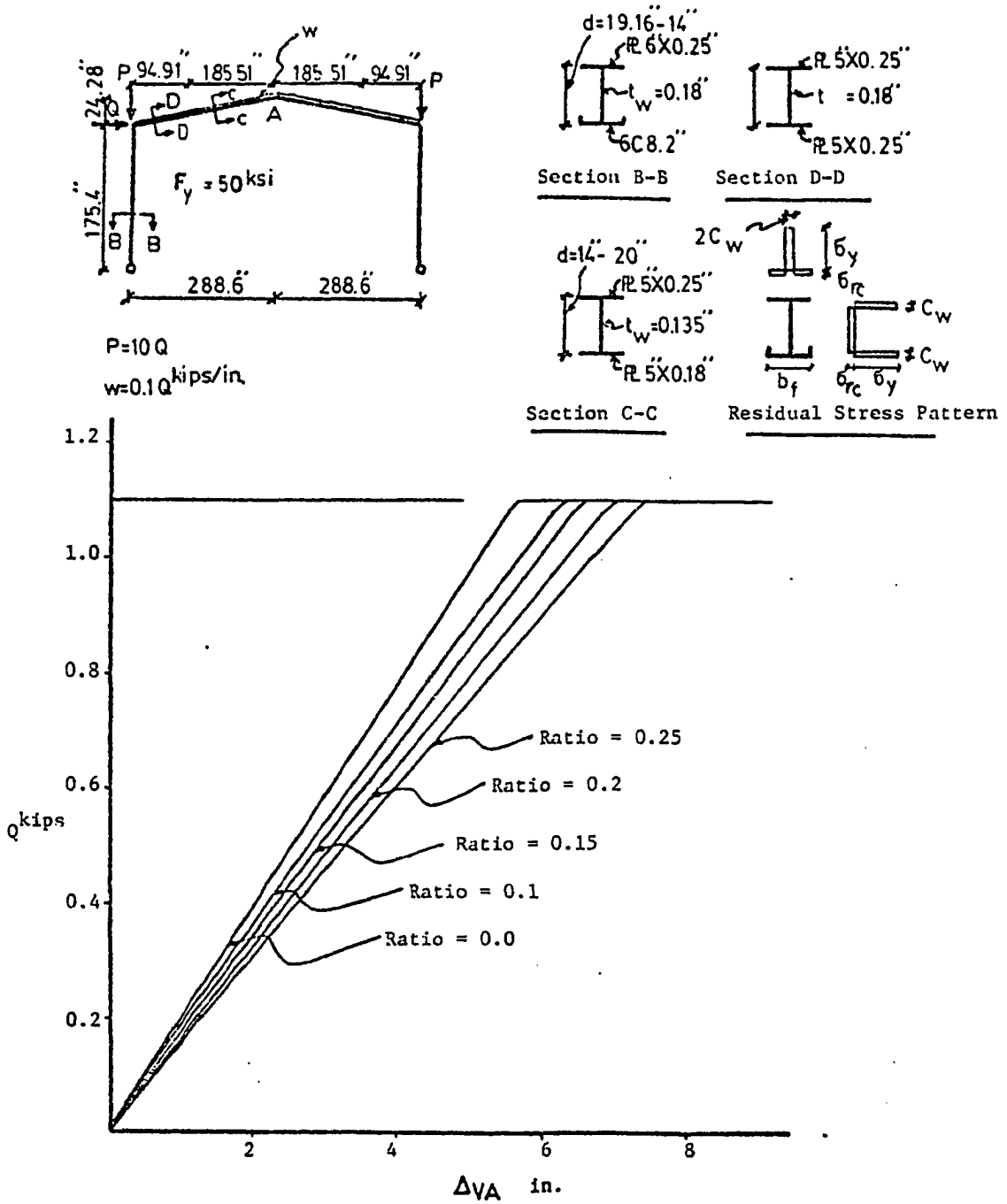

Figure 2.17 Load-Deflection Curves of a Frame for Different Tension Block Width to Flange Width Ratios

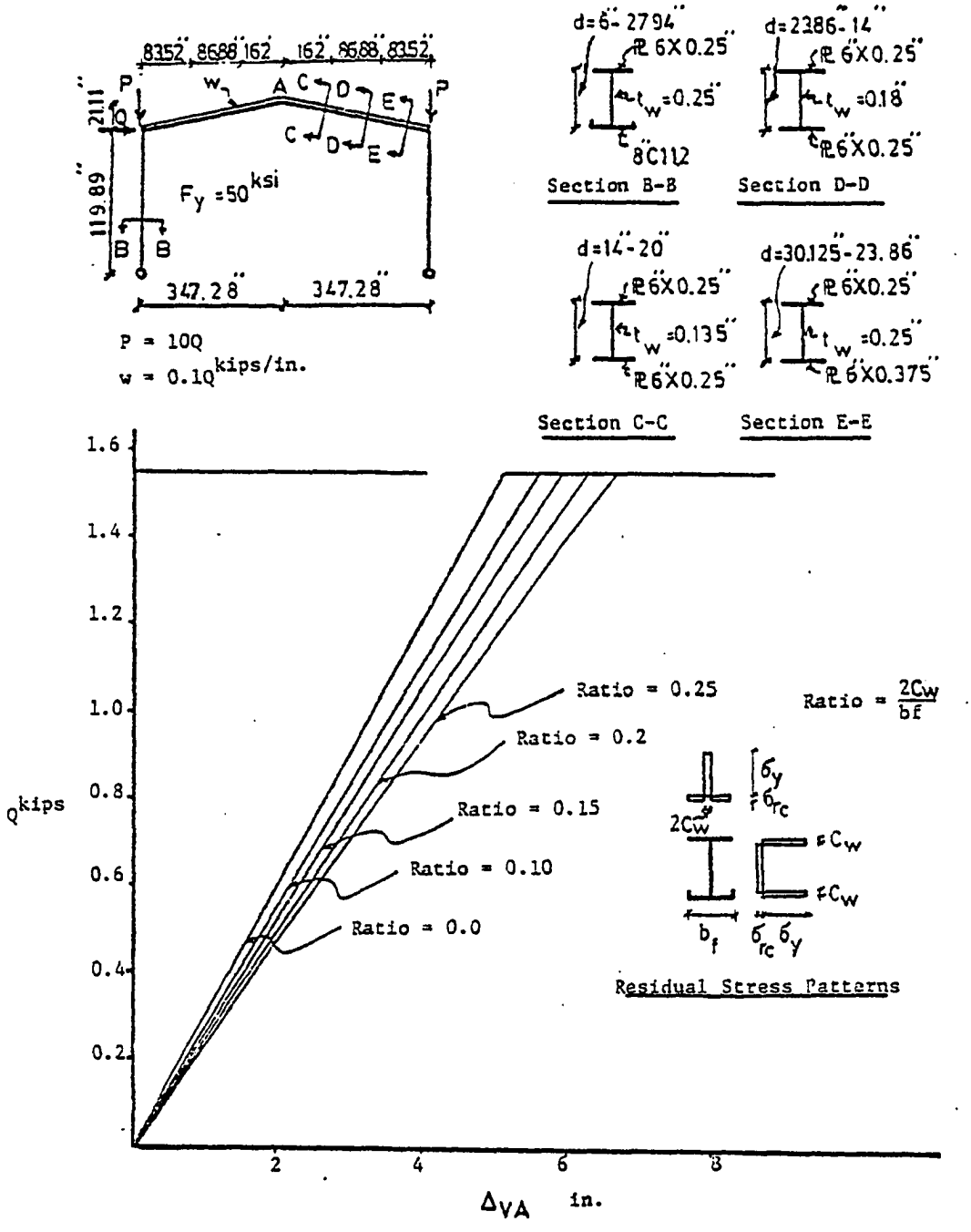

Figure 2.18 Load-Deflection Curves of a Frame for Different Tension Block Width to Flange Width Ratios

block width increases, the stiffness of the members decreases which, in turn, causes an increase in deflection. This effect, however, does not significantly lower maximum load carrying capacity of the frame. When the width of the tension block increases to about 25% of the flange width, the maximum load capacity decreased by only 2.5% in two of the frames and was unchanged in the other two frames. The decrease is attributed to the increase of the second order moments due to increased deflections after the first hinge forms.

In order to study the effect of different types of residual stress patterns on load-deflection curves, the same frames were analyzed using the other two residual stress patterns, Figures 2.9 and 2.10. The results of these analyses show that the deflections for the trapezoidal pattern are less than the deflections which resulted in the frames with rectangular pattern, Figure 2.19 . In both cases the loads were the same, and the deflections for the triangular pattern were less than the other cases for the same loads. Figure 2.19 shows the load-deflection curves for the three patterns which have the same ratio of the tension block to flange width. The maximum load capacity of the frame with rectangular residual pattern decreased by 2% over the same frame with the same ratio but with triangular pattern. This is because of increased deflections of the first case over the second case after the formation of first hinge.

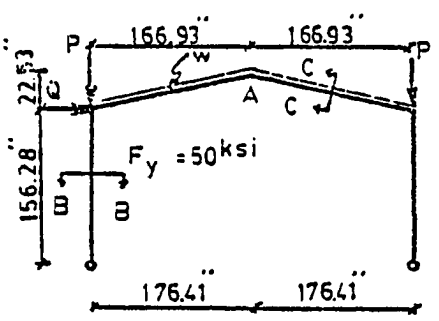

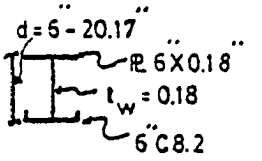

Section B-B

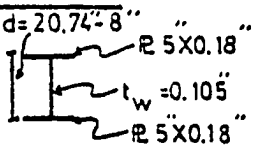

Section C-C

——— Rectangular residual stress pattern

..... Trapezoidal residual stress pattern

- - - - - - Triangular residual stress pattern

p = 10 Q

w = 0.1 Q kips/in.

Ratio = $\frac{2Cw}{bf}$ = 0.2

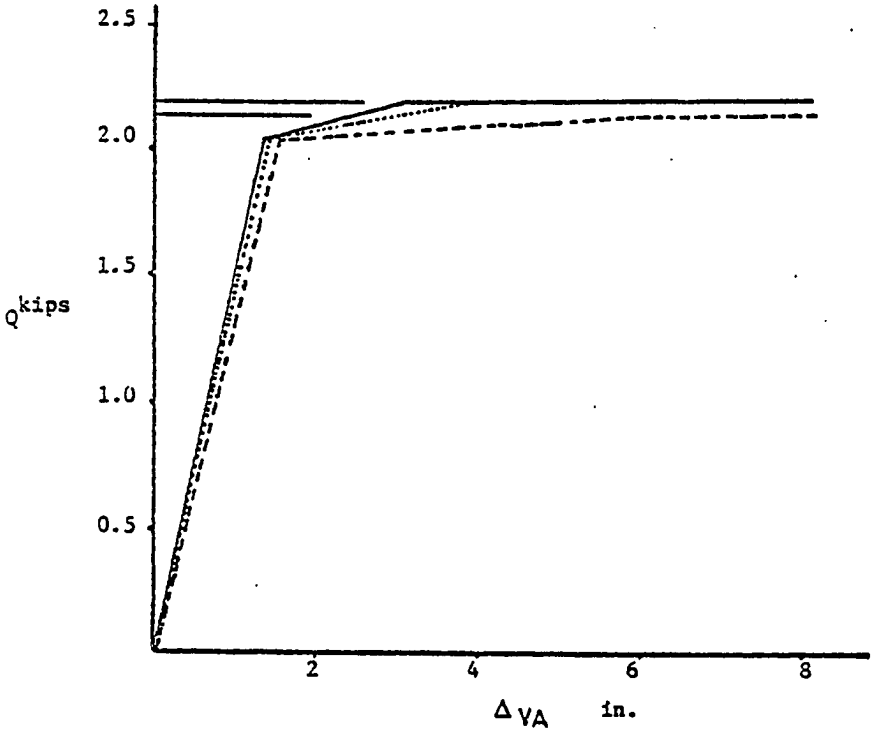

Figure 2.19 Load-Deflection Curves for Three Residual Stress Patterns of Cross-Sections

Effect of Connection Reinforcement

The frame tested at Lehigh University (11) was also analyzed in this study. Assuming that no hinge can form closer than a distance equal to the depth of the column (5.12 inches) on the column to the center of reinforced connections (connection of column to beam) the maximum load was found to be 16.8 kips. In Ref. 11, for a slightly shorter distance (5 inches), the maximum lateral load was 16.9 kips, and in Ref. (12), the maximum lateral load was computed to be 16.75 kips for a distance of 5.225 inches. When the connection reinforcement effect was not considered, the maximum load computed by the computer program was 15 kips. The results of the computer analysis and the results of theoretical and experimental analysis of Ref. (11) are plotted in Figure 2.20.

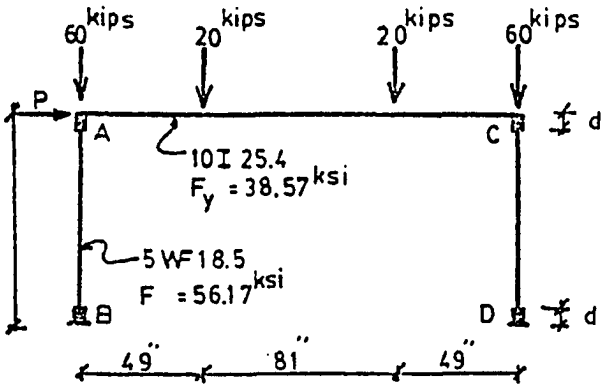

——— Theoretical results of Lehigh U.

------ Experimental results of Lehigh U.

——— Computer program results

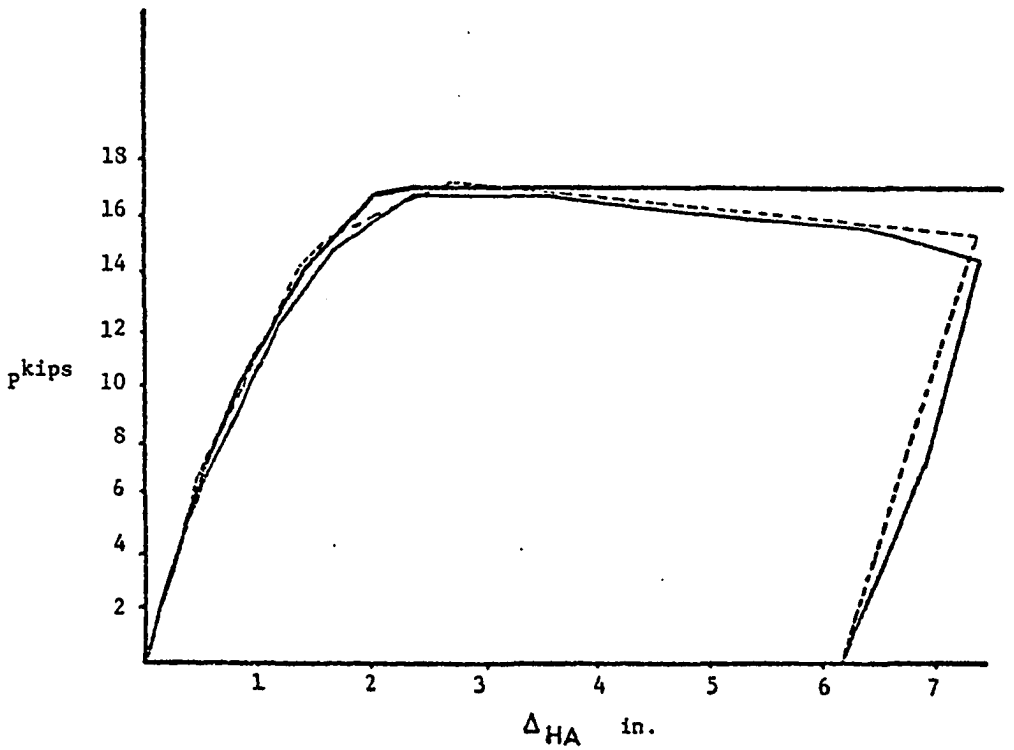

Figure 2.20 Load-Deflection Curves for Lehigh Test Frame

CHAPTER III

TRIAL AND ERROR ANALYSIS OF TAPERED FRAMES

3.1 General

Manual techniques to estimate the load-deflection relationship of tapered gabled frames have not been extensively studied. However, Cheong-Siat-Moy (23,24,25,26,27,28) has thoroughly investigated inelastic sway buckling, secondary effects, and sidesway deflection of unbraced multistory prismatic frames, and Le-Wu-Lu (29), and Liapunov (30) have studied the ultimate strength of primatic steel frames. Procedures discussed in Chapter II, for consideration of residual stresses and elimination of yielded portions of cross sections, incorporated with methods used in the above references, are adapted here to develop a manual technique for the analysis of single bay tapered gabled frames with hinged supports. In the proposed method, slope deflection equations are used to develop formulas for computation of deflections using a trial and error procedure.

3.2 Basic Concepts

As in the previous method (Chapter II), the moment area principle is employed for computation of member stiffness. Integration along members is performed using small elements of the member which are assumed prismatic with constant moment of inertia. The loading is considered in two stages and incrementally increased, until the frame fails due to formation of a plastic mechanism or sidesway buckling.

For each increment of loading, end actions of all members are computed and the stress distribution at all cross-sections obtained. With consideration of residual stresses, the yielded portions of all cross-sections are eliminated and new properties calculated. These properties are then used for reanalysis with the same load increment. The iteration continues until the variation of properties converge. The process of eliminating yielded portions is discussed in Chapter II.

3.3 Development of the Analysis Method

3.3.1 First Stage Loading

The frame CBADE of Figure 3.1, with the following definitons, is used for the analysis:

D_L, D_R = Inclination of columns

e = Rise of beam from the center of connection of beam and column to the ridge line (pitch of roof)

h = Height of column

H = Distance from the center of support to midspan

L_c = Length of column

L_b = Length of beams

θ = Slope of beams.

The frame is loaded with a concenterated horizontal load Q_{T1} at B, a pair of concenterated vertical loads P_{t1}, at B and D, and a uniform load W_{T1} on the beams. It is assumed that the frame is hinged at both supports and all other connections are rigid. The column and beam lengths are:

$$L_c = \sqrt{h^2+D_L} \tag{3.1}$$

$$L_b = \sqrt{(H-D_L)^2+ e^2} \tag{3.2}$$

Figure 3.2 shows the deflected shape of the frame; horizontal deflection Δ_{BT1} and Δ_{DT1} at B and D and vertical deflection V_{AT1} at A.

The vertical reactions P_{CT1}, P_{ET1} at C and E, considering the effect of deflections, are:

$$P_{CT1} = \frac{-P_{T1}(2H-D_L-\Delta_{BT1}) - P_{T1}(D_R-\Delta_{DT1}) - 2W_{T1}L_b(H-\Delta_{AT1}) - Q_{T1}h}{2H} \tag{3.3}$$

$$P_{ET1} = -2P_{T1} - 2W_{T1}L_b - P_{CT1} \tag{3.4}$$

h = Height of column

H = Distance from the center of support to midspan

L_c = Length of column

L_b = Length of beams

θ = Slope of beams.

The frame is loaded with a concenterated horizontal load Q_{T1} at B, a pair of concenterated vertical loads P_{t1}, at B and D, and a uniform load W_{T1} on the beams. It is assumed that the frame is hinged at both supports and all other connections are rigid. The column and beam lengths are:

$$L_c = \sqrt{h^2+D_L} \tag{3.1}$$

$$L_b = \sqrt{(H-D_L)^2+ e^2} \tag{3.2}$$

Figure 3.2 shows the deflected shape of the frame; horizontal deflection Δ_{BT1} and Δ_{DT1} at B and D and vertical deflection V_{AT1} at A.

The vertical reactions P_{CT1}, P_{ET1} at C and E, considering the effect of deflections, are:

$$P_{CT1} = \frac{-P_{T1}(2H-D_L-\Delta_{BT1}) - P_{T1}(D_R-\Delta_{DT1}) - 2W_{T1}L_b(H-\Delta_{AT1}) - Q_{T1}h}{2H} \tag{3.3}$$

$$P_{ET1} = -2P_{T1} - 2w_{T1}L_b - P_{CT1} \tag{3.4}$$

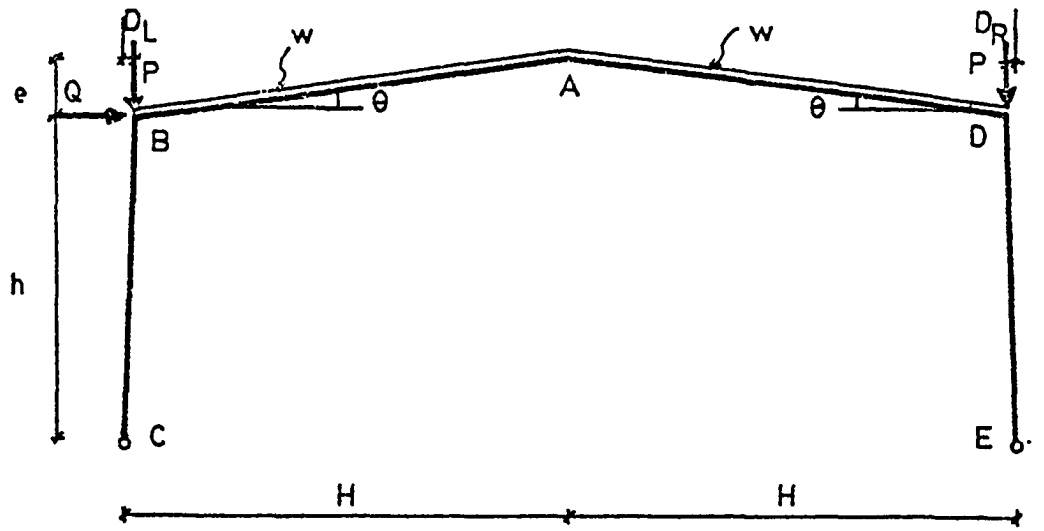

Figure 3.1 Gable Frame Geometry and Loading

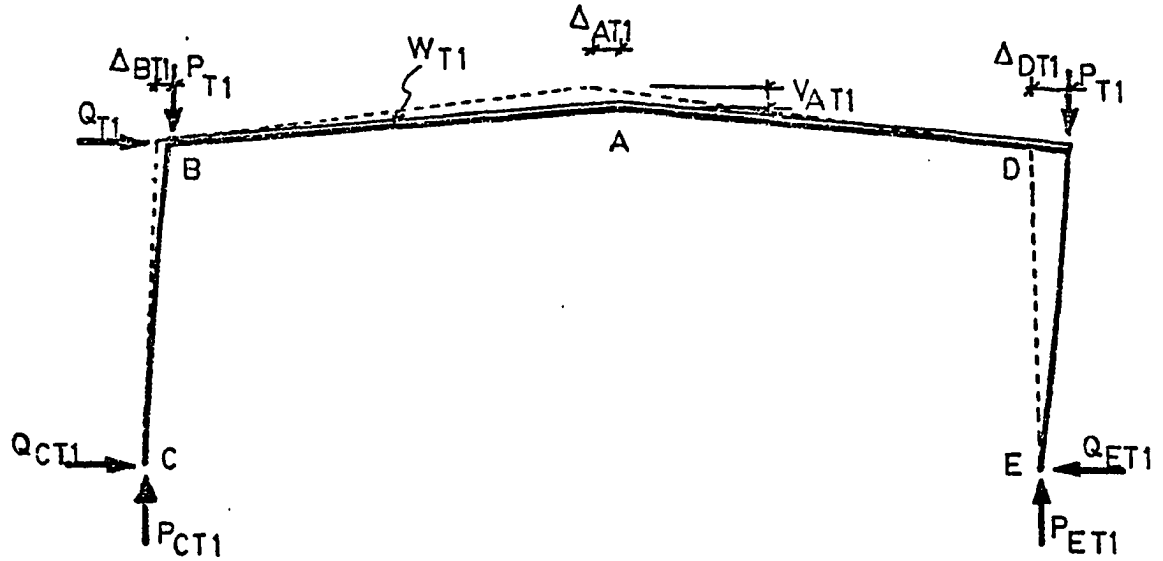

Figure 3.2 Assumed Deflected Shape of Frame

where

$$\Delta_{AT1} = (\Delta_{BT1} + \Delta_{DT1})/2 \tag{3.5}$$

The subscript T1 denotes total load, reaction, or deflection from the start of loading of stage one; subscript 1 indicates the additional loads, reactions, or deflections caused by the last increment of loads.

Since the frame is indeterminate, Q_{c1} and Q_{E1} are computed by trial and error: first a value is assumed for Q_{c1} and then Q_{E1} is computed from

$$Q_{E1} = -Q_1 - Q_{c1} \tag{3.6}$$

The end column and beam moments are then

$$M_{Bc} = -P_{c1}D_L - P_{CT1}\Delta_{B1} + Q_{C1}h \tag{3.7}$$

$$M_{BA} = M_{BC} \tag{3.8}$$

$$M_{AB} = P_{c1}H + P_{CT1}\Delta_{A1} - Q_{c1}(h+e+V_{A1}) + P_1(H-D_L - \frac{\Delta_{BT1}-\Delta_{DT1}}{2}) - Q_1(e+V_{AT1}) + \frac{w_1 L_b}{2}(H-D_L - \frac{\Delta_{BT1}-\Delta_{DT1}}{2}) \tag{3.9}$$

$$M_{AD} = M_{AB} \tag{3.10}$$

$$M_{DE} = P_{E1}D_R - Q_{E1}h + P_{ET1}\Delta_{D1} \tag{3.11}$$

$$M_{DA} = M_{DE} \tag{3.12}$$

The above moments are positive when the inside flange is in compression, otherwise, they are negative.

Based on an assumed value of Q_{c1}, the horizontal deflection of B, with respect to D, is computed by two different procedures, which will be discussed later, and the results compared. If the computed values are equal or are sufficiently close, the assumed value of Q_{c1} is taken as the actual horizontal reaction at c due to additional load increment, otherwise another iteration is required. Once convergence is obtained final deflections, reactions, and end actions are computed. Using these end actions, bending moments and axial force of all cross-sections are found and the stress distribution at all cross-sections obtained. Combining these stresses with residual stresses, yielded portions are eliminated, and new properties of all cross-sections calculated. If no change of properties occurred due to addition of the last load increment, the loading of the frame continues with the next load increment, otherwise, the deflections, moments, and axial forces for the load increment are computed using new properties. The stage of loading ends when all segments at a cross-section are yielded. A hinge is then assumed at the location of this cross section.

The procedures for computing the horizontal deflectic of B with respect to D (Figure 3.2) are as follows:

a) The frame is divided into two subassemblages. A freebody diagram of the deflected shape of left subassemblage is shown in Figure 3.3. The deflection and rotations of this subassemblage are: V_{A1} vertical deflection at A, Δ_{B1} horizontal deflection at B, θ_{BC}, θ_{BA} rotations of BA and BC at their end B. The rotation of column BC due to Δ_{B1} is

$$\frac{\Delta_{B1}}{h} = -\theta_{BC}-\theta_{BA}-\frac{V_{A1}}{H-D_L} \tag{3.13}$$

where θ_{BC} and θ_{BA} are found from

$$\theta_{BC} = \frac{M_{BC}}{EL_C^2} \int_C^B \frac{x^2dx}{I_x} \tag{3.14}$$

and

$$\theta_{BA} = \frac{M_{BA}}{EL_b^2} \int_A^B \frac{x^2dx}{I_x} + \frac{M_{AB}}{EL_b^2} \int_A^B \frac{(L_b-x)xdx}{I_x} +$$

$$\frac{w_1\cos\theta}{EL_b} \int_A^B \frac{(L_b-x)x^2dx}{2I_x} \tag{3.15}$$

substituting θ_{BC} and θ_{BA} into equation 3.13 results in:

$$\frac{\Delta_{B1}}{h} = -\frac{M_{BC}}{EL_C^2}\int_C^B \frac{x^2dx}{I_x} - \frac{M_{BA}}{EL_b^2} \int_A^B \frac{x^2dx}{I_x} - \frac{M_{AB}}{EL_b^2} \int_A^B$$

$$\frac{(L_b-x)xdx}{I_x} - \frac{w_1\cos\theta}{EL_b} \int_A^B \frac{(L_b-x)x^2dx}{I_x} - \frac{V_{A1}}{H-D_L} \tag{3.16}$$

Substituting M_{BC} and M_{BA} from equations 3.7, 3.8, and 3.9 into equation 3.16 yields:

$$\frac{\Delta_{B1}}{h} = \frac{(P_{C1}D_L+P_{CT1}\Delta_{B1}-Q_{C1}h)}{EL_C^2}\int_C^B \frac{x^2dx}{I_x} + \frac{(P_{C1}D_L+P_{CT1}\Delta_{B1}-Q_{C1}h)}{EL_b^2}\int_A^B \frac{x^2dx}{I_x} - \frac{M_{AB}}{EL_b^2}\int_A^B \frac{(L_b-x)xdx}{I_x} - \frac{w_1\cos\theta}{EL_b}\int_A^B \frac{(L_b-x)x^2dx}{2I_x} - \frac{V_{A1}}{H-D_L} \tag{3.17}$$

Rearranging this equation gives

$$\frac{\Delta_{B1}}{h} - \frac{P_{CT1}\Delta_{B1}}{EL_C^2}\int_C^B \frac{x^2dx}{I_x} - \frac{P_{CT1}\Delta_{B1}}{EL_b^2}\int_A^B \frac{x^2dx}{I_x} = \frac{(P_{C1}D_L-Q_{C1}h)}{EL_C^2}\int_C^B \frac{x^2dx}{I_x} + \frac{(P_{C1}D_L-Q_{C1}h)}{EL_b^2}\int_A^B \frac{x^2dx}{I_x} - \frac{M_{AB}}{EL_b^2}\int_A^B \frac{(L_b-x)xdx}{I_x} - \frac{W_1\cos\theta}{EL_b} - \int_A^B \frac{(L_b-x)x^2dx}{2I_x} - \frac{V_{A1}}{H-D_L} \tag{3.18}$$

Defining

$$\alpha = \int_C^B \frac{x^2 dx}{I_x} \tag{3.19}$$

$$\beta = \int_A^B \frac{x^2 dx}{I_x} \tag{3.20}$$

$$\delta = \int_A^B \frac{(L_b - x)\, x\, dx}{I_x} \tag{3.21}$$

$$\rho = \int_A^B \frac{(L_b - x)\, x^2 dx}{2I_x} \tag{3.22}$$

Equation 3.18 can be written in a more simple form as

$$\Delta_{B1} = \frac{(P_{C1}D_L - Q_{C1}h)(\alpha L_b^2 + \beta L_C^2)h - hL_C^2\delta M_{AB} - EL_C^2L_b^2h\left(\frac{V_{A1}}{H-D_L}\right) - \rho w_1 hL_C^2 L_b \cos\theta}{EL_C^2L_b^2 - P_{CT1}h(\alpha L_b^2 + \beta L_C^2)} \tag{3.23}$$

The Freebody diagram of the right subassemblage is shown in Figure 3.4. Using the above procedure the horizontal deflection Δ_{D1} is given by:

$$\Delta_{D1} = \frac{(-P_{E1}D_R - Q_{E1}h)(\alpha L_b^2 + \beta L_C^2)h + hL_C^2\delta M_{AD} + EL_C^2L_b^2h\left(\frac{V_{A1}}{H-D_R}\right) + \rho w_1 hL_C^2 L_b \cos\theta}{EL_C^2L_b^2 - P_{ET1}(\alpha L_b^2 + \beta L_C^2)} \tag{3.24}$$

Since the axial force in the beams is small and the maximum deflection of beams, compared to their length and depth are small, their second order effects are negligible,

and the value of V_{AT1} can be computed from

$$V_{AT1} = \sqrt{L_b^2 - \left(\frac{2H - D_R - D_L + \Delta_{DT1} - \Delta_{BT1}}{2}\right)} - e \qquad (3.25)$$

The difference between values of V_{AT1} before and after application of the last load increment is the same as V_{A1}, which is used in equations 3.23 and 3.24

or

$$V_{A1} = V_{AT1} \text{ after } - V_{AT1} \text{ before} \qquad (3.26)$$

where V_{AT1} after = the total deflection of midspan computed after application of the last load increment, and

V_{AT1} before = the total deflection of midspan computed before application of the last load increment.

Equations 3.23, 3.24 and 3.25 are dependent on each other, and the computation of VA_1, Δ_{B1} and Δ_{D1} is iterative. First, an approximate value is assumed for V_{A1} in equations 3.23 and 3.24, then the computed values of Δ_{D1} and Δ_{B1} are used to compute V_{A1} by equation 3.25. If this second value of V_{A1} is equal or within an acceptable range of difference of the value of V_{A1} used in equations 3.23 and 3.24, the iteration is completed, otherwise, a new value for V_{A1} is assumed and the

process continues until convergence. The procedure for selecting values of V_{A1} is explained in section 3.4.

The horizontal deflection of B with respect to D is then computed by:

$$\Delta_1 = \Delta_{D1} - \Delta_{B1} \tag{3.27}$$

which is used to compare with the result of the next procedure.

b) Girder BAD is separated from the frame, as shown in Figure 3.5. Using the slope deflection method and moment area principle, transverse deflections at B of member AB with respect to A and D of member AB with respect to A are:

$$BB' = \frac{M_{BA}}{EL_b}\int_B^A \frac{(L_b-x)x\,dx}{I_x} + \frac{M_{AB}}{EL_b}\int_B^A \frac{x^2dx}{I_x} + \frac{w_1\cos\theta}{E}\int_B^A \frac{(L_b-x)x^2dx}{2I_x} \tag{3.28}$$

and

$$DD' = \frac{M_{DA}}{EL_b}\int_D^A \frac{(L_b-x)x\,dx}{I_x} + \frac{M_{AD}}{EL_b}\int_D^A \frac{x^2dx}{I_x} + \frac{w_1\cos\theta}{E}\int_D^A \frac{(L_b-x)x^2dx}{2I_x} \tag{3.29}$$

Integrations of the above equations are performed on small elements along the beams as in the previous method (Chapter II).

Using BB′ and DD′ computed by equations 3.28 and 3.29, the horizontal deflection of B with respect to D is:

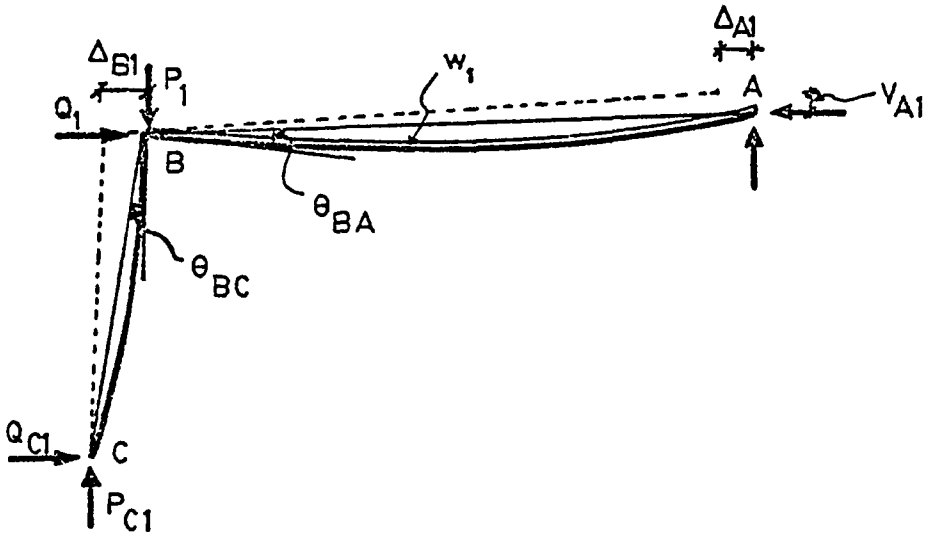

Figure 3.3 Deflected Shape of Left Subassemblage

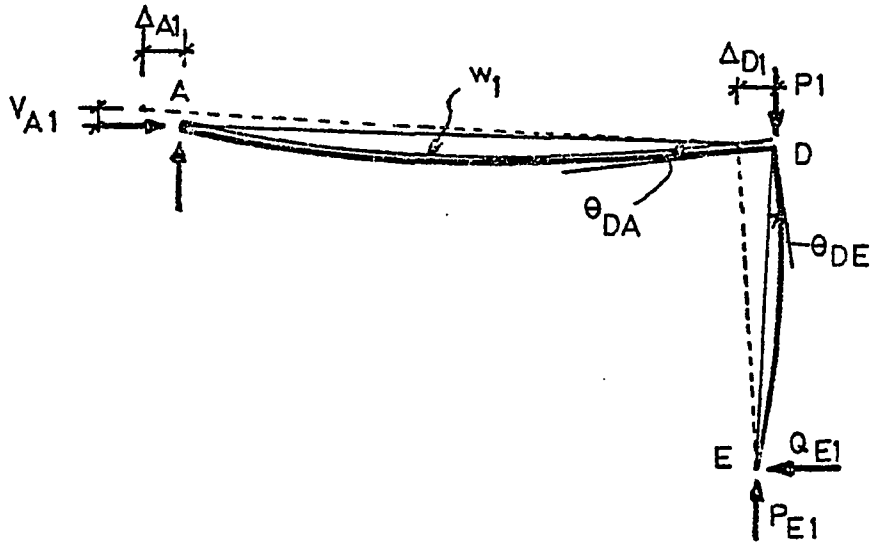

Figure 3.4 Deflected Shape of Right Subassemblage

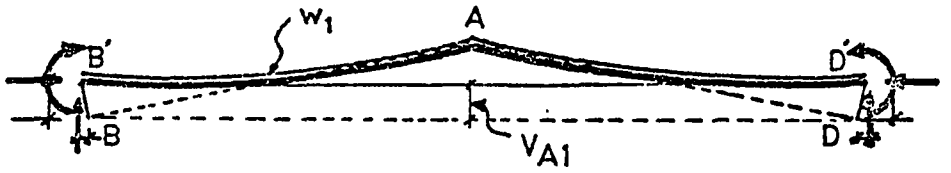

Figure 3.5 Freebody Diagram of Rafter BAD

$$\Delta_1 = -(DD' + BB') \sin\theta \qquad (3.30)$$

The value of Δ_1 computed by equations 3.27 and 3.30 are compared. If the difference of these two values is within an acceptable range the computed values of deflections are correct, otherwise, a new value for reactions are assumed and the process repeated. The procedure for selecting values of horizontal reaction is explained in section 3.4.

3.3.2 Second Stage Loading

In this stage of loading, the frame is determinate because of the additional hinge formed at the end of the first stage. Figure 3.6 shows the frame in second stage of loading with an assumed hinge at point 0. The length of the portion of the beam between 0 and A is

$$L_{0A} = \sqrt{x_{0A}^2 + y_{0A}^2} \qquad (3.31)$$

where X_{0A} and y_{0A} are the horizontal and vertical projections of 0A in the original position of the frame. Summation of moments produced by the loads in the second stage at point 0 is equal to zero, therefore, for subassemblage CBO,

$$Q_{C2}(h+e-y_{0A}+V_{0T}) - P_{C2}(H-x_{0A}+\Delta_{0T}) + Q_2(e-y_{0A}+V_{0T}) - P_2(H-x_{0A}-D_L+\Delta_{0T}-\Delta_{BT}) - w_2(L_b-L_{0A})\left(\frac{H-x_{0A}-D_L+\Delta_{0T}-\Delta_{BT}}{2}\right) + Q_{CT1}V_{02} - P_{CT1}\Delta_{02} + Q_{T1}V_{02} - P_{T1}(\Delta_{02}-\Delta_{B2}) - w_{T1}(L_b-L_{0A})\left(\frac{\Delta_{02}-\Delta_{B2}}{2}\right) = 0 \qquad (3.32)$$

and for subassemblages OADE

$$Q_{E2}(h+e-y_{0A}+V_{0T})+P_{E2}(H+x_{0A}-\Delta_{OT})+P_2(H+x_{0A}-D_R-\Delta_{0T}+\Delta_{DT}) +$$

$$w_2(L_b+L_{0A})\left(\frac{H+x_{0A}-D_R-\Delta_{0T}+\Delta_{DT}}{2}\right)+Q_{ET1}V_{02}-P_{ET1}\Delta_{02} = 0. \qquad (3.33)$$

From summation of vertical forces

$$P_{C2}+P_{E2}+2P_2+2L_bw_2 = 0 \qquad (3.34)$$

From summation of horizontal forces

$$Q_{C2}+Q_{E2}+Q_2 = 0 \qquad (3.35)$$

Where V_{0T} and Δ_{OT} are the total vertical and horizontal deflections at point 0, Δ_{BT} is the total horizontal deflection at B and P_2,Q_2, w_2, Q_{C2}, Q_{E2}, P_{C2} and P_{E2} are the loads and reactions introducted in the second stage, and, finally, Δ_{02}, Δ_{B2}, V_{02} are the deflections at 0 and B for the second stage of loading. Since the change of geometry due to bowing of Beam AB is negligible, it is assumed to be straight at the end of the first stage. Therefore, the vertical and horizontal deflections at 0 can be computed by proportioning the deflections at A and B from the end of the first stage, and adding the deflections of the second stage. Solving equations 3.32 to 3.35 reactions, Q_{C2}, Q_{E2}, P_{C2} and P_{E2} are computed.

Figure 3.7 shows the deflected shape of frame CBOADE including the two subassemblages, CBO and OADE. Figure 3.8 shows the deflected shape of beam BO of subassemblage CBA fixed at B in order to compute the deflections at 0 without consideration of the rotation of joint B. The deflections are

$$V_{0A} = -\theta_{B0}(H-x_{0A}-D_L) \tag{3.36}$$

$$\Delta_{0A} = +\theta_{B0}(e-y_{0A}) \tag{3.37}$$

where V_{0A} and Δ_{0A} are deflections at point 0, when joint B is fixed, and θ_{B0} is the rotation of B with respect to 0´. The rotation θ_{B0} is computed from

$$\theta_{B0} = \frac{+M_{B0}}{E(L_b-L_{0A})^2}\int_0^B \frac{x^2dx}{I_x} + \frac{w_2\cos\theta}{E(L_b-L_{0A})}\int_0^B \frac{(L_b-L_{0A}-x)x^2dx}{I_x} \tag{3.38}$$

and moment M_{B0} is computed from

$$M_{B0} = -P_{C2}(D_L+\Delta_{BT}) + Q_{C2}h - P_{CT1}\Delta_{B2} \tag{3.39}$$

Figure 3.9 shows the deflected shape of rafter 0AD of subassemblage 0ADE fixed at D to compute the deflections at 0 without the consideration of the rotation of Joint A. The deflections are:

$$V_{0D} = V' + V'' + V''' \tag{40}$$

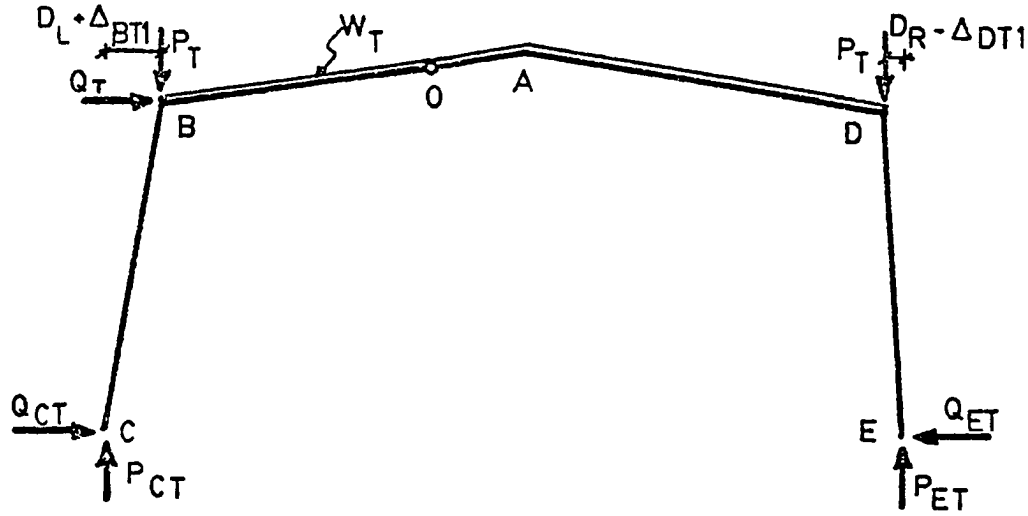

Figure 3.6 Loading at Start of Stage II

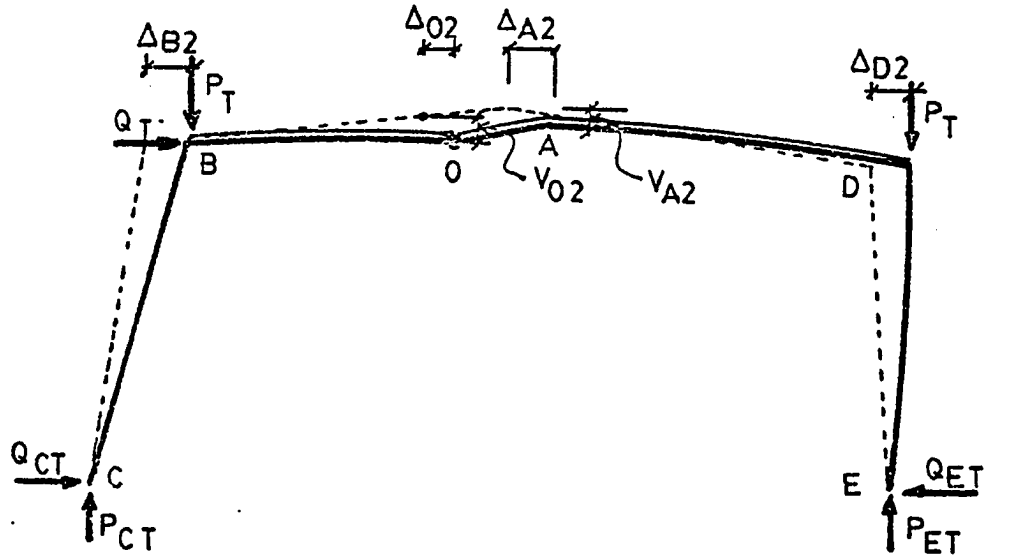

Figure 3.7 Deflected Shape Under Stage II Loading

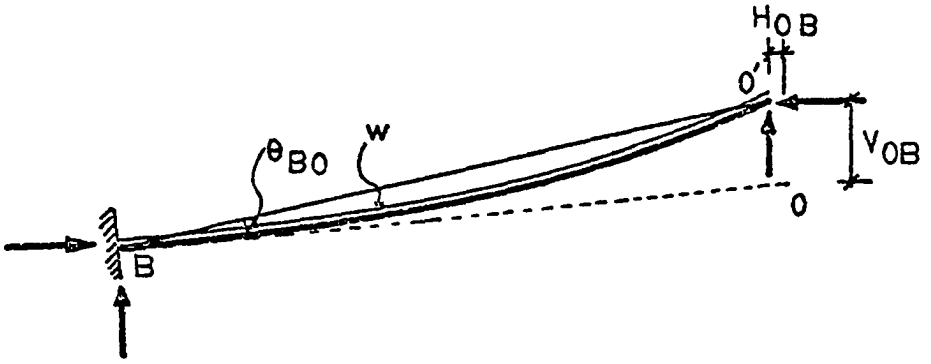

Figure 3.8 Deflected Shape of Member BO without Consideration of Joint Rotation at B

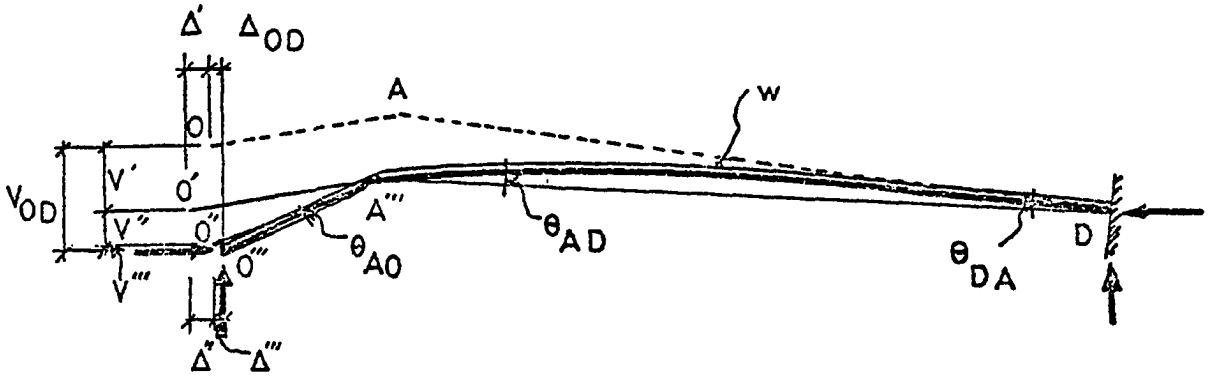

Figure 3.9 Deflected Shape of Member DAO without Consideration of Joint Rotation at D

$$\Delta_{0D} = \Delta' + \Delta'' + \Delta''' \tag{41}$$

where

$$\Delta' = +\theta_{DA}(e-y_{0A}) \tag{3.42}$$

$$\Delta'' = -\theta_{AD}y_{0A} \tag{3.43}$$

$$\Delta''' = -\theta_{A0}t_{0A} \tag{3.44}$$

Therefore

$$\Delta_{0D} = \theta_{DA}(e-y_{0A}) - \theta_{AD}y_{0A} - \theta_{A0}y_{0A} \tag{3.45}$$

and

$$V' = -\theta_{DA}(H-D_R+x_{0A}) \tag{3.46}$$

$$V'' = -\theta_{AD}x_{0A} \tag{3.47}$$

$$V''' = -\theta_{A0}x_{0A} \tag{3.48}$$

Therefore

$$V_{0D} = -\theta_{DA}(H-D_R+x_{0A}) - (\theta_{AD}+\theta_{A0})x_{0A} \tag{3.49}$$

where $\Delta', \Delta'', \Delta'''$, V', V'', V''', θ_{0A}, θ_{AD}, θ_{A0} are deflections and rotations, as shown in Figure 3.9, caused by second stage loading. These rotations are given by

$$\theta_{DA} = \frac{M_{DA}}{EL_b^2}\int_A^D \frac{x^2dx}{I_x} + \frac{M_{AD}}{EL_b^2}\int_A^D \frac{(L_b-x)xdx}{I_x} +$$

$$\frac{w_2\cos\theta}{EL_b}\int_A^D \frac{(L_b-x)x^2dx}{2I_x} \tag{3.50}$$

where

$$M_{DA} = -Q_{E2}h - P_{E2}(D_R-\Delta_{DT}) + P_{ET1}\Delta_{D2} \tag{3.51}$$

$$M_{AD} = Q_{E2}(h+e+V_{AT}) - P_{E2}(H-\Delta_{AT}) - \left(\frac{w_2L_b}{2}\left(H-D_R-\frac{\Delta_{AT}-\Delta_{DT}}{2}\right)\right.$$

$$-Q_{ET1}V_{A2} - P_{ET1}\Delta_{A2} \tag{3.52}$$

and

$$\theta_{AD} = \frac{M_{DA}}{EL_b^2}\int_D^A \frac{(L_b-x)xdx}{I_x} + \frac{M_{AD}}{EL_b^2}\int_D^A \frac{x^2dx}{I_x} +$$

$$\frac{w_2\cos\theta}{EL_b}\int_D^A \frac{(L_b-x)x^2dx}{2I_x} \tag{3.53}$$

$$\theta_{AO} = \frac{M_{AO}}{EL_{AO}^2}\int_O^A \frac{x^2dx}{I_x} + \frac{w_2\cos\theta}{EL_{AO}^2}\int_O^A \frac{(L_{AO}-x)x^2dx}{2I_x} \tag{3.54}$$

where

$$M_{AO} = M_{AD} \tag{3.55}$$

The vertical and horizontal deflections of O in the subassemblage CBO, figure 3.7, are:

$$V_{O2} = V_{OB} - \left(\frac{\Delta_{B2}}{h} + \theta_{BC}\right)(H - x_{OA} - D_R - \Delta_{BT1} + \Delta_{OT1}) \tag{3.56}$$

$$\Delta_{O2} - \Delta_{B2} = \Delta_{OB} + \left(\frac{\Delta_{B2}}{h} + \theta_{BC}\right)(e - y_{OA} + V_{OT1}) \tag{3.57}$$

and the vertical and horizontal deflection of O in the subassemblage OADE, Figure 3. 7, are:

$$V_{O2} = V_{OD} + \left(\frac{\Delta_{D2}}{h} - \theta_{DE}\right)(H + x_{OA} - D_R + \Delta_{DT1} - \Delta_{OT1}) \tag{3.58}$$

$$\Delta_{D2} - \Delta_{O2} = \Delta_{OD} - \left(\frac{\Delta_{D2}}{h} - \theta_{DE}\right)(e - y_{OA} + V_{OT1}) \tag{3.59}$$

Summation of Equations 3.57 and 3.59 gives the horizontal deflection of B with respect to D in the second stage, Δ_2 where

$$\Delta_2 = \Delta_{D2} - \Delta_{B2} = \Delta_{OB} + \Delta_{OD} + \left(\frac{\Delta_{B2}}{h} + \theta_{BC}\right)(e - y_{OA} + V_{OT1})$$

$$- \left(\frac{\Delta_{D2}}{h} - \theta_{DE}\right)(e - y_{OA} + V_{OT1}) \tag{3.60}$$

Since vertical deflections of both subassemblages are equal, at point O, equations 3.56 and 3.58 are equated, hence

$$V_{OB} - (\frac{\Delta_{B2}}{h} + \theta_{BC})(H - x_{OA} - D_R - \Delta_{BT1} + \Delta_{OT1}) =$$

$$V_{OD} + (\frac{\Delta_{D2}}{h} - \theta_{DE})(H + x_{OA} - D_R + \Delta_{DT1} - \Delta_{OT1}) \qquad (3.61)$$

Upon rearrangement of equation 3.60, Δ_{B2} is

$$\Delta_{B2} = \frac{-(\Delta_{OE}+\Delta_{OD})h - (\theta_{DE}+\theta_{BC})(e - y_{OA} + V_{OT1})h}{(e - y_{OA} + V_{OT1} + h)} + \Delta_{D2} \qquad (3.62)$$

Using Δ_{B2} from equation 3.62 and substiuting into equation 3.61 and solving for Δ_{D2}, results in

$$\Delta_{D2} = \frac{(V_{OB} - V_{OD})h}{(2H-D_L-D_R-\Delta_{BT1}-\Delta_{DT1}+2\Delta_{OT1})} -$$

$$\frac{(H-x_{OA}-D_L+\Delta_{BT1}+\Delta_{OT1})h^2\theta_{BC}}{(2H-D_L-D_R-\Delta_{BT1}-\Delta_{DT1}+2\Delta_{OT1})(e-y_{OA}+V_{OT1}+h)} +$$

$$\frac{(H+x_{OA}-D_R-\Delta_{DT1}+\Delta_{OT1})h}{(2H-D_R-D_L-\Delta_{DT1}-\Delta_{BT1}+2\Delta_{OT1})}\ \theta_{DE} +$$

$$\frac{\theta_{DE}\ (H-x_{OA}-D_L-\Delta_{BT1}+\Delta_{OT1})(e-y_{OA}+V_{OT1}+h)}{(2H-D_L-D_R-\Delta_{BT1}-\Delta_{DT1}+2\Delta_{OT1})(e-y_{OA}+V_{OT1}+h)} +$$

$$\frac{(H-x_{OA}-D_L-\Delta_{BT1}+\Delta_{OT1})(\Delta_{OD}+\Delta_{OB})h}{(2H-D_R-D_L-\Delta_{BT1}-\Delta_{DT1}+2\Delta_{OT1})(e-y_{OA}+V_{OT1}+h)} \qquad (3.63)$$

where θ_{DE} and θ_{BC} are computed by

$$\theta_{DE} = \frac{M_{DE}}{EL_c 2} \int_E^D \frac{x^2 dx}{I_x} \tag{3.64}$$

and

$$\theta_{BC} = \frac{M_{BC}}{EL_c 2} \int_C^B \frac{x^2 dx}{I_x} \tag{3.65}$$

When e is small, equations 3.57 and 3.58 give

$$\Delta_{B2} = \Delta_{D2} \tag{3.66}$$

and

$$\Delta_{OB} = \Delta_{OD} = 0 \tag{3.67}$$

Therefore values computed by Equations 3.62 and 3.63 are equal:

$$\Delta_{B2} = \Delta_{D2} = \frac{(V_{OB} - V_{OD})h}{(2H-D_L-D_R-\Delta_{BT1}-\Delta_{DT1}-2\Delta_{OT1})} +$$

$$\frac{(H-x_{OA}-D_L-\Delta_{BT1}+\Delta_{OT1})h^2\theta_{BC}}{(2H-D_L-D_R-\Delta_{BT1}-\Delta_{DT1}-2\Delta_{OT1})(e-y_{OA}+V_{OT1}+h)} +$$

$$\frac{(H-x_{OA}-\Delta_{DT1}+\Delta_{OT1})\theta_{DE}}{(2H-D_R-D_L-\Delta_{BT1}-\Delta_{DT1}-2\Delta_{OT1})} +$$

$$\frac{(H-x_{OA}-D_L-\Delta_{BT1}+\Delta_{OT1})(e-y_{OA}+V_{OT1})h\theta_{DE}}{(2H-D_R-D_L-\Delta_{BT1}-\Delta_{DT1}-2\Delta_{OT1})(e+V_{OT1}-y_{OA}+h)} \tag{3.68}$$

If the first hinge forms in one of the columns, the vertical displacement at the top of the column is equal to the axial deformation of the lower portion of the column which is negligible, Figure 3.10. Also, the shear at 0 in the second stage is equal to zero because Q_{E2} is equal to zero, therefore, the moment at D is equal to zero and the left subassemblage can be identified as shown in Figure 3.11. Figure 3.12 shows the deflected shape of girder BAD without consideration of rotation at Joint B, and vertical deflection DD' is

$$DD' = \theta_{BA}(H-D_L) + (\theta_{AB}+\theta_{BA}+\theta_{AD})(H-D_R) \tag{3.69}$$

The following equation can be written for horizontal deflection at B.

$$\frac{\Delta_{B2}}{h} + \theta_{BC} = \frac{-DD'}{2H-D_R-D_L} \tag{3.70}$$

or

$$\Delta_{B2} = -\theta_{BC}h - \frac{\theta_{BA}(H-D_L)+(\theta_{AB}+\theta_{BA}+\theta_{AD})(H-D_R)}{2H-D_L-D_R} \times h \tag{3.71}$$

where θ_{BC}, θ_{BA}, and θ_{AD} are computed by Equations 3.14, 3.15, 3.53, and θ_{AB} is computed by:

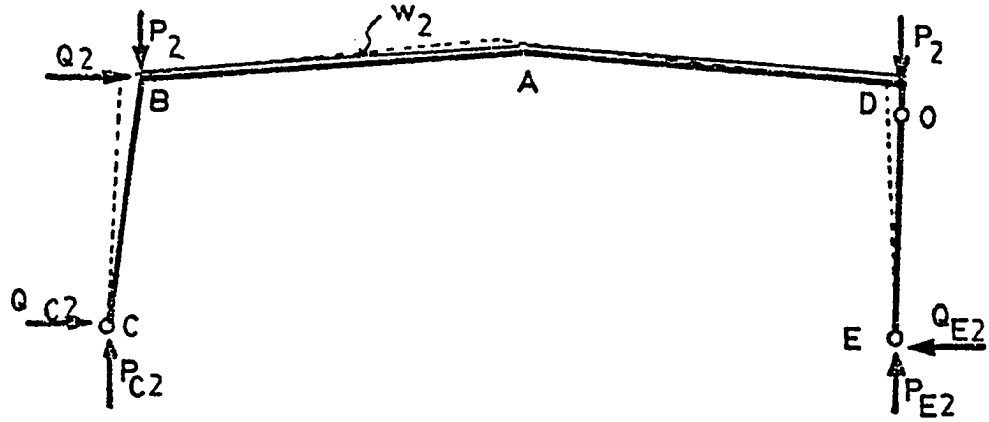

Figure 3.10 Deflected Shape with Hinge in Column DE

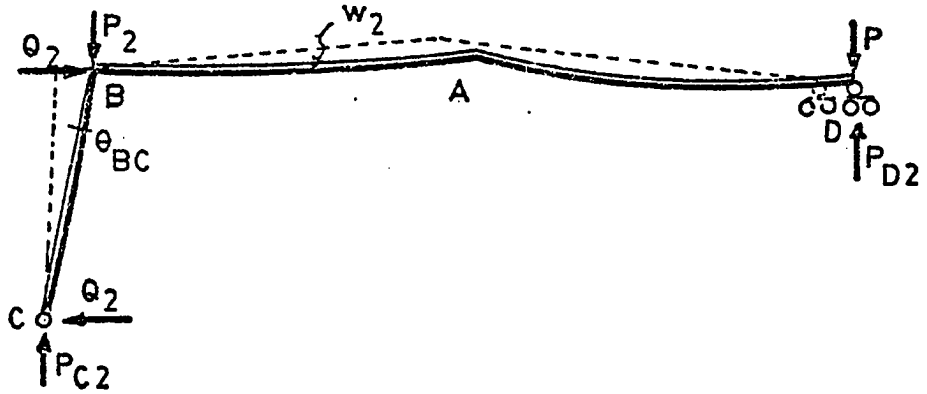

Figure 3.11 Idialized Subassemblage CBAD

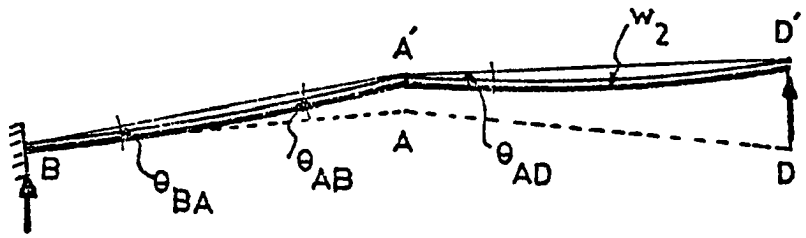

Figure 3.12 Deflected Shape of Rafter when Joint B is Fixed

$$\theta_{AB} = \frac{M_{BA}}{EL_b^2} \int_B^A \frac{(L_b-x)xdx}{I_x} + \frac{M_{AB}}{EL_b^2} \int_B^A \frac{x^2dx}{I_x} +$$

$$\frac{w_2 Cos\theta}{EL_b} \int_B^A \frac{(L_b-x)x^2dx}{2I_x} \qquad (3.72)$$

The vertical deflection at A in second stage loading is

$$V_{A2} = \frac{(\theta_{AB}+\theta_{AD})}{2} \times \frac{(2H-D_R D_L)}{2} \qquad (3.73)$$

and the total horizontal deflection of B with respect to D is

$$\Delta_2 + \Delta_1 = 2(\sqrt{L_b^2 - (e - V_{AT1} - V_{A2})^2} - H) \qquad (3.74)$$

In the second stage of loading, computation of deflections is iterative because the computation of moments is based on the deformed frame. In the first cycle the end moments are computed assuming deflections in the second stage equal to zero. In the remaining cycles, the deflections computed in one cycle are used for computation of end moments of the next cycle. This iteration process continues until convergence occurs with an acceptable tolerance.

In the second stage loads can be applied incrementally. At the end of computations for deflections in a particular load increment, stresses of all segments of cross-sections are checked and yielded segments are eliminated and,

as in the first stage, new properties are computed. If the new properties do not change significantly, the computation proceeds to the next increment of loads, otherwise, new properties are computed and the process repeated for the same load increment. The load is increased until an additional hinge forms on the frame. At this point the frame is considered to have failed.

3.4 Approximation of Horizontal Reactions and Deflections

To start the computation for the initial analysis in the first stage, approximate values are needed for one of the horizontal reactions and the vertical displacement at the ridge of the frame. These approximate values must be within a reasonable range of the actual reaction and displacement, otherwise, the iteration may require a long and tedious computation to converge. Results of a first order analysis of the frame loaded with the first load increment are very useful for this purpose. Subsequent trial values of horizontal reaction in the first stage of loading must also be chosen carefully, if the horizontal deflection of one end of the rafter with respect to other end as computed by methods (a) and (b) of Section 3.3 are to converge in successive trials. For example, if in a trial with an increase of horizontal reaction over the previous trial, the difference between the two calculated values of Δ_1 becomes smaller, then the selection of the trial value is in the right direction, otherwise, the trial value must be decreased. If the sign of the difference

between the two values changes in two successive trials, the rate of increase or decrease of the trial value for the reaction must be reduced.

The starting trial value for midspan deflection of the first increment can be the deflection from a first order analysis. For other load increments, the deflection calculated for the previous load increment can be used as the starting value. Convergence is very dependent on the trial values and with the use of proper values convergence will occur much faster.

In the trial and error method, the computation of Δ_{B1} and Δ_{D1} for an assumed value of horizontal reaction is iterative. The iteration is for the value of vertical deflection of midspan. The iteration process continues until the value computed by Equations 3.23 and 3.24 are equal or within an acceptable range of the value used in these equations. For this purpose, in the first two cycles of iteration, the rate of variation of computed vertical deflection with a change of the value used in Equations 3.23 and 3.24 can be obtained and, using this knowledge, proper values can be found and used in computations until convergence occurs.

In this study the computer program described in Chapter II was used without consideration of P-Δ effects or elimination of the yielded portions. Using this approach for the frames analyzed in the study, the maximum difference between starting and final values of the horizontal reaction was about 3% for the first increment.

CHAPTER IV

SUMMARY AND CONCLUSIONS

The purpose of this study was to investigate the elastic and inelastic behavior of unbraced single span gabled frames constructed using tapered members. Because of adequate lateral bracing it was assumed that no out of plane deformation occurs. The investigation included the effects of residual stresses, and P-Δ effects on the load-deflection relationship of this type of frame. A literature survey was conducted to determine the scope of investigations by other authors. It was found that most suggested solutions concerning the analysis of gabled frames with tapered members were limited to elastic and first order analysis. An approximate solution to determine the allowable stresses in frames with tapered members was found which is based on effective length factor curves and also design provisions for prismatic members. The solution is limited to frames with members having doubly symmetrical cross-sections with flange dimensions, web thickness, and tapering angle of columns and rafters constant.

Two approaches were used in this study to analyze tapered frames: (a) a general approach based on the stiffness

method and, (b) a manual technique based on the slope deflection method. These methods were selected because of their suitability, especially the adaptability of the stiffness method to the computer. Both methods have a broad potential for the analysis of tapered frames. The stiffness method, which is used as a tool of research, was incorporated with P-Δ effects, property changes of the frame members during loading process, and residual stresses. A computer program was developed based on this method. The program treats every straight element of the frame with constant flange dimensions, web thickness, and tapering angle of columns and rafters as an individual member, therefore, it can handle change of slope and cross-section along the frame members. In both methods, the equilibrium equations are formulated on the deformed structure and residual stresses at a cross-section and partial yielding of the members are considered in the loading process. Also, the effects of connection reinforcement are considered, by assuming that a hinge cannot form on a member adjacent to a reinforced connection within a distance equal to the depth of the member. Both methods are iterative and the loads are applied incrementally, and are increased until failure of the frame occurs due to sidesway buckling or a plastic mechanism.

Results obtained from the second order analysis of several tapered frames by the two procedures show very good agreement. A frame with double symmetric H-shaped cross-sections and constant flange dimensions, web thickness, and

tapering angle along columns and rafters was analyzed. The ultimate load obtained by the computer analysis and trial and error method was about 2.7% higher than ultimate load computed by the procedure using the effective length factor curves and AISC design provisions for the same type of loading. A prismatic frame analyzed both experimentally and theoretically at Lehigh University was also analyzed using the proposed methods and the results of the two studies were very close.

From the analyses conducted in this study, it was learned that: 1) the effect of residual stresses is limited to an increase in deflection which, in turn, causes an increase in secondary member end moments which slightly effects the maximum load capacity of the frame; 2) the rate of this increase changes with the type of residual stress pattern. For the three types of patterns examined here, the rate was the highest when the pattern was rectangular, and the lowest when the pattern was triangular. A design practice which ignores the P-Δ effects, overestimates the load carrying capacity of the structure; 3) connection reinforcement increases the stiffness of the ham which increases its load carrying capacity.

BIBLIOGRAPHY

1. Amirikian, A., "Wedge-Beam Framing," Transaction of ASCE, 117, 596, 1952.

2. Lee, G.C., Morrell, M.L., Ketter, R.L., "Design of Tapered Members," Welding Research Council Bulletin, No. 173, June 1972.

3. Moses, F., "Inelastic Frame Buckling," Journal of the Structural Division, ASCE, Vol. 90, No. ST6, December, 1964, pp. 105-121.

4. Specification for the Design, Fabrication and Erection of Structural Steel for Buildings, American Institute of Steel Construction, New York, 1978.

5. Galambos, T.V. Structural Members and Frames, Prentice-Hall Publishing Company, Englewood Cliffs, New Jersey, 1968.

6. Boley, B.A., "On the Accuracy of the Bernoulli-Euler Theory for Beams of Variable Section," Journal of Applied Mechanics, Vol. 30, 1963, pp. 373-378.

7. Fogel, C.M., Ketter, R.L., "Elastic Strength of Tapered Columns," Journal of the Structural Division, ASCE, Vol. 88, No. ST5, October 1962, pp. 67-106.

8. Lee, G.C., Morrell, M.L., "Application of AISC Design Provisions for Tapered Members," Engineering Journal. AISC, Vol. 12, No. 1, First Quarter, 1975, pp. 1-13.

9. Morrell, M.L., Lee, G.C., "Allowable Stress for Web-Tappered Beams with Lateral Resistants," Welding Research Council Bulletin, No. 192, February 1974.

10. Wang, Chu-Kia, Computer Methods in Advanced Structural Analysis, In text Educational Publishers, New York, New York, 1973.

11. Arnold, P., Adams, P.F., Lu, Le-Wu, "Experiental and Analytical Behavior of a Hybrid Frame," Fritz Laboratory Report, No. 297.18, Department of Civil Engineering, Lehigh University, Bethlehem, Pennsylvania, May 1966.

12. Oral, A., "Inelastic Analysis of Planar Steel Frames," Dissertation presented to the University of Texas at Austin, January 1974, in Partial Fulfillment of the Requirements for the Degree of Ph.D.

13. Beaufait, F.W., Rowan, Jr. W.H., Hoadly, P.G., Hackett, R.W., Computer Method of Structural Analysis, Prentice-Hall, Inc., Englewood Cliffs, New Jersey, 1970.

14. Wood, B.R., Beaulieu, D., Adams, P.F., "Column Design by P-Δ Method," Journal of the Structural Division. ASCE, Vol. 102, No. ST2, February 1976, pp. 411-427.

15. Wood, B.R., Beaulieu, D., Adams, P.F., "Further Aspects of Design by P-Δ Method," Journal of the Structural Division, ASCE, Vol. 102, No. ST3, March 1976, pp. 487-500.

16. Nagarajarao, N.R., Marek, P., Tall, L., "Welded Hybrid Steel Columns," Welding Journal, Vol. 51, No. 9, September 1972, pp. 4625-4725.

17. Frost, R.W., Schilling, C.G., "Behavior of Hybrid Beams Subjected to Static Loads," Journal of the Structural Division, ASCE, Vol. 90, No. ST3, June 1964, pp. 55-88.

18. Nethercot, D.A, "Buckling of Welded Hybrid Steel I-Beams," Journal of the Structural Division, ASCE, Vol. 102, No. ST3, March 1976, pp. 461-474.

19. Nethercot, D.A., "Buckling of Welded Beams and Girders," Proceeding of the International Association for Bridge and Structural Engineering, Vol. 34-I, March 1974, pp. 107-121.

20. Bjorhovde, R. et al., "Residual Stress in Thick Welded Plates," Welding Journal, Vol. 51, No. 8, August 1972, pp. 3925-4055.

21. Dwight, J.B., Maxham, K.E., "Welded Steel Plates in Compression," The Structural Engineering, Vol. 47, No. 2, February 1969, pp. 49-66.

22. Handbook of Frame Constants, Portland Cement Association, Skokie, Illinois, 1958.

23. Cheong-Siat-May, F., "Inelastic Sway Buckling of Multistory Frames," Journal of the Structural Division, ASCE, Vol. 102, No. ST1, January 1976, pp. 65-75.

24. Cheong-Siat-Moyf., Erkan Ozer, Le Wu-Lu, "Strength of Steel Frames under Gravity Loads," Journal of the Structural Division, ASCE, Vol. 103, No. ST6, June 1977, pp. 1223-1235.

25. Cheong-Siat-Moy, F., "Consideration of Secondary Effects in Frame Design," Journal of the Structural Division, ASCE, Vol. 103, No. ST10, October 1977, pp. 2005-2019.

26. Cheong-Siat-Moy, F., "Control of Deflection in Unbraced Steel Columns," Proceedings Institute of Civil Engineers, London, England, Part 2, December 1974, pp. 619-634.

27. Cheong-Siat-Moy, F., "Plastic Analysis of Restrained Sway Columns," Journal of the Structural Division, ASCE, Vol. 101, No. ST9, September 1975, pp. 2010-2013.

28. Cheong-Siat-Moy,F., "Multistory Frame Design Story Stiffness Concept," Journal of the Structural Division, ASCE, Vol. 102, No. ST6, June 1976, pp. 1197-1212.

29. Mcnamee, B.M., Lu, Le-Wu,"Inelastic Multistory Frame Buckling," Journal of the Structural Division, ASCE, Vol. 98, No. ST7, July 1972, pp. 1613-1631.

30. Liapunov, S., "Ultimate Strength of Multistory Steel Rigid Frames," Journal of the Structural Division, ASCE, Vol. 100, No. ST8, August 1974, pp. 1643-1655.

31. Manual for Mathematical and Statistical Subroutines, International Mathematical and Statistical Libraries Inc., Houston, Texas, Revised January 1979.

32. Lay, M.G., Galambos, T.V., "The Experimental Behavior of Restrained Columns," Welding Research Council Bulletin, No. 110, November 1960.

33. Tall, L., Yu, C.K., "Significance and Application of Stub-Column Test Results," Journal of the Structural Division, ASCE, Vol. 97, No. ST7, July 1971, pp. 1841-1861.

34. Dwight, J.B., "Prediction of Residual Stress Caused by Welding," Proceedings Colloquium on Centrally Compressed Structures, Paris, France, November 1972.

APPENDIX A

COMPUTER PROGRAM

COMPUTER PROGRAM

A.1 Description of Computer Program

The computer program developed in this study is based on the stiffness method of analysis. The program contains a main program and four subroutines as follows:

Main--Reads and prints the input data; computes joint deflections and member end actions and adds to previous deflections and end actions; calculates a set of imaginary loads, to replace moments in the members form P-Δ effects; modifies the stiffness matrix of the frame using properties at cross-sections computed including the effects of previous loadings; assembles the load matrix for imaginary loads; computes deflections for imaginary loads; iterates until the summation of the absolute values of the set of imaginary loads is less than or equal to a specified value, taken as 0.001 Kip in this study. If a hinge forms on the frame due to application of a load increment before iterating for P-Δ effects, deletes the hinge, deflections and member end actions due to this load increment and re-analyzes using smaller load increments to obtain a more accurate value of load which causes the formation of the hinge. If a hinge forms on the frame due to application of the smaller load increment or while iterating for P-Δ effects, further loading of the frame continues considering

the new hinge location; when the number of hinges reaches the number required for the failure of the frame, the final deflections, member end forces and reactions are printed.

Inrtia--Computes moment of inertia, area, and determines the location of center of gravity of all cross-sections.

RESREC--For rectangular residual stress patterns, combines stresses due to loading with the residual stress of elements at all cross-sections; eliminates yielded portions.

RESTRI--The same as RESREC for when the residual stress pattern is triangular.

RESTRP--The same as RESREC for when the residual stress pattern is trapezoidal.

A.2 Input Data Format

Type 1 — General Parameters (one card)

Cols. 1-5 LNP — Number of frames to be analyzed.

6-10 LTP — A code number for the type of residual stress patterns as follows:

1 = rectangular pattern

2 = triangular pattern

3 = trapezoidal pattern

Data card set for a frame

Type 2 — Frame Parameters (one card per frame)

Col. 1-5 NP	Number of degrees of freedom of frame
6-10 NM	Number of members in frame
11-15 JN	Number of joints in frame
16-20 NLF	Number of larger load increments
21-25 IL	Number of smaller load increments
26-30 JH	Number of hinges at supports
31-35 LC	Number of connections where connection reinforcement is to be considered

Type 3 — Number of Elements (maximum of 16 per card)

Cols. 1-80 NN(K) — Number of elements in each member; five spaces for each number; limited to the number of members

Type 4 — Location of Reinforced Connections (maximum of 16 per card)

Cols. 1-25 JCN(I) Joint numbers where connection reinforcement is to be considered, five spaces for each number, joint numbering sequence is shown in Figure A.1; limited to 5 joints.

Type 5 — Joint Coordinates (one card per joint)

Col. 1-10 XO(I) Horizontal coordinate of joint, inches.

11-20 YO(I) Vertical coordinate of joint, inches.

Type 6 — Member Properties (one card per member)

Cols. 1-8 TF1(K) Outside flange width, inches.

9-16 W1(K) Outside flange thickness, inches.

17-24 TF2(K) Inside flange width, inches.

25-32 W2(K) Inside flange thickness, inches.

33-40 WCF(K) Width of channel section flanges not including web thickness, if used, otherwise leave blank, inches.

41-48 TCF(K) Thickness of channel section flanges, if used, otherwise leave blank, inches.

49-56 TW(K) Thickness of the web, inches.

57-64 HA(K,1) Depth of web at the start end, inches

65-72 HA(K,N) Depth of web at the end end, inches.

Type 7 — Material Properties (one card per member)

Cols. 1-10 YST(K) Yield stress of steel, KSI.

11-24 E(K) Modulus of elasticity of steel, KSI

Type 8 — Width of Tension Block Due to Residual Stresses (one card per member)

Cols. 1-8 WF1(K) — Width of tension block in outside flange, inches.

9-16 WW1(K) — Width of tension block in outside portion of the web, inches.

17-24 WF2(K) — Width of tension block in inside flange, inches.

25-32 WW2(K) — Width of tension block in inside portion of the web, inches.

Type 9 — First Set of Joint Loads (one per each degree of freedom and eight per card)

Cols. 1-80 PBASE(K) — Joint loads, according to degrees of freedom numbering sequence of Figure A.1, KIPS; limited to the number of degrees of freedom.

Type 10 — First Set of Member Loads (one card per member)

Cols. 1-10 CIVLB(K) — Vertical member load, KIPS per inch of member length, in order of the member number, Figure A.1; limited to the number of members.

11-20 CIHLB(K) — Horizontal member load, KIPS per inch of member length, in order of the member number, Figure A; limited to the number of members.

Type 11 — Location of Deflections and Loads for Printout (five spaces for each location)

Cols. 1-25 JH(N) — Degrees of freedom numbers where the deflections and loads are needed to be printed out, Figure A.1; limited to five joints.

Type 12 — Second Set of Joint Loads (one per each degree of freedom and 8 per card)

Cols. 1-80 PBASE(K) — Joint loads, according to degrees of freedom numbering sequence of Figure A.1, KIPS, limited to the number of degrees of freedom.

Type 13 Second Set of Member Loads (one card per member)

Cols. 1-10 CTVLB(K) Vertical member load, KIPS per inch of member length, in order of the member number, Figure A.1; limited to the number of members.

11-20 CTHLB(K) Horizontal member load, KIPS per inch of member length, in order of the member number, Figure A.1; limited to the number of members.

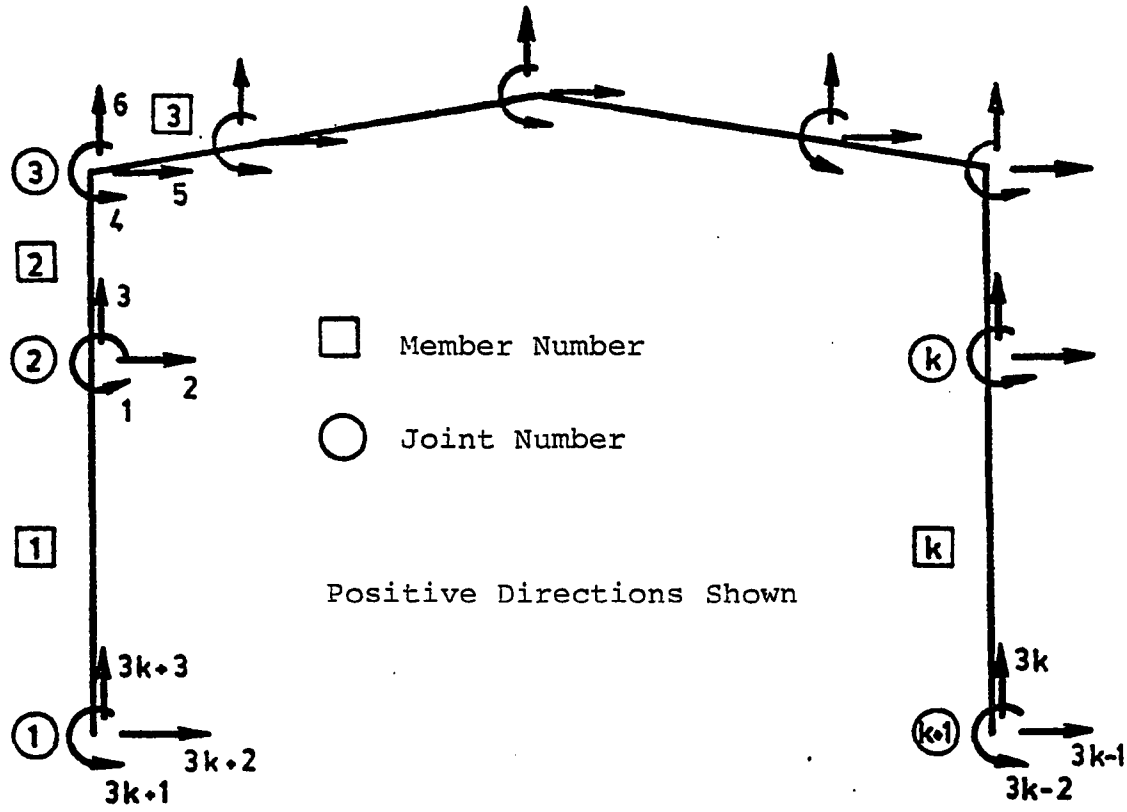

Figure A.1 Degree of Freedom, Member and Joint Numbering Systems

```
      IMPLICIT REAL*8(A-H,O-Z)
      DIMENSION XO(13),YO(13),XLO(12),HC(12),VC(12),XLP(12)
      DIMENSION P(39),P1(39),PBASE(39),PK(39),PP(39),PS(12,6)
      DIMENSION PL(12,6),PL1(12,6),PL2(12,6),JCN(5),MF(6)
      DIMENSION PMAB(12),PMBA(12),FEI(12,6),FEMG(12,6)
      DIMENSION S(6,6),STT(12,6,6),ETSTT(6,6),TSTT(39,39)
      DIMENSION T(12,6,6),TT(12,6,6),DEL(12,6),DELT(12)
      DIMENSION X(39),X1(39),XO(39),XB(12,21,28),XBT(12,21)
      DIMENSION XBT1(12,21),N1(12),NN(12),NPE(12,6),KP(12)
      DIMENSION XBT2(12,21),WIN(12,21),WIN1(12,21),WIN2(12,21)
      DIMENSION AREA(12,21),AREA1(12,21),AREA2(12,21)
      DIMENSION TH(12,21,28),TH1(12,21,28),TV(12,21,28)
      DIMENSION TF1(12),TF2(12),TW(12),W1(12),W2(12),HA(12,21)
      DIMENSION TCF(12),WCF(12),YST(12),E(12),RST(12,21,28)
      DIMENSION A(33,33),AINV(33,33),WK(1188),CTVL1(12)
      DIMENSION CTVL(12),CTHL(12),CTVL2(12),CTHL2(12)
      DIMENSION CTHL1(12),CVLT(12),CHLT(12),CVL(12),CHL(12)
      DIMENSION C1(12),C2(12),C3(12),C4(12),C5(12),C6(12)
      DIMENSION C7(12),CK(12),CL(12),C8(12),SN(12),WI1(12)
      DIMENSION WI2(12),WI3(12),WI4(12),WI5(12),WI6(12)
      DIMENSION WI7(12,21),WF1(12),WW1(12),WF2(12),WW2(12)
      DIMENSION SUP1(6),SUP2(6),SP(28),SPL(28),THH(28)
C     AREA.......AREA OF CROSS-SECTION
C     CS,SN......DIRECTION COSINES OF MEMBER
C     E..........MODULUS OF ELASTICITY OF STEEL
C     YST........YIELD STRESS OF STEEL
C     HA.........DEPTH OF WEB
C     TF1,TF2....THICKNESS OF OUTSIDE AND INSIDE FLANGES
C     W1,W2......WIDTH OF OUTSIDE AND INSIDE FLANGES
C     TW.........THICKNESS OF WEB
C     WCF........WIDTH OF FLANGE OF CHANNEL SECTION, NOT
C                INCLUDING WEB THICKNESS
C     TCF........THICKNESS OF FLANGE OF CHANNEL SECTION
C     TH,TV......DIMENSIONS OF CROSS-SECTION SEGMENT
C     WF1,WF2....PORTION OF OUTSIDE AND INSIDE FLANGES IN
C                TENSION DUE TO RESIDUAL STRESS
C     WW1,WW2....PORTIONS OF WEB IN TENSION DUE TO RESIDUAL
C                STRESSES
C     RST........RESIDUAL STRESS
C     XLO........MEMBER LENGTH
C     XO,YO......JOINT COORDINATES
C     HC,VC......HORIZONTAL AND VERTICAL PROJECTION OF MEMBER
C     WIN........MOMENT OF INERTIA
C     NPE........DEGREE OF FREEDOM NUMBERS
C     PBASE......BASIC LOAD
C     CTVLB......BASIC VERTICAL UNIFORM LOAD
C     CTHLB......BASIC HORIZONTAL UNIFORM LOAD
      NX=33
C     VALUE OF NX MUST BE EQUAL TO THE DIMENSION OF MATRIX A
      READ(5,501) LNP,LTP
      DO 400 LPN=1,LNP
```

```
      PRINT 503
      IF(LTP.EQ.1) PRINT 510
      IF(LTP.EQ.2) PRINT 532
      IF(LTP.EQ.3) PRINT 572
      WRITE(6,578) LPN
      READ(5,502) NP,NM,JN,NLF,IL,JH,LC
      MM=3*JN
      READ(5,506) (NN(K),K=1,NM)
      IF(LC.EQ.0) GO TO 38
      READ(5,556) (JCN(I),I=1,LC)
   38 CONTINUE
      READ(5,520) (XC(I),YC(I),I=1,JN)
      DO 40 K=1,NM
      N1(K)=NN(K)+1
   40 READ(5,516) TF1(K),W1(K),TF2(K),W2(K),WCF(K),TCF(K),
     1TW(K),HA(K,1),HA(K,N1(K))
      READ(5,574) (YST(K),E(K),K=1,NM)
      READ(5,524) (WF1(K),WW1(K),WF2(K),WW2(K),K=1,NM)
C     FIRST SET OF LOADS
      READ(5,504) (PBASE(I),I=1,NP)
      READ(5,520) (CTVLB(K),CTHLB(K),K=1,NM)
      READ(5,560) JH1,JH2,JH3,JH4
C      NUMBERING THE DEGREES OF FREEDOM
      NPE(1,1)=MM-2
      NPE(1,2)=1
      NPE(1,3)=MM
      NPE(1,4)=3
      NPE(1,5)=MM-1
      NPE(1,6)=2
      DO 42 K=2,NM
      NPE(K,1)=3*K-5
      NPE(K,2)=3*K-2
      NPE(K,3)=3*K-3
      NPE(K,4)=3*K
      NPE(K,5)=3*K-4
      NPE(K,6)=3*K-1
   42 CONTINUE
      PRINT 522
      PRINT 542
      WRITE(6,544) (K,TF1(K),W1(K),TF2(K),W2(K),WCF(K),
     1TCF(K),TW(K),HA(K,1),HA(K,N1(K)),YST(K),E(K),K=1,NM)
      PRINT 580
      PRINT 514
      PRINT 515
      WRITE(6,518) (K,(NPE(K,J),J=1,6),XC(K),YC(K),XC(K+1),
     1YC(K+1),K=1,NM)
      PRINT 534
      PRINT 535
      PRINT 546
      WRITE(6,558) (K,WF1(K),WW1(K),WF2(K),WW2(K),K=1,NM)
      PRINT 536
```

```
      PRINT 530
      PRINT 552
      WRITE(6,512) (I,PBASE(I),I=1,NP)
      PRINT 570
      PRINT 554
      DO 46 K=1,NM
      WRITE(6,538) K,CTVLB(K),CTHLB(K)
      CTVL1(K)=CTVLB(K)
      CTHL1(K)=CTHLB(K)
   46 CONTINUE
      DO 48 I=1,NP
   48 P1(I)=PBASE(I)
      IN=1
      EPS=0.001
      EP=0.000001
      KJ=0
      IJ=0
      DO 86 K=1,NM
      KB(K)=0
      N1K=N1(K)
      DO 80 I=1,N1K
C     CALCULATION OF DEPTH OF WEB AT EACH SECTION
      HA(K,I)=HA(K,1)+(HA(K,N1(K))-HA(K,1))*(I-1)/NN(K)
C     CALCULLATION OF TH,TV,XB OF CROSS-SECTION SEGMENTS
      DO 58 N=1,4
      TV(K,I,N)=TF1(K)/4
      TH(K,I,N)=W1(K)-WF1(K)
   58 TH1(K,I,N)=TH(K,I,N)
      DO 60 N=5,8
      TV(K,I,N)=TF1(K)/4
      TH(K,I,N)=WF1(K)
   60 TH1(K,I,N)=TH(K,I,N)
      XB(K,I,1)=HA(K,I)+TF2(K)+7*TF1(K)/8
      XB(K,I,2)=HA(K,I)+TF2(K)+5*TF1(K)/8
      XB(K,I,3)=HA(K,I)+TF2(K)+3*TF1(K)/8
      XB(K,I,4)=HA(K,I)+TF2(K)+TF1(K)/8
      XB(K,I,5)=HA(K,I)+TF2(K)+7*TF1(K)/8
      XB(K,I,6)=HA(K,I)+TF2(K)+5*TF1(K)/8
      XB(K,I,7)=HA(K,I)+TF2(K)+3*TF1(K)/8
      XB(K,I,8)=HA(K,I)+TF2(K)+TF1(K)/8
      DO 62 N=9,12
      TV(K,I,N)=TF2(K)/4
      TH(K,I,N)=W2(K)-WF2(K)
   62 TH1(K,I,N)=TH(K,I,N)
      DO 64 N=13,16
      TV(K,I,N)=TF2(K)/4
      TH(K,I,N)=WF2(K)
   64 TH1(K,I,N)=TH(K,I,N)
      XB(K,I,9)=7*TF2(K)/8
      XB(K,I,10)=5*TF2(K)/8
      XB(K,I,11)=3*TF2(K)/8
```

```
      X3(K,I,12)=TF2(K)/3
      X3(K,I,13)=7*TF2(K)/3
      X8(K,I,14)=5*TF2(K)/3
      X3(K,I,15)=3*TF2(K)/3
      X8(K,I,16)=TF2(K)/8
      DO 66 N=17,20
      TV(K,I,N)=WCF(K)/2
      TH(K,I,N)=TCF(K)
   66 TH1(K,I,N)=TH(K,I,N)
      X8(K,I,17)=TF2(K)+WCF(K)/4
      X8(K,I,18)=TF2(K)+3*WCF(K)/4
      X8(K,I,19)=X8(K,I,17)
      X8(K,I,20)=X8(K,I,18)
      TV(K,I,21)=WW2(K)
      TH(K,I,21)=TW(K)
      TH1(K,I,21)=TH(K,I,21)
      X8(K,I,21)=TF2(K)+WW2(K)/2
      DO 68 N=22,27
      TV(K,I,N)=(HA(K,I)-WW1(K)-WW2(K))/5
      TH(K,I,N)=TW(K)
      X8(K,I,N)=(N-21.5)*TV(K,I,N)+TF2(K)+WW2(K)
   68 TH1(K,I,N)=TH(K,I,N)
      TV(K,I,28)=WW1(K)
      TH(K,I,28)=TW(K)
      TH1(K,I,28)=TH(K,I,28)
      X8(K,I,28)=TF2(K)+HA(K,I)-WW1(K)/2
C     COMPUTATION OF RESIDUAL STRESS OF CROSS-SECTION SEGMENTS
      DO 74 N=1,4
      IF(LTP.EQ.1) RST(K,I,N)=-YST(K)*WF1(K)/(W1(K)-WF1(K))
      IF(LTP.EQ.2) RST(K,I,N)=-YST(K)*WF1(K)/(2*(W1(K)-WF1(K
     1)))
      IF(LTP.EQ.3) RST(K,I,N)=-3*YST(K)*WF1(K)/(4*(W1(K)-WF1
     1(K)))
      M=N+8
      IF(LTP.EQ.1) RST(K,I,M)=-YST(K)*WF2(K)*TF2(K)/((W2(K)-
     1WF2(K))*TF2(K)+2*WCF(K)*TCF(K))
      IF(LTP.EQ.2) RST(K,I,M)=-YST(K)*WF2(K)*TF2(K)/(2*((W2(
     1K)-WF2(K))*TF2(K)+2*TCF(K)*WCF(K)))
      IF(LTP.EQ.3) RST(K,I,M)=-3*YST(K)*WF2(K)*TF2(K)/(4*((W
     12(K)-WF2(K))*TF2(K)+2*TCF(K)*WCF(K)))
   74 CONTINUE
      DO 76 N=5,8
      RST(K,I,N)=YST(K)
      M=N+8
      RST(K,I,M)=YST(K)
      L=N+12
      LJ=L-8
      RST(K,I,L)=RST(K,I,LJ)
   76 CONTINUE
      RST(K,I,21)=YST(K)
      DO 78 N=22,27
```

```
      IF(LTP.EQ.1) RST(K,I,N)=-YST(K)*(WW1(K)+WW2(K))/(HA(K,
     1I)-WW1(K)-WW2(K))
      IF(LTP.EQ.2) RST(K,I,N)=-YST(K)*(WW1(K)+WW2(K))/(2*(HA
     1(K,I)-WW1(K)-WW2(K)))
      IF(LTP.EQ.3) RST(K,I,N)=-3*YST(K)*(WW1(K)+WW2(K))/(4*(
     1HA(K,I)-WW1(K)-WW2(K)))
   78 CONTINUE
      RST(K,I,28)=YST(K)
      WI7(K,I)=(((HA(K,I)-WW1(K)-WW2(K))/6)**3)*TW(K)/12
   80 CONTINUE
      WI1(K)=((TF1(K)/4)**3)*(W1(K)-WF1(K))/12
      WI2(K)=((TF1(K)/4)**3)*WF1(K)/12
      WI3(K)=WI1(K)+WI2(K)
      WI4(K)=((TF2(K)/4)**3)*(W2(K)-WF2(K))/12
      WI5(K)=((TF2(K)/4)**3)*WF2(K)/12
      WI6(K)=WI4(K)+WI5(K)
      DO 82 I=1,6
      PS(K,I)=0.0
   82 PL1(K,I)=0.0
   86 CONTINUE
C     COMPUTATION OF HORIZONTAL AND VERTICAL PROJECTIONS
C     AND LENGTH OF MEMBERS
      DO 94 K=1,NM
      HC(K)=XC(K+1)-XC(K)
      VC(K)=YC(K+1)-YC(K)
      XLC(K)=(DSQRT(HC(K)*HC(K)+VC(K)*VC(K)))
   94 CONTINUE
      DO 96 I=1,MM
      X(I)=0.
      X1(I)=0.
      PP(I)=0.
      PK(I)=0.0
   96 P(I)=0.
      TCLK=0.0
      DO 100 K=1,NM
C     CALCULATION OF MEMBER TRANSFORMATION MATRICES
      DO 98 I=1,6
      DO 98 J=1,6
   98 T(K,I,J)=0.0
      CS(K)=HC(K)/XLC(K)
      SN(K)=VC(K)/XLC(K)
      T(K,1,1)=1.0
      T(K,2,2)=1.0
      T(K,3,3)=CS(K)
      T(K,3,5)=-SN(K)
      T(K,4,4)=CS(K)
      T(K,4,6)=-SN(K)
      T(K,5,3)=SN(K)
      T(K,5,5)=CS(K)
      T(K,6,4)=SN(K)
      T(K,6,6)=CS(K)
```

```
      DO 100 L=1,6
      DO 100 M=1,6
      TT(K,L,M)=T(K,M,L)
  100 CONTINUE
      DO 102 K=1,NM
      CVLT(K)=0.0
      CHLT(K)=0.0
      NIK=NI(K)
      DO 102 I=1,NIK
C     CALCULATION OF MOMENT OF INERTIA, AREA AND THE
C     DISTANCE FROM THE CENTER OF GRAVITY TO THE
C     BOTTOM OF THE INSIDE FLANGE OF THE CROSS-SECTION
      CALL INRTIA(WIN,TH,TV,XS,XBT,K,I,BB,ND)
      AREA(K,I)=BB
      WIN1(K,I)=WIN(K,I)
      AREA1(K,I)=BB
      XBT1(K,I)=XBT(K,I)
  102 CONTINUE
C     CALCULATION OF MEMBER STIFFNESS COEFFICIENTS
      DO 104 K=1,NM
      XLP(K)=XLC(K)/NN(K)
      C1(K)=0.0
      C2(K)=0.0
      C3(K)=0.0
      C4(K)=0.0
      CS(K)=0.0
      CK(K)=0.0
      CL(K)=0.0
      NNK=NN(K)
      DO 104 I=1,NNK
      AWIN=(WIN(K,I)+WIN(K,I+1))/2
      IF(AWIN.EQ.0.0) AWIN=0.0001
      C1(K)=C1(K)+((XLP(K)*I)**2-(XLP(K)*(I-1))**2)*XLC(K)/(
     12*AWIN)
      C2(K)=C2(K)+((XLP(K)*I)**3-(XLP(K)*(I-1))**3)/(3*AWIN)
      CK(K)=CK(K)+((XLP(K)*I)**4-(XLP(K)*(I-1))**4)/(4*AWIN)
      J=NN(K)-I+1
      AWIN=(WIN(K,J)+WIN(K,J+1))/2
      IF(AWIN.EQ.0.0) AWIN=0.0001
      C3(K)=C3(K)+((XLP(K)*I)**2-(XLP(K)*(I-1))**2)*XLC(K)/(
     12*AWIN)
      C4(K)=C4(K)+((XLP(K)*I)**3-(XLP(K)*(I-1))**3)/(3*AWIN)
      CL(K)=CL(K)+((XLP(K)*I)**4-(XLP(K)*(I-1))**4)/(4*AWIN)
      AAREA=(AREA(K,I)+AREA(K,I+1))/2
      IF(AAREA.EQ.0.0) AAREA=0.0001
      CS(K)=CS(K)+XLP(K)/(AAREA*E(K))
  104 CONTINUE
      JF=JH
  110 NF=NLF
      IF(IN.EQ.1) NF=1
      IF(IN.EQ.1) GO TO 111
```

```
      PRINT 525
      PRINT 540
      PRINT 562
      PRINT 564
      PRINT 581
  111 CONTINUE
      DO 350 ILF=1,NF
      JF1=JF
      KS=0
      IF(JF.GE.4) GO TO 350
      DO 112 K=1,NM
      CTVL(K)=CTVL1(K)
      CTHL(K)=CTHL1(K)
      DO 112 I=1,6
      PS(K,I)=0.0
  112 CONTINUE
      DO 114 J=1,NP
  114 P(J)=P1(J)
      JK=0
      LL=0
  116 IF(JK.NE.1) GO TO 129
      DO 120 K=1,NM
      DO 118 I=1,6
  118 PL1(K,I)=PL2(K,I)
      N1K=N1(K)
      DO 120 I=1,N1K
      WIN(K,I)=WIN2(K,I)
      AREA(K,I)=AREA2(K,I)
      XBT(K,I)=XBT2(K,I)
  120 CONTINUE
      DO 122 I=1,NP
  122 X(I)=X2(I)
  124 DO 126 J=1,NP
  126 P(J)=P1(J)/IL
      DO 128 K=1,NM
      CTVL(K)=CTVL1(K)/IL
      CTHL(K)=CTHL1(K)/IL
      DO 128 I=1,6
      PS(K,I)=0.0
  128 CONTINUE
  129 CONTINUE
      JF2=JF
  130 DO 131 J=1,MM
      DO 131 L=1,MM
  131 TSTT(J,L)=0.
      SPE=0.0
      DO 136 K=1,NM
      JP=0
      IF(JF.GE.4) GO TO 134
      IF(KR(K).EQ.1) GO TO 134
      C1(K)=0.0
```

```
      C2(K)=0.0
      C3(K)=0.0
      C4(K)=0.0
      C5(K)=0.0
      CK(K)=0.0
      CL(K)=0.0
      NNK=NN(K)
      DO 132 I=1,NNK
      AWIN=(WIN(K,I)+WIN(K,I+1))/2
      IF(AWIN.EQ.0.0) AWIN=0.0001
      C1(K)=C1(K)+((XLP(K)*I)**2-(XLP(K)*(I-1))**2)*XLO(K)/(
     12*AWIN)
      C2(K)=C2(K)+((XLP(K)*I)**3-(XLP(K)*(I-1))**3)/(3*AWIN)
      CK(K)=CK(K)+((XLP(K)*I)**4-(XLP(K)*(I-1))**4)/(4*AWIN)
      J=NN(K)-I+1
      AWIN=(WIN(K,J)+WIN(K,J+1))/2
      IF(AWIN.EQ.0.0) AWIN=0.0001
      C3(K)=C3(K)+((XLP(K)*I)**2-(XLP(K)*(I-1))**2)*XLO(K)/(
     12*AWIN)
      C4(K)=C4(K)+((XLP(K)*I)**3-(XLP(K)*(I-1))**3)/(3*AWIN)
      CL(K)=CL(K)+((XLP(K)*I)**4-(XLP(K)*(I-1))**4)/(4*AWIN)
      AAREA=(AREA(K,I)+AREA(K,I+1))/2
      IF(AAREA.EQ.0.0) AAREA=0.0001
      C5(K)=C5(K)+XLP(K)/(AAREA*E(K))
  132 CONTINUE
  134 CONTINUE
  136 CONTINUE
      IF(JF.GE.4) GO TO 315
      DO 172 K=1,NM
C     CALCULATION OF STIFFNESS COEFFICIENTS
      CVL(K)=CTVL(K)*C3(K)-CTHL(K)*SN(K)
      CHL(K)=CTVL(K)*SN(K)+CTHL(K)*CS(K)
      C6(K)=CVL(K)*XLO(K)*(XLO(K)*C2(K)-CK(K))/2
      C7(K)=CVL(K)*XLO(K)*(XLO(K)*C4(K)-CL(K))/2
      DO 138 I=1,6
      DO 138 J=1,6
  138 S(I,J)=0.0
C     CALCULATION OF CARRY-OVER FACTORS
      CAB=(C1(K)-C2(K))/C2(K)
      CBA=(C3(K)-C4(K))/C4(K)
C     CALCULATION OF STIFFNESS FACTORS
      DAB=E(K)*(XLO(K)**2)/(C4(K)-CAB*(C3(K)-C4(K)))
      DBA=E(K)*(XLO(K)**2)/(C2(K)-CBA*(C1(K)-C2(K)))
C     CALCULATION OF MEMBER STIFFNESS MATRICES
      S(1,1)=DAB
      S(1,2)=DBA*CBA
      S(1,3)=(DAB+DBA*CBA)/XLO(K)
      S(1,4)=-S(1,3)
      S(2,1)=DAB*CAB
      S(2,2)=DBA
      S(2,3)=(DBA+DAB*CAB)/XLO(K)
```

```
      S(2,4)=-S(2,3)
      S(3,1)=S(1,3)
      S(3,2)=S(2,3)
      S(3,3)=(CAB+CAB*CAB+CBA*CBA+DBA)/(XLC(K)**2)
      S(3,4)=-S(3,3)
      S(4,1)=S(1,4)
      S(4,2)=S(2,4)
      S(4,3)=S(3,4)
      S(4,4)=S(3,3)
      S(5,5)=1/CS(K)
      S(5,6)=-1/CS(K)
      S(6,5)=S(5,6)
      S(6,6)=1/CS(K)
      J1=0
      J2=0
      IF(K.EQ.1) GO TO 140
      K1=K-1
      IF(AREA(K1,N1(K1)).EQ.0.0) J1=1
  140 IF(AREA(K,1).EQ.0.0) J1=1
      IF(K.EQ.NM) GO TO 142
      IF(AREA(K+1,1).EQ.0.0) J2=1
  142 IF(AREA(K,N1(K)).EQ.0.0) J2=1
      IF(K.NE.1) GO TO 144
      IF(JH.NE.0) J1=1
  144 IF(K.NE.NM) GO TO 146
      IF(JH.NE.0) J2=1
  146 CONTINUE
      J3=J1+J2
      IF(J3.EQ.2) GO TO 148
      GO TO 152
  148 DO 150 I=1,4
      DO 150 J=1,4
  150 S(I,J)=0.0
      GO TO 162
  152 IF(J1.EQ.1) GO TO 154
      GO TO 158
  154 DO 156 I=1,4
      DO 156 J=1,4
  156 S(I,J)=0.0
      S(2,2)=(E(K)*(XLC(K))**2)/C2(K)
      S(2,3)=S(2,2)/XLC(K)
      S(2,4)=-S(2,3)
      S(3,2)=S(2,3)
      S(3,3)=S(2,2)/((XLC(K))**2)
      S(3,4)=-S(3,3)
      S(4,2)=S(2,4)
      S(4,3)=S(3,4)
      S(4,4)=S(3,3)
      GO TO 162
  158 IF(J2.NE.1) GO TO 162
      DO 160 I=1,4
```

```
      DO 160 J=1,4
  160 S(I,J)=0.0
      S(1,1)=(E(K)*(XLO(K))**2)/C4(K)
      S(1,3)=S(1,1)/XLO(K)
      S(1,4)=-S(1,3)
      S(3,1)=S(1,3)
      S(3,3)=S(1,1)/((XLO(K))**2)
      S(3,4)=-S(3,3)
      S(4,1)=S(1,4)
      S(4,3)=S(3,4)
      S(4,4)=S(3,3)
  162 CONTINUE
C     ASSEMBLING STIFFNESS MATRIX OF FRAME
      DO 164 L=1,6
      DO 164 M=1,6
      STT(K,L,M)=0.
      DO 164 N=1,6
  164 STT(K,L,M)=STT(K,L,M)+S(L,N)*T(K,N,M)
      DO 166 L=1,6
      DO 166 M=1,6
      ETSTT(L,M)=0.
      DO 166 N=1,6
  166 ETSTT(L,M)=ETSTT(L,M)+TT(K,L,N)*STT(K,N,M)
      DO 168 L=1,6
      L1=NPE(K,L)
      DO 168 M=1,6
      M1=NPE(K,M)
      FEM(K,M)=0.0
  168 TSTT(L1,M1)=TSTT(L1,M1)+ETSTT(L,M)
C     CALCULATION OF FIXED ACTIONS OF MEMBERS DUE TO
C     UNIFORM LOADS
      PMM=C4(K)*C2(K)-(C1(K)-C2(K))*(C3(K)-C4(K))
      PMAB(K)=(C5(K)*(C3(K)-C4(K))-C7(K)*C2(K))/PMM
      PMBA(K)=(C7(K)*(C1(K)-C2(K))-C5(K)*C4(K))/PMM
      FEM(K,1)=-PMAB(K)
      N1K=N1(K)
      IF(AREA(K,1).EQ.0.0) FEM(K,1)=0.0
      IF(AREA(K,N1K).EQ.0.0) FEM(K,1)=C7(K)/C4(K)
      FEM(K,2)=PMBA(K)
      IF(AREA(K,1).EQ.0.0) FEM(K,2)=C6(K)/C2(K)
      IF(AREA(K,N1K).EQ.0.0) FEM(K,2)=0.0
      FEM(K,3)=CVL(K)*XLO(K)/2-(PMAB(K)-PMBA(K))/XLO(K)
      FEM(K,4)=CVL(K)*XLO(K)/2+(PMAB(K)-PMBA(K))/XLO(K)
      IF(CVL(K).EQ.0.0) GO TO 170
      FEM(K,5)=CHL(K)*XLO(K)*FEM(K,3)/(FEM(K,3)+FEM(K,4))
      FEM(K,6)=CHL(K)*XLO(K)*FEM(K,4)/(FEM(K,3)+FEM(K,4))
  170 CONTINUE
      DO 171 I=1,6
      FEMG(K,I)=0.0
      DO 171 J=1,6
  171 FEMG(K,I)=FEMG(K,I)+TT(K,I,J)*FEM(K,J)
```

```
      DO 172 I=1,6
      P(NPE(K,I))=P(NPE(K,I))+PING(K,I)
  172 CONTINUE
      DO 174 I=1,NP
      DO 174 J=1,NP
  174 A(I,J)=TSTT(I,J)
      N=NP
      JR=0
      DO 176 I=1,NP
      IF(A(I,I).NE.0.0) GO TO 176
      JR=JR+1
      MF(JR)=I
      N=N-1
  176 CONTINUE
      IF(JR.EQ.0) GO TO 186
      IH=NP
      DO 184 IP=1,JR
      IT=MF(IP)-IP+1
      IK=IH
      IH=IH-1
      DO 180 I=1,IK
      DO 180 J=IT,IH
  180 A(I,J)=A(I,J+1)
      DO 182 I=IT,IH
      DO 182 J=1,IH
  182 A(I,J)=A(I+1,J)
  184 CONTINUE
  186 CONTINUE
      IDGT=0
C     CALCULATION OF INVERSE OF STIFFNESS MATRIX
      CALL LINV2F(A,N,NX,AINV,IDGT,WK,IER)
      IF(IER.NE.0) GO TO 318
      IF(JR.EQ.0) GO TO 198
      IH=N
      DO 196 IP=1,JR
      IT=MF(IP)
      IK=IH
      IH=IH+1
      DO 190 I=1,IK
      L=IK-I+1
      DO 188 J=IT,IK
      M=IK-J+IT
  188 AINV(L,M+1)=AINV(L,M)
  190 AINV(L,MF(IP))=0.0
      DO 194 J=1,IH
      M=IH-J+1
      DO 192 I=IT,IK
      L=IK-I+IT
  192 AINV(L+1,M)=AINV(L,M)
  194 AINV(MF(IP),M)=0.0
  196 CONTINUE
```

```
  192 CONTINUE
      DO 200 I=1,NP
      X1(I)=0.
      PP(I)=ILF*P1(I)+PK(I)
      IF(JK.EQ.1) PP(I)=(ILF-1)*P1(I)+LL*P1(I)/IL+PK(I)
C     CALCULATION OF DEFLECTIONS
      DO 200 J=1,NP
  200 X1(I)=X1(I)+AINV(I,J)*P(J)
      M=NM/2
      TCL=ILF*CTVL1(M)+TCLK
      IF(JK.EQ.1) TCL=(ILF-1)*CTVL1(M)+LL*CTVL1(M)/IL+TCLK
      DO 202 K=1,NM
      CVLT(K)=CVLT(K)+CVL(K)
      CHLT(K)=CHLT(K)+CHL(K)
      CTVL(K)=0.0
  202 CTHL(K)=0.0
      DO 204 I=1,MM
      P(I)=0.0
  204 X(I)=X(I)+X1(I)
      DO 214 K=1,NM
C     CALCULATION OF MEMBER END ACTIONS
      DO 206 I=1,6
      PL(K,I)=0.
      DO 206 J=1,6
  206 PL(K,I)=PL(K,I)+STT(K,I,J)*X1(NPE(K,J))
      DO 208 I=1,6
      PL(K,I)=PL(K,I)-FEM(K,I)-PS(K,I)
      FEM(K,I)=0.0
      FEMG(K,I)=0.0
      DEL(K,I)=0.
      DO 208 J=1,6
  208 DEL(K,I)=DEL(K,I)+T(K,I,J)*X1(NPE(K,J))
      DELT(K)=DEL(K,4)-DEL(K,3)
      DO 210 I=1,6
      PL1(K,I)=PL1(K,I)+PL(K,I)
      PS(K,I)=0.0
  210 CONTINUE
C     CALCULATION OF LOADS DUE TO SECOND ORDER EFFECTS
      PS(K,3)=DELT(K)*(PL1(K,6)-PL1(K,3))/(2*KLC(K))
      PS(K,4)=-PS(K,3)
      DO 212 I=1,6
      DO 212 J=1,6
  212 P(NPE(K,I))=P(NPE(K,I))+TT(K,I,J)*PS(K,J)
  214 CONTINUE
      DO 215 K=1,NM
      N1K=N1(K)
      DO 215 I=1,N1K
      DO 215 N=1,28
  215 TH(K,I,N)=TH1(K,I,N)
C     INSPECTION OF STRESSES OF CROSS-SECTION SEGMENTS
      DO 270 K=1,NM
```

```
      NIK=N1(K)
      DO 270 I=1,NIK
      IPK=0
      DO 216 N=1,28
      SP(N)=0.0
      SPL(N)=0.0
  216 THH(N)=TH1(K,I,N)/2
      IF(LC.EQ.0) GO TO 219
      IIK=I+K
      IF(IIK.EQ.2) IPK=1
      IF(JH.NE.0) IPK=0
      DO 218 N=1,LC
      IIK=K+1
      IF(K.EQ.JCN(N)) IPK=1
      IF(IIK.EQ.JCN(N)) IPK=1
  218 CONTINUE
      IF(K.NE.NM) GO TO 219
      IF(I.EQ.N1(K)) IPK=1
      IF(JH.NE.0) IPK=0
  219 CONTINUE
      IF(IPK.NE.0) GO TO 270
      IF(AREA(K,I).EQ.0.0) GO TO 270
      WIN(K,I)=WIN1(K,I)
      AREA(K,I)=AREA1(K,I)
      XBT(K,I)=XBT1(K,I)
      CTM1=0.0
      CTM2=0.0
      CTM3=0.0
      CTP1=0.0
      CTP2=0.0
      CTP3=0.0
      F1=0.0
      FF1=0.0
      F2=0.0
      FF2=0.0
      CTP=-PL1(K,5)-CHLT(K)*XLP(K)*(I-1)
      CTM=PL1(K,1)-(PL1(K,1)+PL1(K,2))*(I-1)/NN(K)+CVLT(K)*
     1(XLP(K)**2)*(I-1)*(NN(K)-I+1)/2
      CTP1=CTP
      CTM1=CTM
  220 WW=WIN(K,I)-WI1(K)
      IF(DABS(WW).LE.EP) GO TO 222
      WW=WIN(K,I)-WI2(K)
      IF(DABS(WW).LE.EP) GO TO 222
      WW=WIN(K,I)-WI3(K)
      IF(DABS(WW).LE.EP) GO TO 222
      WW=WIN(K,I)-WI4(K)
      IF(DABS(WW).LE.EP) GO TO 222
      WW=WIN(K,I)-WI5(K)
      IF(DABS(WW).LE.EP) GO TO 222
      WW=WIN(K,I)-WI6(K)
```

```
      IF(DABS(WW).LE.EP) GO TO 222
      WW=WIN(K,I)-WI7(K,I)
      IF(DABS(WW).LE.EP) GO TO 226
      WW=WIN(K,I)-3*WI7(K,I)
      IF(DABS(WW).LE.EP) GO TO 228
      GO TO 230
  222 IF(CTM.NE.0.0) GO TO 224
      IF(CTP.NE.0.0) GO TO 224
      GO TO 230
  224 WIN(K,I)=0.0
      AREA(K,I)=0.0
      KJ=K
      IJ=I
      GO TO 270
  226 N=ND
      HPP=(RST(K,I,N)*AREA(K,I)+CTP)/(YST(K)*TH(K,I,N))
      IF(DABS(HPP).GT.TV(K,I,N)) HPP=TV(K,I,N)
      TKL=((TV(K,I,N)-DABS(HPP))/2)*TH(K,I,N)*YST(K)*(TV(K,I
     1,N)+DABS(HPP))/2
      IF(DABS(CTM).LT.TKL) GO TO 230
      WIN(K,I)=0.0
      AREA(K,I)=0.0
      KJ=K
      IJ=I
      GO TO 270
  228 N=ND
      HPP=(RST(K,I,N)*AREA(K,I)+CTP)/(YST(K)*TH(K,I,N))
      TVN=2*TV(K,I,N)
      IF(DABS(HPP).GT.TVN) HPP=TVN
      TKL=((2*TV(K,I,N)-DABS(HPP))/2)*TH(K,I,N)*YST(K)*(2*TV
     1(K,I,N)+DABS(HPP))/2
      IF(DABS(CTM).LT.TKL) GO TO 230
      WIN(K,I)=0.0
      AREA(K,I)=0.0
      KJ=K
      IJ=I
      GO TO 270
  230 DO 236 N=1,29
      IF(TH(K,I,N).EQ.0.0) GO TO 236
      STRP=CTP/AREA(K,I)
      STRM=CTM*(XB(K,I,N)-XBT(K,I))/WIN(K,I)
      IF(LTP.EQ.1) CALL RESREC(RST,STRM,STRP,YST,F1,FF1,F2,
     1FF2,TH,TV,XB,K,I,N)
      IF(LTP.EQ.2) CALL RESTRI(RST,STRM,STRP,YST,F1,FF1,F2,
     1FF2,TH,TV,TH1,XB,SP,SPL,K,I,N)
      IF(LTP.EQ.3) CALL RESTRP(RST,STRM,STRP,YST,F1,FF1,F2,
     1FF2,TH,TV,TH1,XB,SP,SPL,K,I,N,THH)
  236 CONTINUE
      CALL INRTIA(WIN,TH,TV,XB,XBT,K,I,30,ND)
      AREA(K,I)=88
      IF(F1.EQ.0.0) DIS1=0.0
```

```
      IF(F2.EQ.0.0) DIS2=0.0
      IF(F1.NE.0.0) DIS1=FF1/F1
      IF(F2.NE.0.0) DIS2=FF2/F2
      DIS=DIS2-DIS1
      IF(DIS.EQ.0.0) GO TO 270
      KR(K)=1
      IF(AREA(K,I).EQ.0.0) KJ=K
      IF(AREA(K,I).EQ.0.0) IJ=I
      IF(AREA(K,I).EQ.0.0) GO TO 270
      IF(DABS(F1).LT.DABS(F2)) GO TO 244
      CTM=CTM1-F2*DIS+(F1+F2)*(XBT(K,I)-FF1/F1)+CTP1*
     1(XBT1(K,I)-XBT(K,I))
      CTP=CTP1-F1-F2
      IF(CTM.EQ.CTMI) GO TO 240
      GO TO 242
  240 IF(CTP.EQ.CTPI) GO TO 270
  242 CTMI=CTM
      CTPI=CTP
      GO TO 220
  244 IF(DABS(F2).LT.DABS(F1)) GO TO 252
      CTM=CTM1+F1*DIS+(F1+F2)*(XBT(K,I)-FF2/F2)+CTP1*
     1(XBT1(K,I)-XBT(K,I))
      CTP=CTP1-F1-F2
      IF(CTM.EQ.CTM2) GO TO 246
      GO TO 248
  246 IF(CTP.EQ.CTP2) GO TO 270
  248 CTM2=CTM
      CTP2=CTP
      GO TO 220
  252 CTM=CTM1+F1*DIS
      CTP=CTP1
      IF(CTM.EQ.CTM3) GO TO 254
      GO TO 256
  254 IF(CTP.EQ.CTP3) GO TO 270
  256 CTM3=CTM
      CTP3=CTP
      GO TO 220
  270 CONTINUE
      JF=JH
      DO 280 K=1,NM
      N1K=N1(K)
      DO 280 I=1,N1K
      IF(AREA(K,I).EQ.0.0) JF=JF+1
      IF(K.EQ.1) GO TO 280
      IF(I.GT.1) GO TO 280
      K1=K-1
      AR=AREA(K1,N1(K1))+AREA(K,1)
      IF(AR.GT.0.0) GO TO 280
      JF=JF-1
  280 CONTINUE
      KS1=KS
```

```
      IF(KS.EQ.5) GO TO 316
      KS=KS+1
      DO 314 I=1,MM
  314 SPE=SPE+DABS(P(I))
      IF(SPE.LT.EPS) GO TO 316
      GO TO 130
  316 KS=0
      IF(JK.NE.0) GO TO 318
      IF(JF.GT.JF1) JK=1
      IF(JK.EQ.1) JF=JF1
      IF(JK.EQ.1) GO TO 322
  318 CONTINUE
      IF(JK.NE.1) GO TO 320
      IF(LL.EQ.IL) GO TO 320
      IF(JF.EQ.JF2) GO TO 332
  320 CONTINUE
      IF(IN.EQ.1) GO TO 322
      WRITE(6,348) PP(JH1),PP(JH2),TCL,X(JH1),X(JH3),X(JH4),
     1JF,KS1
  322 CONTINUE
      IF(JK.EQ.0) GO TO 330
      LL=LL+1
      IF(LL.GT.IL) JK=0
      IF(LL.GT.IL) GO TO 330
      IF(JF.GE.4) GO TO 350
      IF(LL.EQ.1) GO TO 116
      IF(JK.EQ.1) GO TO 124
  330 CONTINUE
      DO 332 J=1,NP
  332 X2(J)=X(J)
      DO 340 K=1,MM
      DO 334 I=1,6
      PL2(K,I)=PL1(K,I)
  334 CONTINUE
      NIK=N1(K)
      DO 336 I=1,NIK
      AREA2(K,I)=AREA(K,I)
      WIN2(K,I)=WIN(K,I)
      XBT2(K,I)=XBT(K,I)
  336 CONTINUE
  340 CONTINUE
  350 CONTINUE
      IF(IER.NE.0) GO TO 360
      IN=IN+1
      IF(JF.GE.4) GO TO 366
      IF(IN.GT.2) GO TO 362
      DO 356 I=1,NP
  356 PK(I)=PBASE(I)
C     SECOND SET OF LOADS
      READ(5,504) (PBASE(I),I=1,NP)
      TCLK=CTVLU(6)
```

```
      READ(5,520) (CTVLB(K),CTHLB(K),K=1,NM)
      PRINT 576
      PRINT 530
      PRINT 552
      WRITE(6,512) (I,PBASE(I),I=1,NP)
      PRINT 570
      PRINT 554
      WRITE(6,538) (K,CTVLB(K),CTHLB(K),K=1,NM)
      DO 358 I=1,NP
  358 P1(I)=PBASE(I)/NLF
      DO 359 K=1,NM
      CTVL1(K)=CTVLB(K)/NLF
      CTHL1(K)=CTHLB(K)/NLF
  359 CONTINUE
      GO TO 110
  362 PRINT 550
  366 CONTINUE
      IF(IER.NE.0) GO TO 368
      GO TO 370
  368 PRINT 500
  370 CONTINUE
      PRINT 586
      PRINT 588
      PRINT 590
      PRINT 584
      WRITE(6,566) (K,PL1(K,5),PL1(K,3),PL1(K,1),PL1(K,6),
     1PL1(K,4),PL1(K,2),K=1,NM)
      DO 372 I=1,6
      SUP1(I)=0.0
      SUP2(I)=0.0
      DO 372 J=1,6
      SUP1(I)=SUP1(I)+TT(1,I,J)*PL1(1,J)
      SUP2(I)=SUP2(I)+TT(NM,I,J)*PL1(NM,J)
  372 CONTINUE
      PRINT 592
      PRINT 594
      PRINT 596
      PRINT 582
      WRITE(6,568) SUP1(5),SUP1(3),SUP1(1)
      PRINT 598
      PRINT 596
      PRINT 582
      WRITE(6,568) SUP2(6),SUP2(4),SUP2(2)
      IF(JF.GE.4) PRINT 523
  400 CONTINUE
  500 FORMAT(5X,'THE MATRIX IS ZERO SO IT DOES NOT WORK')
  501 FORMAT(2I5)
  502 FORMAT(7I5)
  504 FORMAT(8F10.2)
  506 FORMAT(15I5)
  508 FORMAT('1','SECOND ORDER ANALYSIS OF RIGID FRAMES'//)
```

```
510 FORMAT('0','RESIDUAL STRESS PATTERN IS RECTANGULAR'/)
512 FORMAT(6X,I3,6X,F3.3)
514 FORMAT('0',' MEMBER NP1  NP2  NP3  NP4  NP5  NP6',5X,
   1'XI',8X,'YI',8X,'XJ',8X,'YJ')
515 FORMAT(42X,'IN.',7X,'IN.',7X,'IN.',7X,'IN.'/)
516 FORMAT(9F8.3)
518 FORMAT(1H ,7I5,1X,4F10.3)
520 FORMAT(2F10.3)
522 FORMAT('0','MEMBER AND MATERIAL PROPERTIES,'
   1,1X,' IN , AND KSI'/)
524 FORMAT(4F8.3)
526 FORMAT('1','VALUES OF JOINT LOADS, UNIFORM LOADS,',1X,
   1'DEFLECTIONS, AND NUMBER OF HINGES AND ITERATIONS'/)
528 FORMAT('-',5X,'END OF PROBLEM---- THE FRAME FAILED')
530 FORMAT('0',3X,'JOINT LOADS, KIPS'/)
532 FORMAT('0','RESIDUAL STRESS PATTERN IS TRIANGULAR'/)
534 FORMAT('1','WIDTH OF PORTION OF FLANGE AND WEB IN')
535 FORMAT(1X,'TENSION DUE TO RESIDUAL STRESSES, IN.'/)
536 FORMAT('1','FIRST SET OF LOADS'/)
538 FORMAT(I5,2F10.2)
540 FORMAT('0','HORIZ. LOAD',4X,'VERT. LOAD',2X,'CONT. VE'
   1,3X,'HORIZ. DEFL.',2X,'VERT. DEFL.',3X,'ROTIZ. DEFL.')
542 FORMAT('0','MEMBER',2X,'TF1',4X,'W1',5X,'TF2',4X,'W2',
   15X,'WCF',4X,'TCF',4X,'TW',4X,'HA(SE)',2X,'HA(EE)',
   23X,'YST',6X,'E'/)
544 FORMAT(I5,1X,7F7.3,3F8.3,F10.2)
546 FORMAT('0','MEMBER',4X,'WF1',7X,'WW1',7X,'WF2',7X,'WW2'/)
548 FORMAT(F10.4,5X,F10.4,1X,F10.4,2X,E13.5,1X,E13.5,E14.5
   1,2X,I5,3X,I5)
550 FORMAT(5X,'END OF PROBLEM')
552 FORMAT(4X,'LOCATION',5X,'LOAD'/)
554 FORMAT('0','MEMBER',2X,'VERTICAL',2X,'HORIZONTAL'/)
556 FORMAT(5I5)
558 FORMAT(I5,4F10.3)
560 FORMAT(4I5)
562 FORMAT(1X,'AT THE TOP OF',2X,'AT THE TOP',2X,'RT. LOAD'
   1,3X,'AT TOP OF',5X,'AT MID SPAN',2X,'AT TOP OF',7X
   2,'NO. OF',2X,'NO. OF')
564 FORMAT(1X,'LEFT COLUMN',4X,'OF COLUMNS',2X,'OF RAFTER'
   1,2X,'LEFT COLUMN',3X,'OF RAFTER',4X,'RIGHT COLUMN',4X
   2,'HINGES',2X,'ITER.S')
566 FORMAT(I5,4X,F10.4,5F12.4)
568 FORMAT('0',3F10.4)
570 FORMAT('-','UNIFORM LOADS, KIPS/IN.')
572 FORMAT('0','RESIDUAL STRESS PATTERN IS TRAPEZOIDAL'/)
574 FORMAT(F10.2,F14.3)
576 FORMAT('1','SECOND SET OF LOADS'/)
578 FORMAT('0','ANALYSIS OF FRAME NUMBER',I3/)
580 FORMAT('-',///,1X,'DEGREE OF FREEDOM NUMBERS AND',1X,
   1'MEMBER END COORDINATES, IN.'/)
581 FORMAT(1X,'KIPS',11X,'KIPS',8X,'KIPS/IN.',3X,'IN.',
```

```
   111X,'IN.',10X,'IN.'/)
582 FORMAT(4X,'KIPS',7X,'KIPS',5X,'KIPS-IN.')
584 FORMAT(13X,'KIPS',5X,'KIPS',4X,'KIPS-IN.',6X,'KIPS',
   18X,'KIPS',6X,'KIPS-IN.'/)
586 FORMAT('-',///,1X,'FINAL END ACTIONS OF MEMBERS')
588 FORMAT('0',24X,'END I',31X,'END J')
590 FORMAT('0','MEMBER',5X,'AXIAL',7X,'SHEAR',6X,'MOMENT',
   17X,'AXIAL',7X,'SHEAR',6X,'MOMENT')
592 FORMAT('1','REACTIONS AT SUPPORTS'//)
594 FORMAT('-',9X,'LEFT SUPPORT')
596 FORMAT('0','HORIZONTAL',2X,'VERTICAL',3X,'MOMENT')
598 FORMAT('-',9X,'RIGHT SUPPORT')
    STOP
    END
```

```
      SUBROUTINE INRTIA(WIN,TH,TV,XB,XBT,K,I,BB,ND)
      IMPLICIT REAL*8(A-H,O-Z)
      DIMENSION WIN(12,21),TH(12,21,28),TV(12,21,28)
      DIMENSION XB(12,21,28),XBT(12,21)
      BB=0.00
      DO 2 N=1,28
      IF(TH(K,I,N).GT.0.0) ND=N
    2 BB=BB+TH(K,I,N)*TV(K,I,N)
      AK=0.00
      DO 3 N=1,28
    3 AK=AK+TH(K,I,N)*TV(K,I,N)*XB(K,I,N)
      WIN(K,I)=0.00
      IF(BB.EQ.0.0) GO TO 5
      XBT(K,I)=AK/BB
      DO 4 N=1,28
    4 WIN(K,I)=WIN(K,I)+(TH(K,I,N)*TV(K,I,N)**3)/12+
     1TH(K,I,N)*TV(K,I,N)*(XBT(K,I)-XB(K,I,N))**2
    5 RETURN
      END
```

```
      SUBROUTINE RESREC(RST,STRM,STRP,YST,F1,FF1,F2,FF2,TH,
     1TV,XB,K,I,N)
      IMPLICIT REAL*8(A-H,O-Z)
      DIMENSION RST(12,21,28),YST(12),TH(12,21,28)
      DIMENSION TV(12,21,28),XB(12,21,28)
      STR=RST(K,I,N)+STRM+STRP
      IF(DABS(STR).LT.YST(K)) GO TO 4
      IF(STR.GE.YST(K)) GO TO 2
      F1=F1-(YST(K)+RST(K,I,N))*TH(K,I,N)*TV(K,I,N)
      FF1=FF1-(YST(K)+RST(K,I,N))*TH(K,I,N)*TV(K,I,N)*XB(K,I,N)
      TH(K,I,N)=0.0
      GO TO 4
    2 F2=F2+(YST(K)-RST(K,I,N))*TH(K,I,N)*TV(K,I,N)
      FF2=FF2+(YST(K)-RST(K,I,N))*TH(K,I,N)*TV(K,I,N)*XB(K,I,N)
      TH(K,I,N)=0.0
    4 CONTINUE
      RETURN
      END
```

```
      SUBROUTINE RESTFI(RST,STRM,STRP,YST,F1,FF1,F2,FF2,TH,
     1TV,TH1,XB,SP,SPL,K,I,N)
      IMPLICIT REAL*8(A-H,O-Z)
      DIMENSION TH(12,21,28),TV(12,21,28),XB(12,21,28),SP(28)
      DIMENSION SPL(28),YST(12),TH1(12,21,28),RST(12,21,28)
      IF(N.LE.4) GO TO 6
      IF(N.LE.8) GO TO 12
      IF(N.LE.12) GO TO 6
      IF(N.LE.16) GO TO 12
      IF(N.LE.20) GO TO 6
      IF(N.EQ.21) GO TO 12
      IF(N.LE.27) GO TO 6
      IF(N.EQ.28) GO TO 12
    6 STR=RST(K,I,N)+STRM+STRP
      IF(DABS(STR).LT.YST(K)) GO TO 16
      IF(STR.GE.YST(K)) GO TO 8
      F1=F1-(YST(K)+RST(K,I,N))*TH(K,I,N)*TV(K,I,N)
      FF1=FF1-(YST(K)+RST(K,I,N))*TH(K,I,N)*TV(K,I,N)*XB(K,I,N)
      TH(K,I,N)=0.0
      GO TO 16
    8 F2=F2+(YST(K)-RST(K,I,N))*TH(K,I,N)*TV(K,I,N)
      FF2=FF2+(YST(K)-RST(K,I,N))*TH(K,I,N)*TV(K,I,N)*XB(K,I,N)
      TH(K,I,N)=0.0
      GO TO 16
   12 STR=STRM+STRP
      IF(STR.GT.0.0) GO TO 14
      SYT=YST(K)-SPL(N)
      IF(DABS(STR).LT.SYT) GO TO 16
      SP(N)=STR+SYT
      TP=-TH1(K,I,N)*SP(N)/YST(K)
      IF(TP.GT.TH(K,I,N)) SP(N)=-2*YST(K)+SYT
      IF(TP.GT.TH(K,I,N)) TP=TH(K,I,N)
      TH(K,I,N)=TH(K,I,N)-TP
      F1=F1+(-YST(K)+SPL(N)+SP(N)/2)*TP*TV(K,I,N)
      FF1=FF1+(-YST(K)+SPL(N)+SP(N)/2)*TP*TV(K,I,N)*XB(K,I,N)
      SPL(N)=SPL(N)+SP(N)
      GO TO 16
   14 IF(STR.LE.SPL(N)) GO TO 16
      SP(N)=STR-SPL(N)
      TP=TH1(K,I,N)*SP(N)/YST(K)
      IF(TP.GT.TH(K,I,N)) SP(N)=YST(K)-SPL(N)
      IF(TP.GT.TH(K,I,N)) TP=TH(K,I,N)
      TH(K,I,N)=TH(K,I,N)-TP
      F2=F2+(SPL(N)+SP(N)/2)*TP*TV(K,I,N)
      FF2=FF2+(SPL(N)+SP(N)/2)*TP*TV(K,I,N)*XB(K,I,N)
      SPL(N)=SPL(N)+SP(N)
   16 CONTINUE
      RETURN
      END
```

```
      SUBROUTINE RESTRP(RST,STRM,STRP,YST,F1,FF1,F2,FF2,TH,
     1TV,TH1,XB,SP,SPL,K,I,N,THH)
      IMPLICIT REAL*8(A-H,O-Z)
      DIMENSION TH(12,21,28),TV(12,21,28),TH1(12,21,28)
      DIMENSION XB(12,21,28),RST(12,21,28),YST(12),SP(28)
      DIMENSION SPL(28),THH(28)
      TY=TH1(K,I,N)/2
      IF(N.LE.4) GO TO 6
      IF(N.LE.8) GO TO 12
      IF(N.LE.12) GO TO 6
      IF(N.LE.16) GO TO 12
      IF(N.LE.20) GO TO 6
      IF(N.EQ.21) GO TO 12
      IF(N.LE.27) GO TO 6
      IF(N.EQ.28) GO TO 12
    6 STR=RST(K,I,N)+STRM+STRP
      IF(DABS(STR).LT.YST(K)) GO TO 16
      IF(STR.GE.YST(K)) GO TO 3
      F1=F1-(YST(K)+RST(K,I,N))*TH(K,I,N)*TV(K,I,N)
      FF1=FF1-(YST(K)+RST(K,I,N))*TH(K,I,N)*TV(K,I,N)*XB(K,I,N)
      TH(K,I,N)=0.0
      GO TO 16
    3 F2=F2+(YST(K)-RST(K,I,N))*TH(K,I,N)*TV(K,I,N)
      FF2=FF2+(YST(K)-RST(K,I,N))*TH(K,I,N)*TV(K,I,N)*XB(K,I,N)
      TH(K,I,N)=0.0
      GO TO 16
   12 STP=STRM+STRP
      IF(STP.GT.0.0) GO TO 14
      SYT=YST(K)-SPL(N)
      IF(DABS(STP).LT.SYT) GO TO 16
      SP(N)=STP+SYT
      TP=-TH1(K,I,N)*SP(N)/(2*YST(K))
      TLH=TH(K,I,N)-TY
      IF(TP.GT.TLH) SP(N)=-2*YST(K)+SYT
      IF(TP.GT.TLH) TP=TLH
      TH(K,I,N)=TH(K,I,N)-TP
      F1=F1+(-YST(K)+SPL(N)+SP(N)/2)*TP*TV(K,I,N)
      FF1=FF1+(-YST(K)+SPL(N)+SP(N)/2)*TP*TV(K,I,N)*XB(K,I,N)
      SPL(N)=SPL(N)+SP(N)
      IF(TH(K,I,N).GT.TY) GO TO 16
      F1=F1-YST(K)*TH1(K,I,N)*TV(K,I,N)
      FF1=FF1-YST(K)*TH1(K,I,N)*TV(K,I,N)*XB(K,I,N)
      TH(K,I,N)=0.0
      GO TO 16
   14 IF(STP.LT.SPL(N)) GO TO 16
      SP(N)=STP-SPL(N)
      TP=TH1(K,I,N)*SP(N)/(2*YST(K))
      TLH=TH(K,I,N)-THH(N)
      IF(TP.GT.TLH) SP(N)=YST(K)-SPL(N)
      IF(TP.GT.TLH) TP=TLH
      TH(K,I,N)=TH(K,I,N)-THH(N)-TP
```

```
      F2=F2+(SPL(N)+SP(N)/2)*TP*TV(K,I,N)
      FF2=FF2+(SPL(N)+SP(N)/2)*TP*TV(K,I,N)*CS(K,I,N)
      SPL(N)=SPL(N)+SP(N)
      THH(N)=0.0
   10 CONTINUE
      RETURN
      END
```

SECOND ORDER ANALYSIS OF RIGID FRAMES

RESIDUAL STRESS PATTERN IS RECTANGULAR

ANALYSIS OF FRAME NUMBER 1

MEMBER AND MATERIAL PROPERTIES, IN. AND KSI

MEMBER	TF1	W1	TF2	W2	WCF	TCF	TW	HA(SE)	HA(EE)	YST	E
1	0.252	6.000	0.200	6.000	1.720	0.348	0.200	5.548	18.523	55.000	29000.00
2	0.252	6.000	0.450	6.000	1.720	0.348	0.200	18.523	20.704	55.000	29000.00
3	0.256	4.925	0.256	4.925	0.0	0.0	0.185	20.053	19.421	55.000	29000.00
4	0.256	4.925	0.256	4.925	0.0	0.0	0.185	19.421	13.488	55.000	29000.00
5	0.256	4.940	0.181	4.940	0.0	0.0	0.139	13.563	19.670	55.000	29000.00
6	0.256	4.940	0.181	4.940	0.0	0.0	0.139	19.670	13.563	55.000	29000.00
7	0.256	4.925	0.256	4.925	0.0	0.0	0.185	13.488	19.421	55.000	29000.00
8	0.256	4.925	0.256	4.925	0.0	0.0	0.185	19.421	20.053	55.000	29000.00
9	0.252	6.000	0.450	6.000	0.348	1.720	0.200	20.704	18.523	55.000	29000.00
10	0.252	6.000	0.200	6.000	0.348	1.720	0.200	18.523	5.548	55.000	29000.00

DEGREE OF FREEDOM NUMBERS AND MEMBER END COORDINATES, IN.

MEMBER	NP1	NP2	NP3	NP4	NP5	NP6	XI IN.	YI IN.	XJ IN.	YJ IN.
1	31	1	33	3	32	2	0.0	0.0	7.271	156.940
2	1	4	3	6	2	5	7.271	156.940	8.128	175.440
3	4	7	6	9	5	8	8.128	175.440	27.528	177.736
4	7	10	9	12	8	11	27.528	177.736	102.609	186.621
5	10	13	12	15	11	14	102.609	186.621	286.773	199.160
6	13	16	15	18	14	17	286.773	199.160	474.937	186.621
7	16	19	18	21	17	20	474.937	186.621	550.018	177.736
8	19	22	21	24	20	23	550.018	177.736	569.416	175.440
9	22	25	24	27	23	26	569.418	175.440	570.275	156.940
10	25	28	27	30	26	29	570.275	156.940	577.546	0.0

WIDTH OF PORTION OF FLANGE AND WEB IN TENSION DUE TO RESIDUAL STRESSES, IN.

MEMBER	WF1	WW1	WF2	WW2
1	0.948	0.474	1.112	0.556
2	0.948	0.474	1.112	0.556
3	1.054	0.527	1.054	0.527
4	1.054	0.527	1.054	0.527
5	0.456	0.228	0.600	0.300
6	0.456	0.228	0.600	0.300
7	1.054	0.527	1.054	0.527
8	1.054	0.527	1.054	0.527
9	0.948	0.474	1.112	0.556
10	0.948	0.474	1.112	0.556

FIRST SET OF LOADS

JOINT LOADS, KIPS

LOCATION	LOAD
1	0.0
2	0.0
3	0.0
4	0.0
5	0.0
6	0.0
7	0.0
8	0.0
9	0.0
10	0.0
11	0.0
12	0.0
13	0.0
14	0.0
15	0.0
16	0.0
17	0.0
18	0.0
19	0.0
20	0.0
21	0.0
22	0.0
23	0.0
24	0.0
25	0.0
26	0.0
27	0.0

UNIFORM LOADS, KIPS/IN.

MEMBER	VERTICAL	HORIZONTAL
1	0.0	0.0
2	0.0	0.0
3	0.0	0.0
4	0.0	0.0
5	0.0	0.0
6	0.0	0.0
7	0.0	0.0
8	0.0	0.0
9	0.0	0.0
10	0.0	0.0

SECOND SET OF LOADS

JOINT LOADS, KIPS

LOCATION	LOAD
1	0.0
2	0.0
3	0.0
4	0.0
5	5.000
6	-20.000
7	0.0
8	0.0
9	0.0
10	0.0
11	0.0
12	0.0
13	0.0
14	0.0
15	0.0
16	0.0
17	0.0
18	0.0
19	0.0
20	0.0
21	0.0
22	0.0
23	0.0
24	-20.000
25	0.0
26	0.0
27	0.0

UNIFORM LOADS, KIPS/IN.

MEMBER	VERTICAL	HORIZONTAL
1	0.0	0.0
2	0.0	0.0
3	-0.20	0.0
4	-0.20	0.0
5	-0.20	0.0
6	-0.20	0.0
7	-0.20	0.0
8	-0.20	0.0
9	0.0	0.0
10	0.0	0.0

VALUES OF JOINT LOADS, UNIFORM LOADS, DEFLECTIONS, AND NUMBER OF HINGES AND ITERATIONS

HORIZ. LOAD AT THE TOP OF LEFT COLUMN KIPS	VERT. LOAD AT THE TOP OF COLUMNS KIPS	CONT. VERT. LOAD OF RAFTER KIPS/IN.	HORIZ. DEFL. AT TOP OF LEFT COLUMN IN.	VERT. DEFL. AT MID SPAN OF RAFTER IN.	HORIZ. DEFL. AT TOP OF RIGHT COLUMN IN.	NO. OF HINGES	NO. OF ITERS.
0.5000	-2.0000	-0.0200	0.83739D-01	-0.10925D+01	0.26018D+00	2	2
1.0000	-4.0000	-0.0400	0.16723D+00	-0.21341D+01	0.51189D+00	2	2
1.5000	-6.0000	-0.0600	0.25638D+00	-0.31805D+01	0.77008D+00	2	3
2.0000	-8.0000	-0.0800	0.35157D+00	-0.42319D+01	0.10352D+01	2	3
2.5000	-10.0000	-0.1000	0.45328D+00	-0.52862D+01	0.13076D+01	2	3
2.9500	-11.8000	-0.1180	0.54655D+00	-0.62411D+01	0.15549D+01	4	1

FINAL END ACTIONS OF MEMBERS

MEMBER	END I AXIAL KIPS	END I SHEAR KIPS	END I MOMENT KIPS-IN.	END J AXIAL KIPS	END J SHEAR KIPS	END J MOMENT KIPS-IN.
1	44.7232	-13.4697	0.0	-44.7232	13.4697	-2111.4412
2	44.7231	-13.4699	2111.4412	-44.7231	13.4699	-2351.3577
3	22.1376	29.8570	2351.3577	-21.8660	-27.5678	-1784.7285
4	21.8663	27.5680	1784.7285	-20.8179	-18.7085	-6.9993
5	19.8462	19.7382	6.9993	-18.3666	2.2311	1663.1270
6	18.4999	0.2520	-1663.1270	-19.9795	21.7153	-383.4748
7	21.0510	-20.6783	383.4748	-22.0994	29.5379	-2305.7320
8	22.0998	-29.5376	2305.7320	-22.3707	31.8268	-2908.8963
9	46.8411	16.3250	2908.8963	-46.8411	-16.3250	-2612.1443
10	46.8412	16.3247	2612.1443	-46.8412	-16.3247	0.0

REACTIONS AT SUPPORTS

LEFT SUPPORT

HORIZONTAL KIPS	VERTICAL KIPS	MOMENT KIPS-IN.
15.5250	44.0519	0.0

RIGHT SUPPORT

HORIZONTAL KIPS	VERTICAL KIPS	MOMENT KIPS-IN.
-18.4750	46.0355	0.0

END OF PROBLEM----- THE FRAME FAILED

APPENDIX B

EXAMPLES OF FRAME ANALYSIS

EXAMPLES OF FRAME ANALYSIS

B.1--Example 1

The frame analyzed in this example is shown in Figure B.1. It is a single story, single bay frame with a multiple tapered rafter and single symmetric H-shaped cross-sections. The columns have single symmetric cross-sections with channel sections used for the inside flanges. A vertical uniform load along the rafter is applied incrementally. All web to flange welds are assumed continuous and one side only with the size of the weld dependent on the thickness of flanges and web. Shear force in the weld is assumed not to govern.

Rectangular patterns are assumed for the residual stress distribution of all cross-sections. The procedure presented in section 2.5 of Chapter II is used for computation of width of tension blocks. The computation of tension blocks of section F-F of Figure B.1 is as follows:
According to minimum weld table in the AISC specification the size of the weld is based on the thickness of plates to be joined. In the case of cross-section F-F the web 0.2 inch, governs and the minimum weld size is 3/16 in.

Thus w_e = 3/16 in.

and the approximate area of the weld is (Eqn. 2.10)

$A = 0.6\ w_e^2 = 0.0211\ \text{in.}^2$

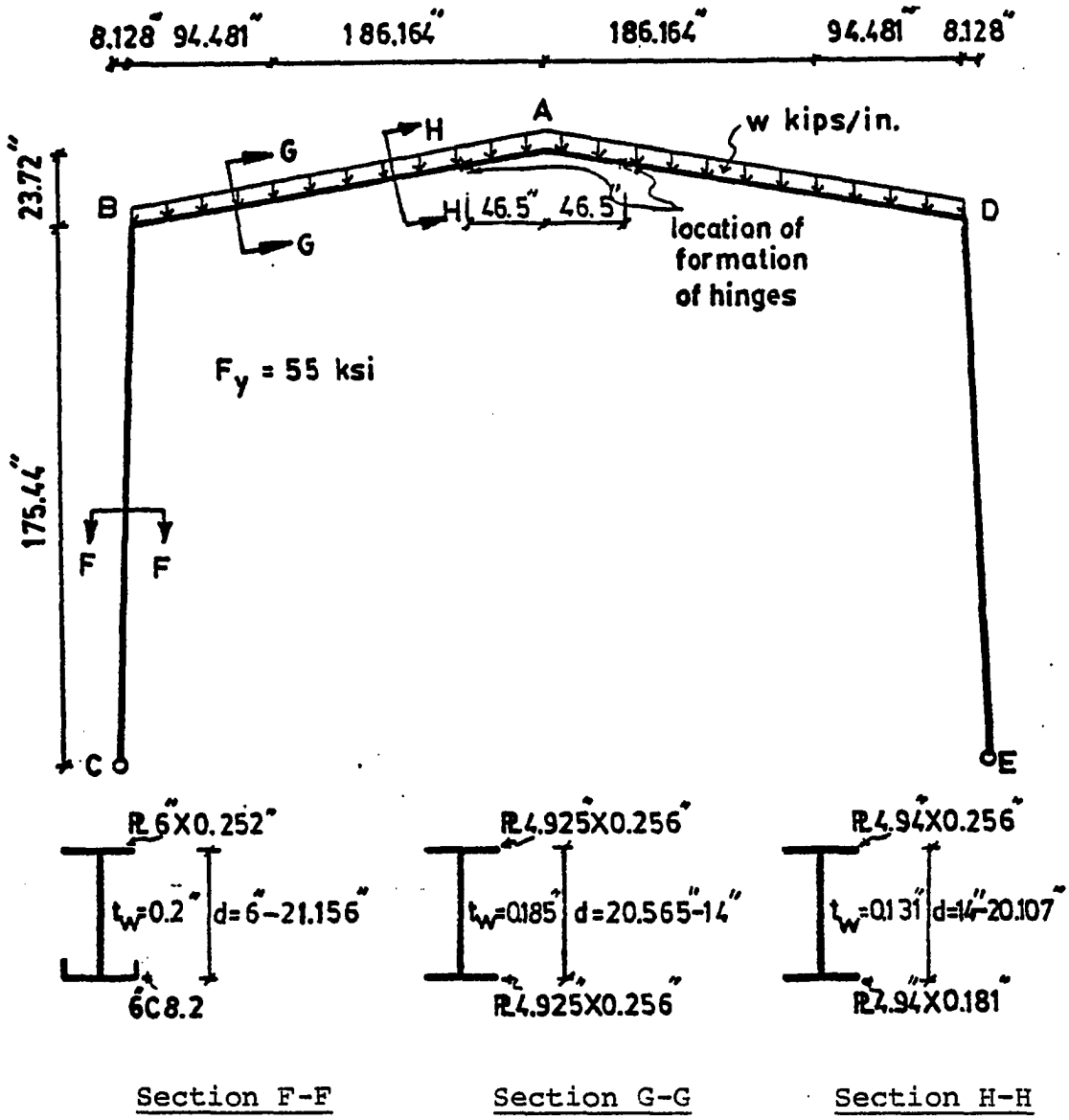

Figure B.1 Frame Geometry and Loading for Example 1

The shrinkage force of the weld is computed from Eqn. 2.9

$F = C_v A$

where C_v = 870 Kips/in., hence

$F = 870 \times 0.0211 = 18.35$ Kips.

The width of tension blocks are then, using Eqn. 2.41,

in outside flange:

$$2C_w = \frac{2F}{\sigma_y \Sigma t} = \frac{2 \times 18.35}{55(2 \times 0.252 + 0.2)} = 0.948 \text{ in.}$$

in outside portion of web: $C_w = 0.074$ in.

in inside flange:

$$2C_w = \frac{2F}{\sigma_y \Sigma t} = \frac{2 \times 18.35}{55(2 \times 0.2 + 0.2)} = 1.112 \text{ in.}$$

in inside portion of web: $C_w = 0.556$ in.

The residual stress level of these tension blocks is assumed equal to the yield stress of the steel which is taken as 55 KSI. The residual stress of the remainder of the flanges and web area are compressive, balancing their respective tension forces. By the same procedure tension blocks for other cross-sections are computed.

The reinforcement effect of connections is taken into account by assuming that the yield stress of the portions of the rafter and columns adjacent to the column-rafter connections to be higher than 55 ksi, so that no yielding will occur in these areas during the loading process. The length of each

portion is taken equal to the depth of the cross-section at the narrow end of the portion.

Because of the rafter configuration and the single symmetric cross-sections, the effective length factor approach of AISC specification is not applicable, and the proposed stiffness method (in the form of the computer program) and the proposed trial and error method are used for the analysis of the frame.

Analysis by Trial and Error Method

From Figure B.1 the length of the beams and columns are, respectively,:

L_b = 281.646 in.

L_c = 175.628 in.

The following values are computed by integrating over small elements of each member, using Eqns. 3.19, 3.20, 3.21 and 3.22:

$$\alpha = \int_C^B \frac{x^2 dx}{I_x} = 6685.44$$

$$\beta = \int_A^B \frac{x^2 dx}{I_x} = 36207.68$$

$$\delta = \int_A^B \frac{(L_b - x)\,x\,dx}{I_x} = 21011.69$$

$$\rho = \int_A^B \frac{(L_b - x)\,x^2 dx}{2I_x} = 1507062.93$$

Since the loading and the frame are symmetric, the deflection and reactions of only one subassemblage needs to be computed. The first load increment is assumed to be

$W_1 = 0.02$ kips/in.

Trial 1

Results of a first order computer analysis yields

$V_{A1} = 1.1$ in.

$P_{C1} = P_{E1} = 5.6326$ kips

$Q_{c1} = -Q_{E1} = 2.75$ kips

Based on these values the member end moments are

$M_{BA} = M_{BC} = 436.68$ kips-in.

$M_{DA} = M_{DE} = 436.68$ kips-in.

$M_{AB} = M_{AD} = 288.47$ kips-in.

From eqn. 2.23:

$$\Delta_{B1} = \Delta_{D1} = \frac{(P_{C1}-Q_{C1}h)(\alpha L_b^2-\beta L_c^2)h-L_c^2\delta h M_{AB}-EL_b^2L_c^2h\left(\frac{V_{A1}}{H-D_L}\right)-w_1\rho L_b L_c^2 h\cos\theta}{EL_b^2\ L_c^2-P_{CT}h(\alpha L_b^2-\beta L_c^2)}$$

because this computation is for the first load increment

$P_{CT} = P_{C1}$

Substituting values of the frame parameter into Eqn. 3.23

$\Delta_{B1} = -\Delta_{D1} = -0.0171$ in.

and

$\Delta_{B1} = \Delta_{BT1}$

$\Delta_{D1} = \Delta_{DT1}$

From Eqn. 3.25

$$V_{AT1} = \sqrt{L_b^2 = \left(\frac{2H-D_R-D_L+\Delta_{DT1}-\Delta_{BT1}}{e}\right)} - e$$

thus

$V_{AT1} = -0.203$ in. > -1.1 in.

Hence try

$V_{A1} = -1$ in.

and Eqn. 3.23 gives

$\Delta_{B1} = -\Delta_{D1} = 0.0469$ in.

Using these values, Eqn. 3.25 gives

$V_{A1} = -0.562$ in. > -1 in.

Hence try

$V_{A1} = -0.95$ in.

then

$\Delta_{B1} = -\Delta_{D1} = -0.0789$ in.

and

$V_{A1} = -0.953$ in. $\quad -0.95$ in. $\quad$ say O.K.

Then from Eqn. 3.27

$\Delta_1 = \Delta_{D1} - \Delta_{B1} = 0.1578$ in.

Because of symmetrical loading and symmetrical frame

$BB' = DD'$ (see Figure 3.5)

Using Eqn. 3.28

$$BB' = \frac{M_{BA}}{EL_b}\int_B^A \frac{(L_b-x)x\,dx}{I_x} + \frac{M_{AB}}{EL_b}\int_B^A \frac{x^2dx}{I_x} + \frac{w_1\cos\theta}{E}\int_B^A \frac{(L_b-x)x^2dx}{2I_x}$$

and integrating over small elements of the rafter gives

$$\frac{1}{EL_b}\int_B^A \frac{(L_b-x)x\,dx}{I_x} = 0.0025718$$

$$\frac{1}{EL_b}\int_B^A \frac{x^2dx}{I_x} = 0.0043744$$

$$\frac{w_1\cos\theta}{E}\int_B^A \frac{(L_b-x)x^2dx}{2In} = -0.9980246$$

Substituting these values and the values of the moments in Eqn. 3.28 gives

$BB' = DD' = -1.137$ in.

and from Eqn. 3.30

$\Delta_1 = - (BB' + DD') \sin \theta$

which gives

$\Delta_1 = 0.1914$ in. > 0.1578 in. (computed by Eqn. 3.27)

Trial 2

Assuming $Q_{C1} = 2.80$ kips

and using deflections from the previous trial gives

$M_{BC} = M_{BA} = 445.90$ kips-in.

$M_{DA} = M_{DE} = 445.90$ kips-in.

$M_{AB} = M_{AD} = -281.17$ kips-in.

The values of V_{A1} used in Eqn. 3.23 and its computed value by Eqn. 3.25 for Trial 2 are arranged in Table B.1.

Table B.1: Assumed and Computed Values of V_{A1} for Q_{C1} = 2.80 kips

V_{A1} (used in Eqn. 3.23)	V_{A1} (computed in Eqn. 3.25)
-0.95 in.	-1.559 in.
-1.00 in.	-1.157 in.
-1.02 in.	-0.999 in.
-1.018 in. *	-1.016 in. *

For V_{A1} = 1.016 in. Eqn. 3.23 gives

$\Delta_{B1} = -\Delta_{D1} = -0.0839$ in.

and using Eqn. 3.27

$\Delta_1 = \Delta_{D1} - \Delta_{B1} = 0.1679$ in.

Computing BB´ by Eqn. 3.28

BB´ = -1.0182 in.

where

BB´ = DD´

and Eqn. 3.30 gives

$\Delta_1 = -(BB'+DD')\sin\theta = 0.1866$ in.> 0.1679 in. (computed by Eqn. 3.27)

Trial 3

Assuming Q_{C1} = 2.833 kips and using the preceeding procedure, the final values of Δ_1 by Eqn. 3.27 and 3.30 are

Δ_1 = 0.1739 in. (by Eqn. 3.27)

Δ_1 = 0.1748 in. (by Eqn. 3.30)

which are not sufficiently close, therefore a lower value for Q_{C1} must be tried.

Trial 4

Assuming Q_{C1} = 2.831 kips and final values of Δ_1, are:

Δ_1 = 0.1754 in. (by Eqn. 3.27)

Δ_1 = 0.1752 in. (by Eqn. 3.30)

These two values are close enough and the other deflections and reactions for this load increment are then found to be

$\Delta_{B1} = -\Delta_{D1} = -0.0877$ in.

$V_{A1} = -1.063$ in.

$P_{C1} = P_{E1} = 5.626$ kips

$Q_{E1} = -2.831$ kips

Using the procedure described in section 2.6 and the computed member forces, the yielded portions of every cross-section were determined and new section properties computed. For this increment additional yielding did not occure besides those portion yielded due to residual stresses and the values of α, β, δ and ρ are unchanged and iteration was not necessary.

With the same procedure, deflections and reactions for additional load increments are computed and shown in Table B.2.

At w_{T1} = 0.121 kips/in., two hinges formed on the rafter, near the peak causing frame instability. The locations of these hinges are symmetrical with respect to Point A as shown in Figure B.1.

The frame was also analyzed by computer (modified stiffness method). The load-deflection relationships of the two analyses are shown in Figure B.2. Good agreement was found until w_{T1} = 0.1 kips/in. Between w_{T1} = 0.1 kips/in. and the failure load, the trial and error method predicted higher deflections, and the failure load computed by this method is slightly lower than the failure load obtained by the computer program.

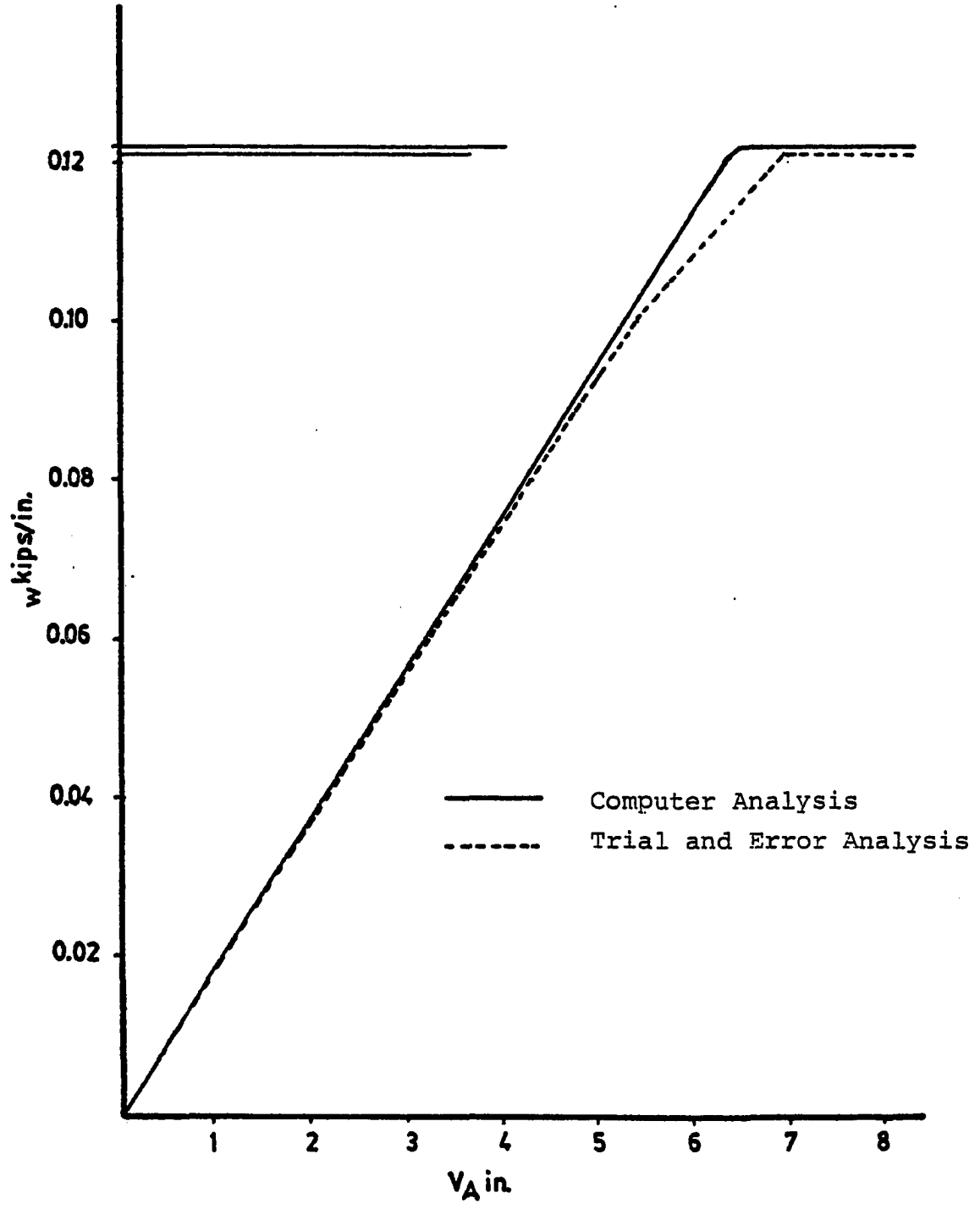

Figure B.2 Load-Deflection Relationships for Example 1

Table B.2: Results of Trail and Error Analysis of Example 1

W_{T1} kips/in.	Q_{CT} kips	P_{CT} kips	V_{AT} in.	Δ_{BT} in.	Δ_{DT} in.
0.02	2.831	5.6326	-1.063	-0.087	0.087
0.04	5.666	11.2652	-2.144	-0.173	0.173
0.06	8.494	16.8978	-3.227	-0.255	0.255
0.08	11.324	22.5304	-4.315	-0.332	0.332
0.10	14.154	28.163	-5.456	-0.408	0.408
0.121	17.126	34.077	-6.97	-0.502	0.502

B.2 Example 2

The frame shown in Figure B.3 is analyzed in this example. The frame is constructed of members with doubly symmetric H-shaped cross-sections and with constant tapering angle. The effect of connection reinforcement and residual stresses are considered in the same manner as in Example 1. The frame is subjected to a uniform load distributed along the length of the rafter in additon to a single concenterated lateral load at the eave. The loading was incremented in two stages: The first stage continued until a single hinge formed. The second stage was from this load to collapse.

First Stage Loading

Results of an analysis by the trial and error method for the first stage loading are tabulated in Table B.3. The procedure used was described in Example 1.

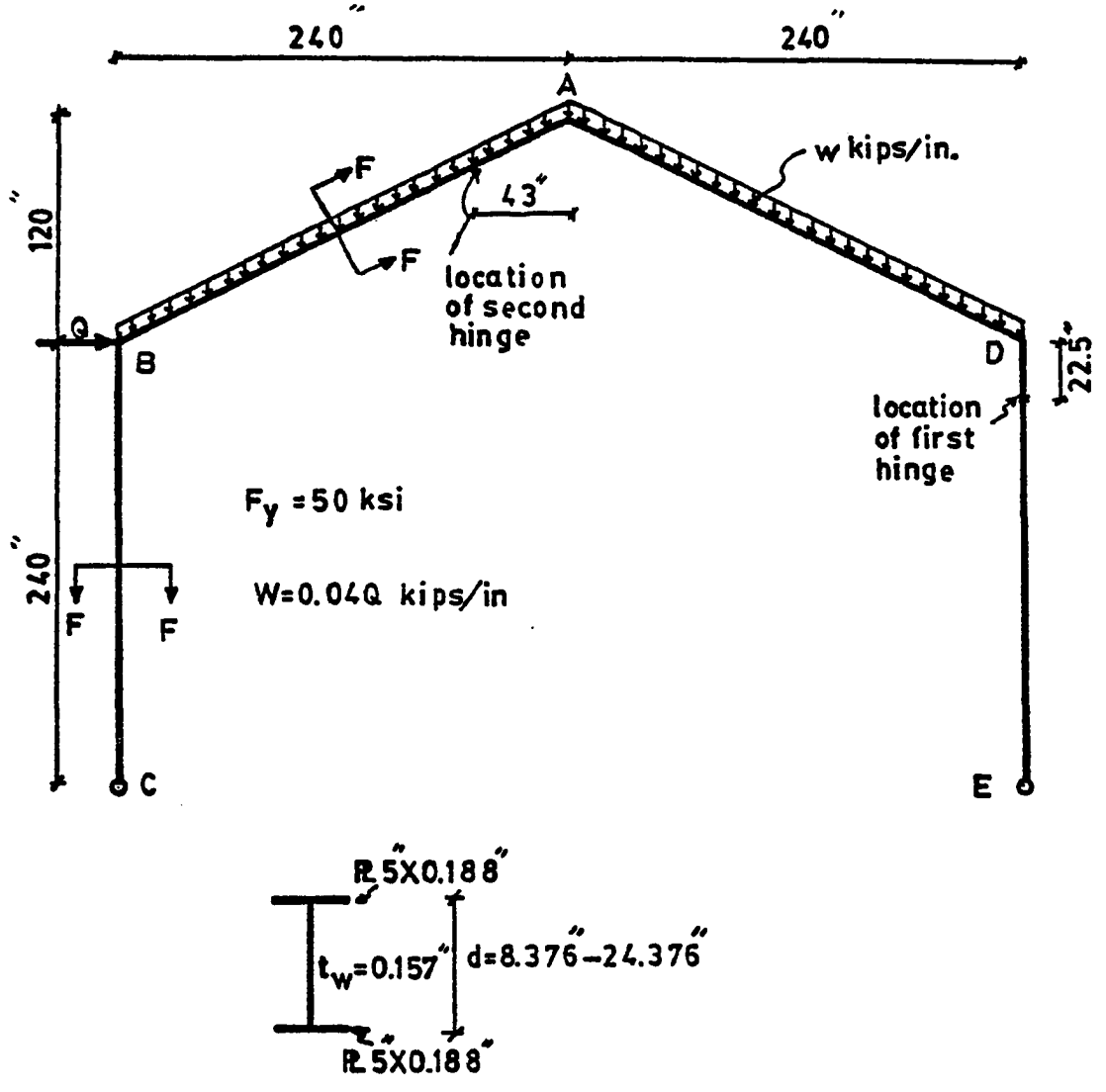

Section F-F

Figure B.3 Frame Geometry and Loading for Example 2

Second Stage Loading

At the end of the first stage of loading a hinge formed on column DE, at a distance 22.5 in. from the center of connection D. Due to formation of this hinge, the frame is determinate for further analysis. The loading for this stage was identical to that of the first stage. A second hinge formed when $w_2 = 0.004$ kips/in. and $Q_2 = 0.1$ kip.

The horizontal deflection at B due to these loads is computed using Eqn. 3.71.

$$\Delta_{B2} = -\theta_{BC}h - \frac{\theta_{BA}(H-D_L)+(\theta_{AB}+\theta_{BA}+\theta_{AD})(H-D_R)}{2H-D_L-D_R} \times h$$

where θ_{BC}, θ_{BA}, θ_{AB} and θ_{AD} are computed by Eqns. 3.14, 3.15 3.69 and 3.53.

$$\theta_{BC} = \frac{M_{BC}}{EL_c^2} \int_C^B \frac{x^2 dx}{I_x}$$

$$\theta_{BA} = \frac{M_{BA}}{EL_b^2} \int_A^B \frac{x^2 dx}{I_x} + \frac{M_{AB}}{EL_b^2} \int_A^B \frac{(L_b-x)x dx}{I_x} + \frac{w_2 \cos\theta}{EL_b} \int_A^B \frac{(L_b-x)x^2 dx}{2I_x}$$

$$\theta_{AB} = \frac{M_{BA}}{EL_b^2} \int_B^A \frac{(L_b-x)x dx}{I_x} + \frac{M_{AB}}{EL_b^2} \int_B^A \frac{x^2 dx}{I_x} + \frac{w_2 \cos\theta}{EL_b} \int_B^A \frac{(L_b-x)x^2 dx}{2I_x}$$

$$\theta_{AD} = \frac{M_{AD}}{EL_b^2} \int_D^A \frac{x^2 dx}{I_x} + \frac{w_2 \cos\theta}{EL_b} \int_D^A \frac{(L_b-x)x^2 dx}{2I_x}$$

Integrating over small elements yields

$$\frac{1}{EL_b^2} \int_A^B \frac{x^2 dx}{I_x} = 1.345 \times 10^{-6}$$

$$\frac{1}{EL_b^2} \int_A^B \frac{(L_b - x) x dx}{I_x} = 1.509 \times 10^{-6}$$

$$\frac{\cos\theta}{EL_b} \int_A^B \frac{(L_b - x) x^2 dx}{2I_x} = 1.607 \times 10^{-2}$$

$$\frac{1}{EL_b^2} \int_B^A \frac{(L_b - x) x dx}{I_x} = 1.517 \times 10^{-6}$$

$$\frac{1}{EL_b^2} \int_B^A \frac{x^2 dx}{I_x} = 7.551 \times 10^{-6}$$

$$\frac{\cos\theta}{EL_b} \int_B^A \frac{(L_b - x) x^2 dx}{2I_x} = 3.943 \times 10^{-2}$$

$$\frac{1}{EL_b^2} \int_D^A \frac{x^2 dx}{I_x} = 6.12 \times 10^{-6}$$

$$\frac{\cos\theta}{EL_b} \int_D^A \frac{(L_b-x)x^2dx}{2I_x} = 2.661 \times 10^{-2}$$

$$\frac{1}{EL_c^2} \int_C^B \frac{x^2dx}{I_x} = 1.578 \times 10^{-6}$$

Based on the deflected shape of the frame at the end of the first stage loading the reaction due to Q_2 and w_2 are

P_{C2} = 1.023 kips

Q_{C2} =-0.1 kip

P_{E2} = 1.124 kips

Q_{E2} = 0

and the member end moments are

$M_{BA} = M_{BC}$ = -24.46 kips-in.

$M_{AB} = M_{AD}$ = -142.30 kips-in.

M_{DA} = 0 (See Figure 3.11)

For these moments, the member end rotations are

$\theta_{BA} = -3.1191 \times 10^{-4}$ rad.

$\theta_{AB} = -1.2693 \times 10^{-3}$ rad.

$\theta_{AD} = -9.7732 \times 10^{-4}$ rad.

$\theta_{BC} = -3.86 \times 10^{-5}$ rad.

and Eqn. 3.71 gives

$\Delta_{B2} = 0.3537$ in.

Using Eqn. 3.73 for vertical deflection at A

$$V_{A2} = \frac{(\theta_{AB} + \theta_{AD})}{2} \times \frac{(2H - D_R - D_L)}{2}$$

$V_{A2} = -0.2723$ in.

From rafter geometry (Eqn. 3.74)

$$\Delta_2 + \Delta_1 = 2(\sqrt{L_b^2 - (e - V_{AT1} - V_{A2})^2} - H)$$

$\Delta_2 + \Delta_1 = 4.9974$ in.

The deflection Δ_1 was computed in the first stage loading to be

$\Delta_1 = 4.74$ in.

therefore

$\Delta_2 = 0.2574$ in.

since

$\Delta_2 = \Delta_{D2} - \Delta_{B2}$

Substitution of the values of Δ_2 and Δ_{B2} gives

$\Delta_{D2} = 0.6111$ in.

and

$$\Delta_{A2} = \frac{\Delta_{B2} + \Delta_{D2}}{2} = 0.4824 \text{ in.}$$

The above results do not consider the P-Δ effects in the second stage loading. Recalculation including these effects results in the following:

$\Delta_{B2} = 0.395$ in.

$V_{A2} = 0.3014$ in.

$\Delta_2 = 0.285$ in.

$\Delta_{D2} = 0.6801$ in.

$\Delta_{A2} = 0.5375$ in.

Because of the increase, a second iteration is required.

$\Delta_{B2} = 0.3983$ in.

$V_{A2} = -0.3037$ in.

$\Delta_2 = 0.287$ in.

$\Delta_{D2} = 0.6856$ in.

$\Delta_{A2} = 0.542$ in.

Since the difference in respective deflections between this cycle and the previous cycle is sufficiently small, the iteration is stopped and these deflections are taken as the final deflections in the second stage.

With these loads a new hinge formed at 43 in. from Point A on beam AB and the frame failed. The deflection and reactions of the frame at several load increments for the first and second stage loadings are tabulated in Table B.3.

Load-deflection curves from the trial and error analysis and form a computer analysis are plotted in Figure B.4. As in Example 1, the trial and error method predicted slightly higher deflection at loads near the failure load of the frame.

Table B.3 Results of Trial and Error Analysis of Example 2

Q kips	Qc kips	Pc kips	ΔB in.	Δ	VA in.
0.5	1.282	5.101	0.075	0.891	-0.0970
1	2.557	10.19	0.155	1.794	-1.855
2	5.057	20.292	0.330	3.752	-3.795
2.5	6.261	25.235	0.452	5.192	-4.861
2.6	6.161	26.27	0.850	5.878	-5.165

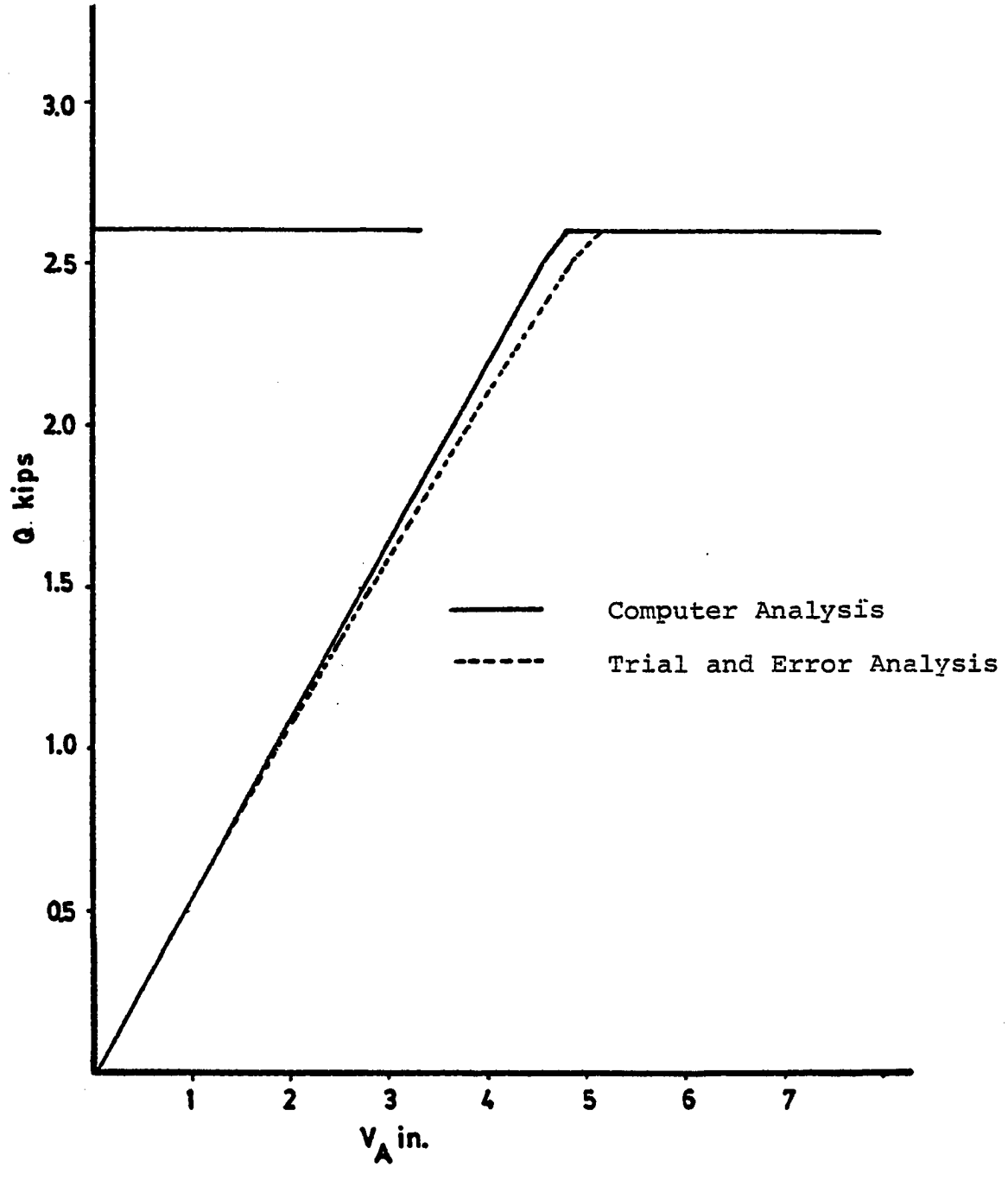

Figure B.4 Load-Deflection Relationships for Example 2

Computation of Maximum Allowable Load of the Frame Using AISC Design Provisions

Since the frame contains double symmetric H-shpaed members with constant tapering angle, the maximum allowable stress for all members can be determined using the design provisions of the AISC specification as explained in Reference 8. In this procedure, the beams and columns of a frame are judged adequate for a given load, when the value of an interaction equation for every member of the frame is less than 1.0.

Figure B.5 shows the moment diagram for a first order analysis of the frame for Q = 1 kip and w = 0.04 kips/in. The moment and axial force of a cross-section for a value of Q and w (same ratio of Q/w as diagram) can be determined by multiplying the values from the diagram by Q. The adequacy of beams and columns of the frame was checked for several values of Q and w, and the maximum values obtained were Q = 2.53 kips and w = 0.1012 kips/in. The computations for this value of Q and w are as follows:

I. Beam AD

For column DE the tapering ratio is

$$\gamma_c = \frac{dD}{dE} - 1 = 1.91.$$

The carry-over-factors and stiffness factor of the column are

$$C_{ED} = -0.9083$$

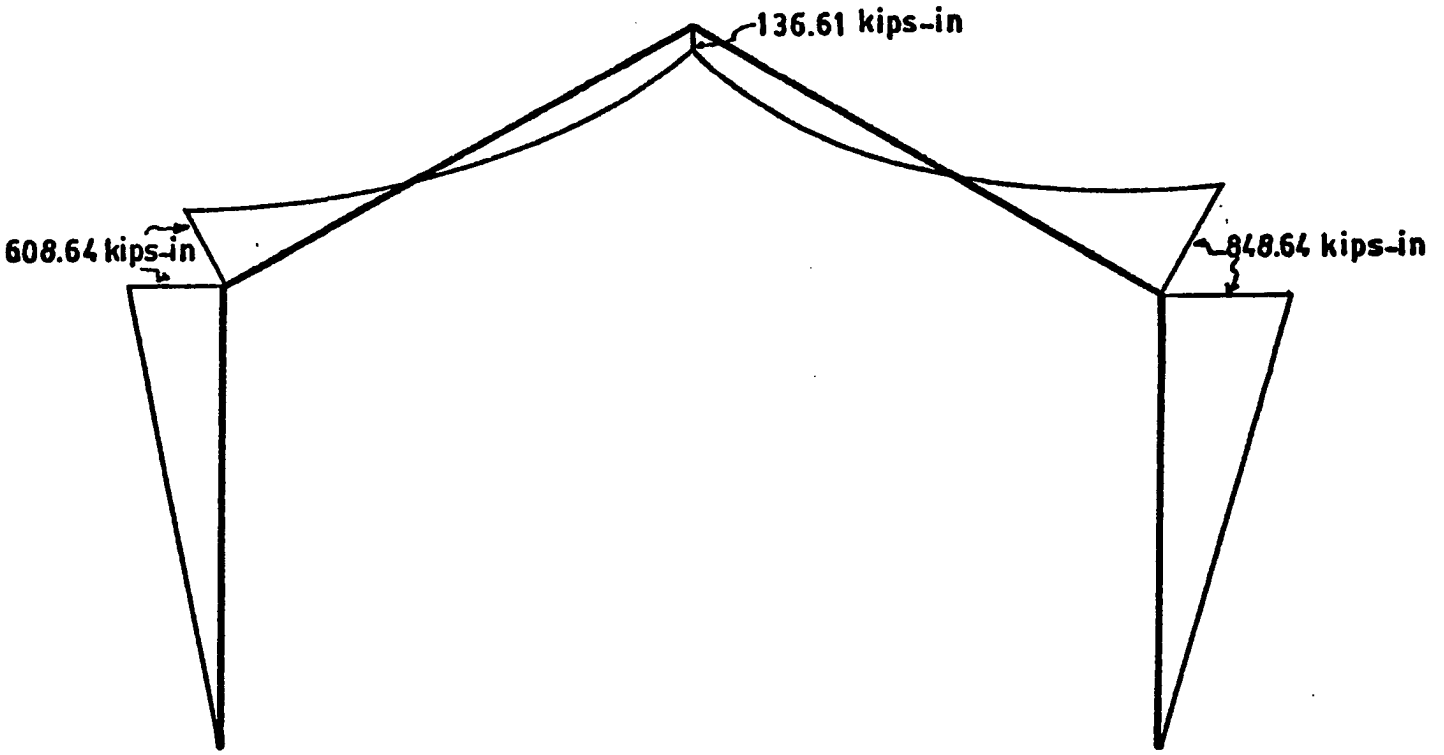

Figure B.5 First Order Analysis Moment Diagram for Frame of Example 2

$C_{DE} = -0.2643$

$k_{DE} = 125161.81$

The equivalent moment of inertia of the column is

$$I_{ec} = \frac{bT}{3E} k_{DE}(1-C_{DE}C_{ED}) = \frac{240}{3x29000} \times 125161.81 \ (1-0.9083x0.2643)$$

$$= 262.39 \text{ in.}^4$$

$$G_D = \frac{bTI_{at\ E}}{LbIec} = \frac{240x38.215}{268.33x262.39} = 0.1304$$

Assuming the frame is hinged at B, $G_A = 10$ (AISC recommended for pinned end) and using the AISC design aid charts

$k_{x\gamma} = 0.9$

At the narrow end $r_x = 3.491$ in. and

$$\frac{k_x \gamma L_b}{r_x} = \frac{0.9x268.33}{3.491} = 69.18$$

AISC specification Table 1-50 gives

$F_{a\gamma} = 21.2$ ksi

From plastic design provisions of AISC

$P_{cr} = 1.7\ F_{a\gamma}A = 36.04A$

Also

$$P_{e'\gamma} = \frac{\pi^2 EA}{(k_{x\gamma x} Lb/rx)^2} = 59.95A$$

The interaction equation is

$$\frac{P}{P_{cr}} + \frac{C_m M}{(1-P/P_{e'\gamma})M_p} \leq 1$$

where $C_m = 0.85$ when sidesway is permitted.

The interaction equation was evaluated at 21 sections along the beam AD. Pertinent parameters and results computed are shown in Table B.4. The moments and axial forces along the beam AB are less than along beam AD, therefore, AD is adequate by inspection.

II. Column DE

The tapering ratio of the beam AD is

$$\gamma_B = \frac{d_D}{d_A} - 1 = 1.91$$

and the carry-over-factors and stiffness factor of the beam are

$$C_{DA} = -0.2643$$

$$C_{AD} = -0.9083$$

$$k_{DA} = 112085.2$$

Table B.4 AISC Analysis of Beam AD, Example 2

Distance in.	Mp kips-in.	A $in.^2$	Moment kips-in.	P kips	$\frac{P}{P_{cr}}$	$\frac{Cm}{1-\frac{P}{P_{e'Y}}}$	$\frac{P}{P_{cr}} + \frac{CmM}{(1-\frac{P}{P_{e'Y}})Mp}$
0	2253.86	5.648	2147.06	-20.491	0.1007	0.9075	0.9628
22.65	2143.47	5.4109	1655.2	-19.464	0.0998	0.9042	0.798
26.80	2068.06	5.3968	1570.7	-19.276	0.0996	0.9039	0.786
40.20	1928.56	5.2712	1309.79	-18.67	0.0983	0.9034	0.7118
53.60	1825.10	5.1456	1067.04	-18.06	0.0974	0.9029	0.625
67.00	1724.14	5.02	842.46	-17.45	0.0965	0.9023	0.537
80.40	1625.65	4.8944	636.05	-16.85	0.0955	0.9018	0.448
93.80	1529.66	4.7688	447.82	-16.24	0.0945	0.9012	0.358
107.20	1436.16	4.6432	277.76	-15.63	0.0934	0.9006	0.268
120.60	1345.14	4.5176	125.87	-15.03	0.0923	0.8999	0.177
134.00	1256.62	4.392	-7.85	-14.42	0.0911	0.8992	0.097
147.40	1170.58	4.2664	-123.40	-13.81	0.0898	0.8985	0.185
160.80	1087.03	4.1408	-220.78	-13.20	0.0885	0.8977	0.271
174.20	1005.96	4.0152	-299.98	-12.6	0.0871	0.8970	0.355
187.60	927.39	3.8896	-361.02	-11.99	0.0855	0.8961	0.434
201.00	851.32	3.764	-403.88	-11.38	0.0839	0.8951	0.509
214.40	777.72	3.6384	-428.571	-10.77	0.0821	0.8941	0.574
227.80	706.61	3.5128	-435.09	-10.17	0.0803	0.8931	0.63
241.20	637.99	3.3872	-423.44	-9.56	0.0783	0.8920	0.67
254.60	571.86	3.2616	-393.61	-8.95	0.0761	0.8908	0.689
268.00	508.22	3.136	-345.62	-8.35	0.0739	0.8895	0.679

The equivalent moment of inertia of beam AD is

$$I_{eB} = \frac{bT}{3E} k_{DA}(1-C_{DA}C_{AD}) + \frac{268.33}{3x29000} \times 112085.2(1-0.2643x0.9083)$$

$$= 262.71 \text{ in.}^4$$

and

$$G_D = \frac{268.33x38.215}{240x262.71} = 0.1626$$

$G_E = 10$ (AISC recommended for pinned end)

Using AISC design aid charts

$K_{x\gamma} = 0.91$

At the narrow end $r_x = 3.491$ and

$$\frac{K_{x\gamma}L_b}{r_x} = 69.13$$

AISC specification Table 1-50 gives

$F_{a\gamma} = 22.27$ KSI

From plastic design provisions of AISC

$P_{cr} = 1.7\ F_{a\gamma}A = 37.86A$

also

$$P_{e'\gamma} = \frac{\pi^2 EA}{(K_{x\gamma x}L_b/r_x)^2} = 73.13A$$

The interaction equation is

$$\frac{P}{P_{cr}} + \frac{CmP}{(1 - \frac{P}{P_{e'\gamma}})M_p} \leq 1$$

where Cm = 0.85 when sidesway is permitted.

The values of interaction equation for 21 sections along the column DE are shown in Table B.5. At a point 48 in. from D, the value of interaction equation was maximum, slightly less than 1.0, and is the critical section. Since the moments and axial forces along column BC are less than moments and axial forces along column DE, column DE is not critical. Thus, Q = 2.53 kips and 2 = 0.1012 kips/in. is the load capacity of the frame by the AISC.

The maximum load computed using the modified stiffness technique described in Chapter II was Q = 2.6 kips and w = 0.104 kips/in. The AISC procedure prediction is 2.7% lower.

Table B.5 AISC Analysis of Column DE, Example 2

Distance in.	Mp kips-in.	A $in.^2$	Moment kips-in.	P kips	$\frac{P}{P_{cr}}$	$\frac{Cm}{1-\frac{P}{P_{e'Y}}}$	$\frac{P}{P_{cr}} + \frac{CmM}{(1-\frac{P}{P_{e'Y}})Mp}$
0	489.09	3.136	0.0	-25.89	0.2181	0.9582	0.2181
12	553.06	3.2616	107.35	-25.89	0.2097	0.9535	0.3948
24	619.55	3.3872	214.71	-25.89	0.2019	0.9492	0.5309
36	688.55	3.5128	322.06	-25.89	0.1947	0.9453	0.6369
48	760.07	3.6384	429.41	-25.89	0.1879	0.9416	0.7199
60	834.09	3.764	536.77	-25.89	0.1817	0.9382	0.7855
72	910.63	3.8896	644.12	-25.89	0.1758	0.9351	0.8372
84	989.67	4.0152	751.47	-25.89	0.1703	0.9322	0.8781
96	1071.23	4.1408	858.82	-25.89	0.1651	0.9295	0.9103
108	1155.31	4.2664	966.18	-25.89	0.1603	0.9269	0.9355
120	1241.89	4.3920	1073.53	-25.89	0.1557	0.9245	0.9549
132	1330.99	4.5176	1180.88	-25.89	0.1514	0.9223	0.9697
144	1422.59	4.6432	1288.24	-25.89	0.1473	0.9202	0.8906
156	1516.71	4.7688	1395.59	-25.89	0.1434	0.9182	0.9883
168	1613.35	4.8944	1502.94	-25.89	0.1397	0.9163	0.9933
180	1712.49	5.0200	1610.29	-25.89	0.1362	0.9145	0.9961
192	1814.41	5.1456	1717.65	-25.89	0.1329	0.9128	0.9972*
204	1918.31	5.2712	1825	-25.89	0.1297	0.9112	0.9966
217.5	2038.85	5.4125	1945.77	-25.89	0.1264	0.9095	0.9945
228	2134.19	5.5224	2039.71	-25.89	0.1238	0.9082	0.9918
240	2245.89	5.6480	2147.06	-25.89	0.1211	0.9068	0.9880

*Critical section